The role of growth in metabolic scaling: a case study across habitats and life histories

Thesis submitted in accordance with the requirements of the University of Liverpool for the degree of Doctor in Philosophy by Guillermo García Gómez

February 2023

Abstract

The role of growth in metabolic scaling: a case study across habitats and life histories
Guillermo García Gómez

All life processes are powered by metabolism, and thus the metabolic rate of organisms provide a measure of their pace of life. Metabolic rate is linked to body size by many biological processes, involving self-maintenance, biomass production, and activity, all three ultimately related to fitness. Explaining the degree of variation in metabolic rate with body size has therefore become a central topic for ecologists, yet the mechanism(s) underlying this relationship, often termed metabolic scaling, remain enigmatic. In this thesis, I investigate the variation in metabolic scaling in response to different ecological and organismal factors in a broad diversity of ectotherms from extremely different habitats. First, using a meta-analytic approach, I determine the change in metabolic scaling within species of ectothermic vertebrates under both increasing temperature and activity level, exploring differences between air- (i.e., reptiles and amphibians) and water-breathing organisms (i.e., teleost fish and elasmobranchs). I demonstrate that scaling slopes become shallower as metabolic level (i.e., the elevation of the metabolic rate *vs.* body mass relationship) increases with warming only in water-breathers, whereas slopes steepen as metabolic level increases with locomotory activity only in air-breathers. I explain these contrasting findings by combining various, complementary hypotheses involving mechanisms that evolved to protect aerobic scope in fish. Second, I show that allometric (log-log) metabolic scaling slopes decrease with increased maximum growth rates across species of teleost fish, suggesting that growth demands influence metabolic scaling. Using a theoretical model, I then characterise the energetic demands at rest in these teleost species, and show that growth costs remain largely invariant with species body size, lifestyle, and evolutionary history. These results highlight that systematic differences in metabolic scaling are important to understand different energy allocation strategies of species. Last, I examine ontogenetic shifts and sexual differences in metabolic scaling in a model crustacean species (*Artemia franciscana*), showing that variation in scaling slopes can be affected by changes in costs of biomass production between ontogenetic phases and reproductive modes. The potential roles of the cellular mode of growth on production costs and hence on metabolic scaling in this species are discussed. Overall, this thesis combines multiple mechanisms including evolutionary adaptations, plastic responses, and metabolic costs of various organismal activities, to explain the variation in the mass-scaling of energy use among

ectotherms and at various levels of biological organisation. Such a multi-mechanistic perspective may be crucial not only for a comprehensive understanding of metabolic scaling, but also to predict the impact of global change on animal communities.

Acknowledgments

Author contributions

Guillermo García (GG) wrote **Chapter 1**, which was improved with comments and suggestions from David Atkinson (DA) and Andrew Hirst (AH). GG, AH, and DA designed the study and developed the hypotheses in **Chapter 2**. GG and Matt Spencer (MS) wrote the R code for the Bayesian models. GG collected and analysed the data. All authors contributed to writing this chapter. GG, DA, and AH designed the study and hypotheses of **Chapter 3**. GG and MS developed the methods. GG collected the data and conducted the statistical analyses. All authors contributed to writing this chapter. GG, DA, and AH designed the study and wrote **Chapter 4**. GG performed the experimental work, collected the data, and conducted the statistical analyses. GG wrote **Chapter 5**, which was further improved with comments and suggestions from DA and AH.

TABLE OF CONTENTS

LIST OF FIGURES

LIST OF TABLES

Chapter 1: General introduction

A curious Ringneck blenny (*Ophioblennius atlanticus*)

General introduction

From the smallest mites crawling through sand interstices to the largest whales gliding in the ocean, evolution has favoured a vast span of body size and lifespan among animals (Andersen et al., 2016; Brown et al., 2018). The size and tempo of living beings are linked by a plethora of organismal features ranging from physiological to ecological traits (Kozłowski et al., 2020; Glazier, 2022a). Body size and the pace of biological processes (tempo) have drawn much attention from scientists for over a century (Bergmann, 1847; Rubner, 1883), and tend to be closely related (Hatton et al., 2019; Brown et al., 2022; Glazier, 2022a). Biological rates are related to body mass through fitness-related activities, such as biomass production, i.e., growth and reproduction (von Bertalanffy, 1957; Gillooly et al., 2002; Hirst & Forster, 2013; Kiørboe & Hirst, 2014), and metabolic expenditure (Kleiber, 1932; Hemmingsen, 1960; Peters, 1983; Brown et al., 2004; DeLong et al., 2010). Understanding the mechanisms underlying the relationship between biological processes and body mass is crucial because it involves energy flows across all levels of biological organisation, from cells to communities (Kozłowski et al., 2003; Barneche et al., 2014). Among these processes, metabolism is a fundamental property of organisms as it fuels all life functions (Brown et al., 2018). Metabolic rates therefore reflect the pace of life, i.e., the speed at which a variety of complex biochemical processes turn resources from the environment into energy to support organismal activities (Glazier, 2015; Brown et al., 2022).

1. Metabolic rate and the pace of life

Organisms obtain resources from the environment and often store them in reserves (Fig. 1.1). These reserves can be mobilised to supply monomers for building new biomass (the 'anabolic' pathway) as well as to be transformed into usable energy through metabolism (the 'catabolic' pathway) (Clarke, 2017, 2019). Metabolic energy is principally contained in energy-rich molecules of ATP (i.e., adenosine triphosphate), which fuel virtually all physiological processes of organisms. Because the regeneration of ATP from ADP (adenosine diphosphate) requires oxygen in aerobic life during phosphorylation in the mitochondria, metabolic rate of animals can be estimated through rates of oxygen consumption (Clarke, 2017).

In principle, metabolic energy firstly powers life-sustaining processes, often termed 'maintenance' (Wieser, 1994; Kooijman, 1986; Glazier, 2005; Rombough, 2011). Maintenance is a major metabolic component that involves repairing and replacing tissues, which is crucial to maintain their function and hence sustain life (Wieser, 1994; Glazier, 2005). In adult humans, for instance, cell biomass is almost entirely replaced over a period of a year (Sender & Milo, 2021). Moreover, since oxygen is necessary but also potentially dangerous due to the production of reactive intermediates during cellular respiration (Davies, 1995), animals need to invest energy to mitigate oxidative stress on cellular components. Hence, maintenance is generally considered primarily as protein turnover (Wieser, 1994; Rombough, 2011), because this activity requires most of the ATP in non-growing organisms (e.g., Siems et al., 1992; Rolfe & Brown, 1997; see review in Rombough, 2011). Besides protein turnover, ion regulation dictates much of the maintenance demands (Wieser, 1994; Verberk et al., 2021). These costs are largely due to ion pumps (i.e., Na^+- K^+- and Ca^{+2}- ATPases) that maintain ion gradients across membranes, i.e., the rate at which passive loss of ions matches that of active transport (Brand, 1990). Biomass production, on the other hand, requires monomers (e.g., amino acids, sugars, fatty acids) to build macromolecules (e.g., proteins, polysaccharides, lipids) that will form new tissue, but also metabolic energy to assemble macromolecules from monomers. Furthermore, the assemblage of those macromolecules involves indirect costs such as the transport of monomers and ATP to production sites (Clarke, 2017, 2019).

While resting metabolic rate powers maintenance and biomass production, organisms also require energy to power muscular work involved in activities such as locomotion, escape responses from predators, foraging, or mating, which comprise the active metabolic rate (Fig. 1.1). Activity is seen as the most flexible component of the energy budget (Wieser, 1994), as these energetic demands are often adjusted following increased costs of maintenance or production (Gittleman & Thompson, 1988; Given, 1988; Pauly, 2010). All three energy-demanding components, i.e., maintenance, growth, and activity, are hence intrinsically linked to body mass through metabolic rates.
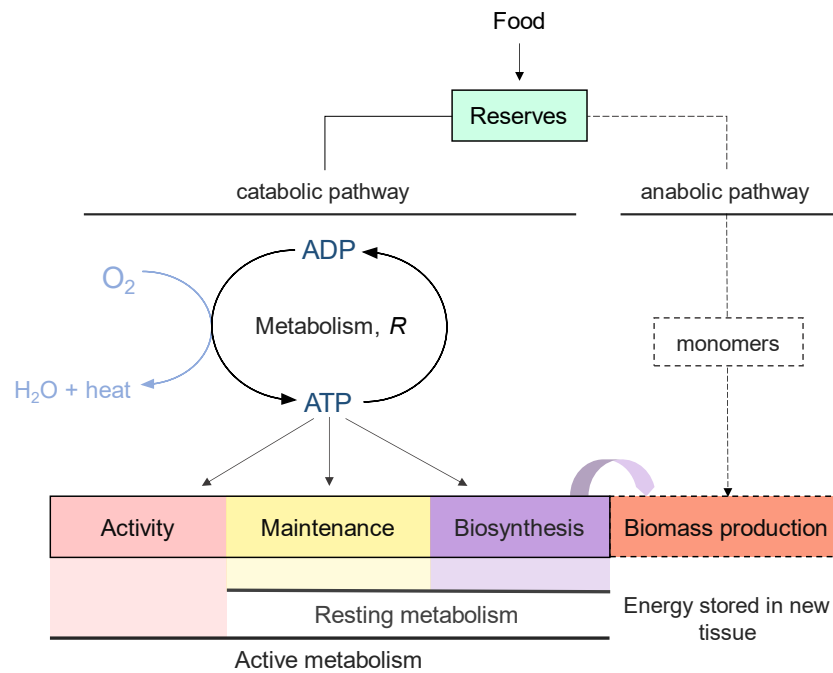
Figure 1.1. Energy flows in an organism (following Clarke, 2017). Energy is assimilated from food and stored in reserves, and then mobilised between metabolism (catabolic pathway) and biomass production (anabolic pathway) *via* growth or reproduction. Metabolism, typically approximated by respiration rate R, captures energy as ATP through the reduction of oxygen in the mitochondria. At rest, metabolic energy is allocated between biosynthesis and self-maintenance functions as regulation of electrochemical gradients or tissue turnover (resting metabolism). Production of new tissue requires monomers as well as metabolic energy, which is dissipated as heat. The rates of metabolism and biomass production are hence intrinsically linked through the costs of biosynthesis. Moreover, organisms need to invest a fraction of metabolic energy in other activities involving muscular work, such as foraging or mating (active metabolism).

2. The relationship between metabolic rate and body mass: a long-standing puzzle

The metabolic rate, often approximated by respiration (R) in animals, increases typically with body mass (m), whose relationship can be expressed by the power function:

$$R = am^b,$$ [1]

where a is the scaling coefficient and b is the scaling exponent, or the allometric slope in a linear regression between $\log R$ vs $\log m$. In this equation, the allometric slope (b) describes the change in metabolic rate as body mass increases (Kleiber, 1932; Bertalanffy, 1957). Remarkably, metabolic rate tends to increase to a lesser extent than body mass does among

4

animals, meaning that large organisms generally require lower rate of energy use per unit mass than small organisms (Kleiber, 1932; White, 2010). Initial evidence of metabolic scaling in endothermic animals showed an intraspecific (i.e. within-species) exponent of $b = 2/3$ (Sarrus & Rameaux, 1839; Rubner, 1883). Such metabolic scaling was then explained by surface-area (SA) principles, arguing that maintaining body temperature in endotherms requires metabolic rate to offset heat loss, which is proportional to body SA, and so both scale as $m^{2/3}$ (Rubner, 1883). The proposed SA-related mechanism associated with thermoregulation, however, excluded most life forms, such as most ectotherms whose body temperatures depend on external heat. Further observations showed an interspecific scaling of $b \approx 3/4$ across a wide diversity of species, initially mammals (Kleiber, 1932; Brody & Proctor, 1932), but later extending to unicellular organisms, plants, and other animals (Brown et al., 2004). Such an apparently consistent, general allometric slope was coined the '3/4-power scaling law' (Hemmingsen, 1960; West et al., 1999; Savage et al., 2004).

The assertion of a 'universal' ¾-power metabolic scaling was initially supported by the vascular oxygen transport system in organisms (Kleiber, 1932), which was further developed theoretically to arise from limits imposed by fractal resource-transport networks (RTN; West et al., 1997, 1999). This hypothesis of West, Brown and Enquist, termed WBE, predicts that internal distribution networks (e.g., blood circulatory system) limit resource supply to cells as body mass, and so network branching, enlarges (Fig. 1.2). The mechanism proposed by the WBE set the basis for the Metabolic Theory of Ecology (MTE; Brown et al., 2004), which explains the variation in metabolic rate across levels of organisation through a fixed scaling with body mass ($b = ¾$) and a constant temperature effect (Gillooly et al., 2001; Brown et al., 2004). While the MTE has been widely used (e.g., Kearney & White, 2012; Price et al., 2012), this model has also attracted much criticism due to its restrictive assumptions (e.g., see Banavar et al., 2002; Ricklefs, 2003; van der Meer, 2006). Indeed, fractal geometry of transport networks in which the MTE is based, has little application in organisms without well-developed circulatory systems (Glazier, 2022a), as is the case for many aquatic invertebrates (Kooijman, 2000; van der Meer, 2006; Glazier, 2005, 2014). Moreover, this so-called 'canonical' ¾-power scaling has been challenged by growing evidence in the literature that shows systematic variation in scaling slopes (b) among taxa, lifestyles, environmental conditions, physiological states, activity levels, or ontogenetic stages (e.g., DeLong et al., 2010; Killen et al., 2010; Glazier 2014, 2020; Hirst et al., 2014; Carey & Sigwart, 2014; Glazier & Paul, 2017) (Fig. 1.2). Indeed, while some species show a nearly constant or increased metabolic rate per gram as they

grow ($b \geq 1$), others exhibit a marked reduction over ontogeny ($b << 1$) (e.g., Bokma, 2004; Killen et al., 2010; Hirst et al., 2014). Among aquatic invertebrates, for instance, more active pelagic species tend to exhibit steeper slopes b, often close to 1, than their sluggish counterparts (Glazier, 2006).
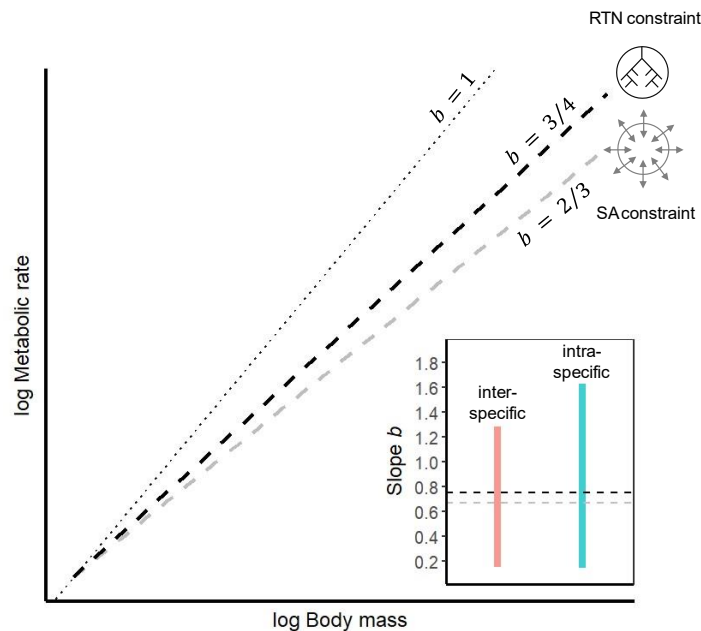
Figure 1.2. The two hypothesised relationships between metabolic rate and body mass, and the mechanisms originally proposed to explain these relationships, i.e., metabolic scaling is constrained by surface-area (SA) or by resource-transport networks (RTN). Inset plot shows the ranges of interspecific and intraspecific variation in the scaling slopes (b) observed over the history of metabolic scaling research (b range from Glazier, 2022a).

Explaining the degree of variation in respiration rate with body size has become a central topic for ecologists, yet the mechanism(s) underlying the slope of this relationship remain enigmatic (Glazier, 2005, 2014, 2022a; Hatton et al., 2019). As a result, a variety of hypotheses and models have been developed based on four main mechanisms, i.e., (*i*) resource supply through exchange surfaces or (*ii*) through circulatory systems, (*iii*) changes in body composition, and (*iv*) resource demands of various metabolic processes (Glazier, 2014). The emphasis of these models has gradually shifted from (a) biophysical constraints on resource supply due to SA- or RTN-related limits, to (b) evolutionarily adaptive, context-dependent effects of various resource demanding processes that power fitness-related activities of organisms (Glazier, 2022a).

2.1. Context-dependent influences on resource supply

Instead of a single mechanism and a fixed metabolic scaling slope, the 'Metabolic-Level Boundaries Hypothesis' (MLBH; Glazier, 2005, 2010, 2014) offers a multi-mechanistic explanation to the variation in metabolic scaling slope (b). The MLBH proposes that factors related to body volume (V) and surface area (SA) set boundaries on b, with its value between these boundaries being influenced by various physiological, developmental and ecological factors. The relative influences of SA-related limits of resource supply and V-related resource demands on b is modulated by the metabolic level (L), i.e., the mass-specific elevation of the metabolic scaling relationship. According to the MLBH, the scaling of metabolic rate with body mass should increasingly approach limits set by the area of exchange surfaces (for resource supply or excretory losses), or by limits set by internal resource distribution systems, as resting metabolic rate increases (i.e. high L). Specifically, in isomorphic growing organisms, whose body shape is maintained throughout ontogeny, b should approach 2/3 (Rubner, 1883) due to a constraint of SA processes by external exchange surfaces, or 3/4 if limits by resource-transport networks are predominant (West et al., 1997; Brown et al., 2004). How gill SA varies with body mass, for example, has been hypothesised to be a crucial geometric constraint for many water-breathing animals associated with growth rate, adult body size, and lifestyle (Pauly, 2010; Gillooly et al., 2016; Bigman et al., 2018). In contrast, in organisms with low energy demands, resource supply is likely not influenced by SA-related processes; instead, energy use is only dictated by total tissue maintenance, which is proportional to body V (or mass) and so b should approach 1. This hypothesis has received support from a wide variety of taxa, as diverse as unicellular organisms (Glazier, 2009a, 2010), terrestrial and aquatic ectotherms (Glazier, 2009b; Killen et al., 2010; Glazier, 2020), and endotherms (Glazier, 2008, 2018a).

According to the MLBH, ecological factors that influence L, such as environmental temperature can therefore result in variation of b (Fig. 1.3A). As temperature increases, resting metabolic demands and so L increase, MLBH predicts that fluxes through exchange surfaces ($m^{2/3}$ in isomorphic growers) become more influential on resource supply and ultimately dictate the mass-scaling of metabolic rates. Intrinsic factors such as organismal activity, on the other hand, may also affect L and so the slope b (Glazier, 2005, 2008, 2010). Indeed, the MLBH predicts that increasing levels of activity and so energy demands of muscle work can increase the slope b from its value at rest (Fig. 1.3B). Hence, from resting to maximum L, metabolic

7

rates are expected to be gradually dictated by the demands of muscle mass, which is proportional to body V or mass (Weibel & Hoppeler, 2005; Glazier, 2009c).

More recently, Rubalcaba et al. (2020) developed a model based on MTE principles, in which oxygen supply explicitly constrains metabolic rates in fish following an increase in temperature and activity level. Their results indicated that temperature might reduce the aerobic scope of larger fish, as warming waters can disproportionally curtail their activity and physiological performance. Hence, this model predicts that metabolic scaling in fish decreases from the typical $b = 0.75$ proposed by the MTE as temperature and activity both increase, yet the resulting slope depends on how the capacity of individuals to supply oxygen is affected by size, which may vary among species according to their mass-scaling of ventilation rates or gill SA.
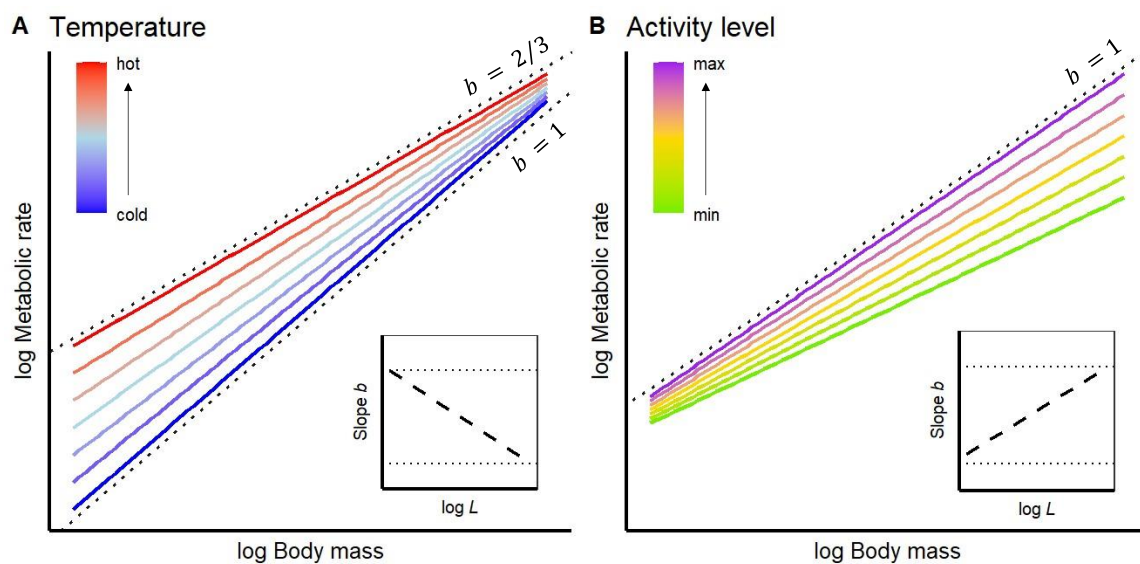
Figure 1.3. Schematic of the expected relationship between metabolic rates and body mass according to the 'Metabolic-Level Boundaries Hypothesis' (MLBH; Glazier, 2010). The metabolic scaling slope (b) varies with metabolic level (L, mass-specific metabolic rate at the geometric mass midpoint of the scaling regression) following the limits set by volume-related ($V \sim m^1$) and surface-area related ($SA \sim m^{2/3}$) processes, here indicated by dotted lines. (**A**) In cold temperatures (deep blue), the energetic demands of resting organisms are low and sufficiently met by SA-related processes, and hence body maintenance dictates metabolic rates ($b \approx 1$). As metabolic rates and so L increase with warming (blue to red), resource supply become more influenced by SA-related processes, which leads b to approach 2/3. (**B**) With raising activity levels (green to purple), metabolism becomes gradually dictated by the energy demands of muscular mass (proportional to body V), which leads b to approach 1 when L is

near its maximum during strenuous exercise. Note that the MLBH predicts a linear relationship between b and log-transformed L (inset plots).

2.2. Resource demand of various metabolic processes

Since all living forms are products of evolution, life-history theory predicts that organisms have evolved under selective pressures to maximise fitness by typically increasing energy gains relative to energy demands (Burger et al., 2021). Instead of biophysical constraints on resource supply mentioned above, this approach attempts to explain the variation in metabolic scaling through changes in energy allocation between biomass production and other metabolic activities (Glazier, 2005; Moses et al., 2008; Kooijman, 2010; White et al., 2022). Pütter (1920) and Bertalanffy (1938, 1957) first postulated that sigmoidal growth trajectories occur when the overall catabolic rate (i.e., non-growth metabolic processes) increases more rapidly with body size than the rate of assimilation (i.e. resource acquisition; Atkinson et al., 2022), which may describe different metabolic scaling patterns over ontogeny (reviewed in Glazier, 2005). The von Bertalanffy growth model (VBG) described the growth dm/dt of an organism with mass m in the form:

$$\frac{dm}{dt} = \alpha m^h - \beta m \qquad [2]$$

where αm^h typically describes the resources available for organismal growth whereas βm, comprises all non-growth metabolic processes. Note that the non-growth processes, often referred as 'maintenance metabolism', are assumed to increase isometrically with body mass. The VBG has proved useful to describe growth among a wide range of organisms, especially in fish (Froese & Pauly, 2010). In effect, when corrected by body mass, the increase in body mass over time exhibits generally similar sigmoidal trajectories among different taxa (Karkach, 2006; Hou et al., 2008). Exceptions to this generality are often seen in aquatic invertebrates with diverse growth trajectories, including exponential, yet these variety of growth types can be incorporated in growth models by changing the anabolic exponents (h) (Lee et al., 2020).

However, like the VBG (von Bertalanffy, 1957), most early models aiming to describe growth and metabolism in ectotherms (e.g., Paloheimo & Dickie, 1965; Ursin, 1967; Bayne et al., 1976), assumed erroneously that anabolism (biosynthesis) and catabolism (metabolism) were two independent processes using the same energy source (Makarieva et al., 2004). In contrast, Parry's model (Parry, 1983) noted that in ectotherms biosynthesis required an

important fraction of metabolism (17 – 29% of metabolic rate), and explicitly incorporated the overhead costs of growth, i.e., the heat production due to biosynthesis. Building upon MTE assumptions, this concept was further developed by the ontogenetic growth model (OGM; West et al., 1997, 2001; Gillooly et al., 2002), which divided total metabolic rate into body maintenance, growth, and activity (Moses et al., 2008; Hou et al., 2008), and linked growth rates to metabolic rates through the metabolic costs of growth. Although mathematically similar, the OGM differs from the VBG in their assumptions: (1) the metabolic costs of mass production are explicitly incorporated; (2) body maintenance is assumed to comprise catabolic as well as anabolic processes, such as protein turnover; and (3) the scaling term αm^h refers to the assimilation of metabolic energy with body mass, which is assumed to be $h = 0.75$, following the ¾-power metabolic scaling in the MTE (Barneche & Allen, 2018). Hence, although the OGM incorporates the costs of growth, it is still unable to capture the variation in metabolic scaling slopes.

While the metabolic costs of growth were largely overlooked during the early history of metabolic scaling, the Dynamic Energy Budget theory (DEB; Kooijman, 1986, 2000, 2010) incorporated growth costs to explain metabolic scaling, and proposed that different metabolic activities of organisms are subjected to various SA- and V-related influences. Specifically, DEB theory divides body mass into 'reserves' (e.g., lipid deposits) and 'structure' (e.g., muscular tissue). Structural mass dictates the costs of body maintenance, which is assumed to be proportional to body volume (V), or mass. The mobilisation of reserves, on the other hand, is assumed to scale with surface-area (SA) due to the influence of reserve exchange surfaces (van der Meer, 2006; Kooijman, 2010; Maino et al., 2014). Hence, according to DEB, the mass-scaling of metabolic rates during ontogeny results from the various SA-related and V-related processes, whereas the scaling slope b can vary between 1 and 2/3 depending on the relative contribution of these processes to overall metabolism. However, changes in body composition can also affect metabolic scaling. Since reserves are metabolically inert and hence require no maintenance (Kooijman, 2010), DEB predicts hypo-allometric scaling slopes ($b < 1$) when organisms grow with disproportionately increasing reserves, leading to a decrease in mass-specific demands as body mass increases. This is evidenced during embryo development, when eggs containing almost entirely reserves require low metabolic demands, whereas metabolic rates in growing embryos increase steeply with body mass (often $b > 1$) until hatching (Maino et al., 2017).

10

More recently, building on predictions of whole-body energy demands proposed by Glazier (2005), the 'growth-scaling hypothesis' (GSH; Tan et al., 2019) posited that the contribution of the overhead costs required to fuel growth to resting metabolic rates may help explain differences in metabolic scaling during ontogeny seen across species. According to the GSH, the cost of growth and its ontogenetic trajectory may thus influence metabolic scaling. Indeed, since overhead costs of growth contribute substantially to metabolic rate even at resting or routine states (Parry, 1983; Rosenfeld et al., 2015), a decrease in mass-specific growth demands over ontogeny would lead to shallower metabolic scaling (i.e., low *b*). These predictions seem to be borne out by comparisons between whole-body metabolic demands of cephalopod and fish species, on which Tan et al.'s (2019) study was based. Specifically, in animals whose mass-specific growth rates decline during ontogeny such as teleost fish, the GSH predicts that slopes *b* decrease as growth demands increase from slow- to rapid-growing organisms (Fig. 1.4). Conversely, when growth is exponential or more sustained over ontogeny as occurs in rapid-growing cephalopods, slopes *b* are expected to increase with increasing growth rates (Tan et al., 2019).
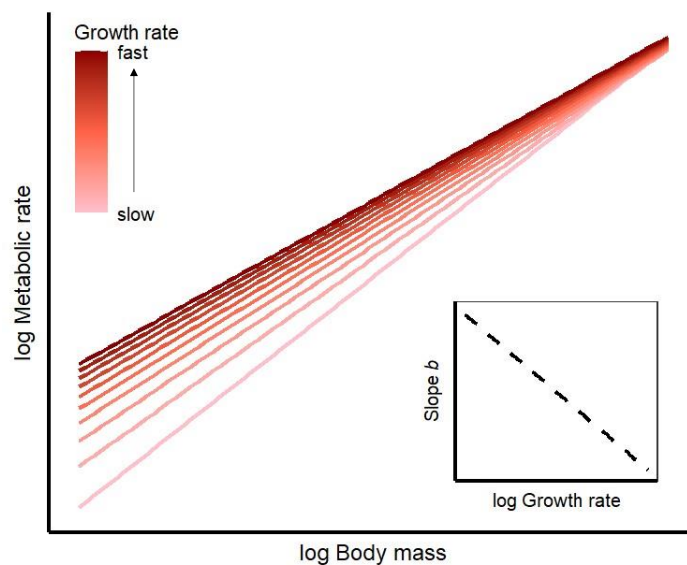
Figure 1.4. Schematic of the expected relationship between resting or routine metabolic scaling and growth rate according to the 'Growth Scaling Hypothesis' (GSH; Tan et al., 2019). In animals whose mass-specific growth rates decline over ontogeny, higher growth rate and so its contribution to metabolism will lead to shallower increases in metabolic rate with body mass. Hence, from slow- to fast-growing organisms, metabolic scaling slopes (*b*) will decrease as growth rates increase.

3. Variation in metabolic scaling within species

Besides the differences in mass-scaling of metabolic rate during ontogeny seen among major animal groups (e.g., Bokma, 2004; Hatton et al., 2019), and species (e.g., Glazier, 2009b; Killen et al., 2010; Tan et al., 2019), metabolic scaling may also change during ontogeny and differ between sexes (e.g., Post & Lee, 1996; Strauss & Reinhold, 2010; Sears et al., 2012; Moffett et al., 2022), whereas the mechanism(s) explaining this variation are still unclear (Wieser, 1984, Glazier, 2005, 2020; Glazier et al., 2015; Somjee et al., 2022). During the ontogeny of many kinds of animals, from copepods to humans, metabolic scaling often shifts from steep slopes b during early or postembryonic stages, to shallow slopes b in older, adult stages (Wieser, 1984; Glazier, 2005, 2014; Glazier et al., 2015). Various, complementary hypotheses have been proposed to explain such ontogenetic shifts in mass-scaling of metabolic rates (Fig. 1.5), which involve changes in resource supply and demands as well as in body composition. Indeed, these metabolic scaling shifts are most typically associated with changes in growth trajectories (Glazier, 2005), as growth and so its overhead costs require a substantial fraction of total metabolic energy (Parry, 1983; Wieser, 1994; Clarke, 2017). While high, often exponential growth rates in early ontogenetic stages are thought to entail steep increases in metabolic rate with body mass (e.g., Kamler, 1992; Post & Lee, 1996; Sears et al., 2012), lower, declining mass-specific growth rates as organisms enlarge in older stages should require much shallower increases of metabolic rate with size (Riisgård, 1998; Glazier, 2005, 2022b).

Alternatively, the cellular mode of growth has been proposed as a mechanism underpinning changes in resource-supply capacity of organisms as they grow, and hence changes in metabolic scaling (Kozłowski et al., 2003; Glazier, 2022b). This hypothesis is grounded in the relative contribution of cell multiplication and cell expansion to organismal growth. Effectively, during early life stages (i.e., embryos or larval phases) of most organisms, growth is dominated by cell multiplication, usually accompanied by cell size reduction (e.g., Wesley et al., 2020), which maintains high total cell surface-area (SA) relative to body volume (V), as well as small intracellular transport distances as the body size increases. Consequently, this sustained (or increased) resource-supply capacity can support steep increases in metabolic rate with body mass ($b \geq 1$; e.g., Alami-Durante et al., 1997; Arendt, 2000; Gaitán-Espitia et al., 2013). Conversely, growth is generally dominated by cell expansion during later life stages (i.e., old juveniles and adults; Goss, 1966; e.g., Higgins & Thorpe, 1990), which decreases total cell SA/V and increases intracellular transport distances. This reduction in resource-supply

capacity of large, old individuals leads to shallower metabolic scaling with mass ($b < 1$). Concomitantly, the accumulation of higher proportions of reserves (e.g., lipid deposits), and other metabolically inert materials (e.g., cuticle) in larger individuals is also thought to reduce energetic requirements relative to body mass, and hence contribute to lowering the slope b in late life stages (Kooijman, 2010; Glazier, 2022b).
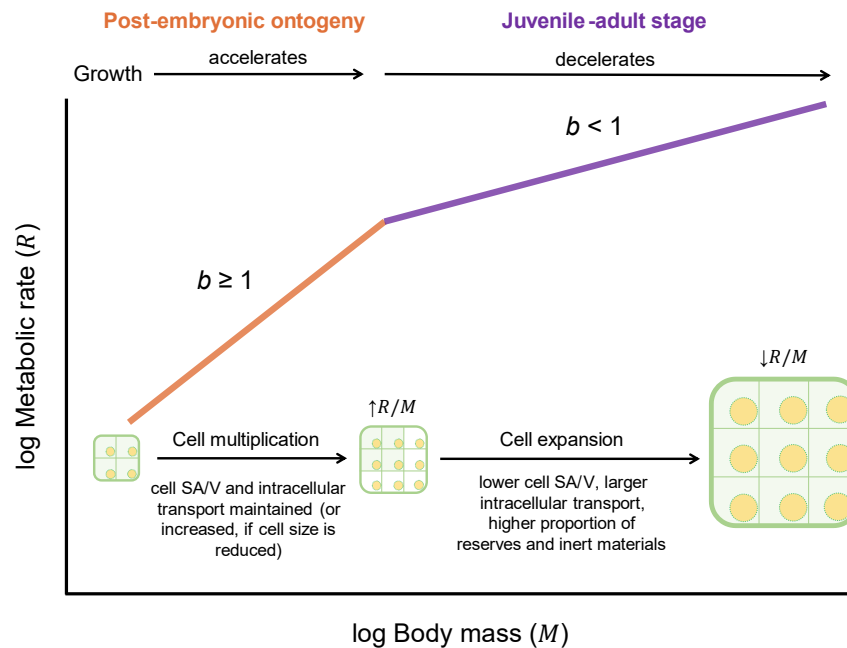
Figure 1.5. Schematic of the ontogenetic variation in metabolic rates with body mass. Steep metabolic scaling typically occurs during postembryonic ontogeny ($b \geq 1$; red line), and it is associated with exponential growth in postnatal and young juveniles. Shallower metabolic scaling, by contrast, occurs generally later in ontogeny ($b < 1$; purple line), as mass-specific growth rates decline with body size in juveniles and adults. The cellular mode of growth and associated changes in body composition may also underpin these ontogenetic shifts (Kozłowski et al., 2003; Glazier, 2022b). Early growth occurs primarily by cell multiplication, maintaining or often reducing cell size, which keeps total cell surface-area (SA) relative to body volume (V), as well as similar intracellular transport and composition. This allows high mass-specific resource-supply rates as body size enlarges (higher R/M), and hence high b. Conversely, growth later in ontogeny involves greater cell differentiation and expansion, which leads to lower SA/V and larger intra-cellular transports. Moreover, cells accumulate greater proportions of metabolically inter materials (e.g., cuticle or lipid reserves; here indicated by thicker border and yellow circles). Consequently, mass-specific supply rates as well as energetic demands decrease with body size in older, larger individuals (lower R/M).

While studies of intraspecific metabolic scaling typically focus on ontogenetic scaling (i.e., variation in metabolic rates during organismal growth), sexual differences among adult

individuals have received much less attention (Somjee et al., 2022). Indeed, while females and males often show stark differences in traits such as body mass, morphology, or behaviour (see Cornwallis & Uller, 2010, for a review), differences in metabolic demands with size are less explored. Despite females bearing the costs of offspring production, sexes can experience different selective pressures and converge on similar energetic demands through various mechanisms (Parker et al., 2018), which may scale differently with body mass (Somjee et al., 2022). Hence, reproductive investment may reflect differences in energy allocation between sexes (Stearns, 1989; Somjee et al., 2022; Moffett et al., 2022). Metabolic demands in females are elevated by producing energy-costly gametes, maintaining ovarian tissues, and developing offspring that involves egg production, gestation, and sometimes carrying offspring during pregnancy (Hayward & Gillooly, 2011; Angilletta & Sears, 2000; Finkler et al., 2014; Ducret et al., 2020). Males, on the other hand, often bear higher metabolic demands of maintaining sexually selected traits used to compete with rivals or attract females (Somjee et al., 2018; Somjee, 2021), higher levels of activity during mating (e.g., chasing or acoustic calling), and consequently higher proportions of muscle mass to support those activities. Such differences in biomass production, body composition, and activity levels can ultimately shape different patterns in metabolic scaling between females and males according to current theory (Glazier, 2005, 2009c; Kooijman, 2010).

4. Integrating approaches to explain metabolic scaling across and within taxa

As literature grows, it becomes more evident that a single, 'universal' mechanism cannot explain the wide and systematic variation in metabolic scaling observed both across (e.g., DeLong et al., 2010) and within taxa (e.g., Bokma, 2004). Consequently, recent models have offered new mechanisms to explain systematic deviations from the proposed SA- and RTN-constraints (e.g., Banavar et al., 2010; Hirst et al., 2014; Glazier et al., 2015). Given this ongoing change in perspective, Glazier (2014, 2018a, 2022a) claims for a comprehensive theory following a multi-mechanistic, context-dependent approach, where various mechanisms can simultaneously influence the relationship between metabolic rates and body mass, responding to both intrinsic and extrinsic factors. While developing such a holistic model falls outside the scope of my thesis, here I do combine multiple theoretical approaches to formulate new hypotheses involving various, synergetic mechanisms to explain metabolic scaling.

5. Thesis outline

In this thesis, I explore the variation in the mass-scaling of metabolic rates at different levels of biological organisation in a diverse array of ectothermic animals. Firstly, I investigate how metabolic ontogenetic scaling changes in ectothermic vertebrates with increasing environmental temperatures and levels of locomotory activity, emphasising the differences between air- (reptiles and amphibians) and water-breathing (teleost fish and elasmobranchs) animals. Then, I focus on teleost fishes, exploring the relationship between ontogenetic metabolic scaling and maximum growth rates across species, as well as analysing the effects of various ecological traits on the energetic demands of growth and self-maintenance. Finally, I use a model crustacean to investigate the link between metabolism and biomass production, and how this relationship aligns with ontogenetic shifts and sexual differences in metabolic scaling in this species.

Chapter 2 analyses the intraspecific variation in metabolic scaling among air- and water-breathing ectothermic vertebrates. Using a meta-analytic approach, I quantify the change in metabolic scaling slopes as metabolic rates increase with temperature (523 scaling regressions from 111 species) and activity level (281 regressions from 47 species). I found that scaling slopes decline with warming only in water-breathers (fish), whereas slopes steepen with increasing activity only in air-breathers (herptiles). I here combine various, complementary hypotheses to improve the predictions of metabolic scaling in ectothermic animals, proposing adaptive mechanisms to protect aerobic scope in water-breathers.

Chapter 3 investigates the interspecific variation in metabolic scaling in relation to maximum growth rates across 118 species of teleost fish, and uses a theoretical model to quantify the energetic costs of growth and maintenance in 114 of these species. I demonstrate that metabolic scaling slopes covary negatively with maximum growth rates across species. Moreover, I show that the relative contribution of growth demands to resting metabolism remain similar with temperature in these species, whereas maintenance demands in pelagic fishes are relatively higher than in less active lifestyles. I further show that growth efficiency is largely independent of species ecology and phylogenetic relationships. Finally, I highlight the importance of accounting for metabolic scaling variation to understand energy allocation strategies between species.

Chapter 4 investigates experimentally ontogenetic shifts and sexual differences in metabolic scaling, as well as the associated costs of biomass production in a model crustacean, *Artemia franciscana*. I demonstrate that the rates of metabolism and growth change simultaneously during ontogeny, and show that metabolic scaling becomes similar between males and females in reproductive animals. I further show that such variation in metabolic scaling slopes can be explained by differences in the cost of biomass production between ontogenetic phases (larvae *versus* post-larval individuals) and reproductive modes (ovi- *vs*. ovoviviparous). Here, I discuss the potential role of the cellular mode of growth seen in this species to explain differences in production costs and metabolic scaling.

Chapter 5 discusses the main findings of this thesis and explores new hypotheses and research avenues that emerged from this investigation. Overall, my findings contrast with a general metabolic scaling across or within species, showing that the relationship between metabolic rate and body mass can be influenced by extrinsic (temperature) as well as intrinsic factors (biomass production, activity). To explain such variation in metabolic scaling, this thesis uses different, complementary perspectives based on evolutionary adaptations, plastic responses, and various energy demanding activities of organismal metabolism.

Chapter 2: Combining theoretical approaches to understanding the intraspecific variation in metabolic scaling: responses to temperature and activity differ between water- and air-breathing ectothermic vertebrates

A Diamond lizardfish (*Synodus synodus*) resting on the seafloor

Combining theoretical approaches to understanding the intraspecific variation in metabolic scaling: responses to temperature and activity differ between water- and air-breathing ectothermic vertebrates

Abstract

Metabolism underpins all life-sustaining processes, and quantifying and explaining the variation in metabolic rate with organismal body size is crucial in ecology. The relationship between metabolic rates (R) and body mass (m), usually termed metabolic scaling, can be affected by environmental temperature and locomotory activity. Warming and increasing activity not only elevate metabolic level (L) of organisms, but often lead to changes in the body mass-scaling exponent (or slope b, in log R vs. log m). Such variation in slopes b has been explained through the change in L, depending on whether this change is mainly dictated by volume (V)- or surface-area (SA)-related processes. Another hypothesis proposes that water-breathers have evolved to restrict metabolic costs in large individuals experiencing warming, thus avoiding oxygen shortage. Here, I test these predictions using intraspecific metabolic scaling responses to temperature (523 regressions) and activity (281 regressions) in a range of ectothermic vertebrates, including teleost fish, elasmobranchs, reptiles, and amphibians. Through a meta-analysis, I quantitatively compare the change in b when L is increased by either temperature or locomotor activity within these species. I show that b decreases with temperature-increased L only in water-breathers, supporting a SA-related avoidance of oxygen shortage, whereas b increases with activity-increased L only in air-breathers, following influences from V-related muscular demands. Overall, this new quantitative theoretical approach extends explanatory power to incorporate different influences (warming, locomotion) and respiration modes (aquatic or aerial) to predict changes in energy use with body size.

Keywords: Ecophysiology; Oxygen Limitation; Animal Locomotion; Bioenergetics; Body mass; Metabolic Theory; Metabolic-Level Boundaries Hypothesis; Allometry

1. Introduction

Metabolism is a fundamental property of life, comprising all biochemical processes that transform energy and materials from the environment into life-sustaining functions and body structures (Humphries & McCann, 2014). Metabolic rate (indirectly estimated by respiration rate R in aerobic organisms) is strongly linked to body size (m), through a relationship

commonly expressed as a power function, $R = am^b$ (Kleiber, 1932; Bertalanffy, 1957), where *a* is the scaling coefficient, and *b* is the scaling exponent, or allometric slope of a linear regression between log *R* and log *M*. The slope *b* describes the change in log respiration rate as log body mass increases. Understanding and quantifying the influence of body size on respiration rate has become a central topic in ecology, where the emphasis is placed on combinations of both physical principles and organismal adaptations (Brown et al., 2004; Kooijman, 2010; Glazier, 2005, 2022a; White et al., 2022). The classic description of *b* as having a value of 0.75 across all life forms (Hemmingsen, 1960; West et al., 1999; Savage et al., 2004) is challenged by systematic variation in its value across taxa, lifestyles, ontogeny, as well as with environmental conditions and physiological states (White et al., 2007; DeLong et al., 2010; Hirst et al., 2014; Tan et al., 2019; Glazier, 2010, 2014, 2020, 2022a).

The 'Metabolic-Level Boundaries Hypothesis' (MLBH; Glazier, 2005, 2010, 2014) offers a mechanistic explanation for the variation in metabolic scaling. This hypothesis proposes that variation in the allometric slope *b* is influenced by factors related to body volume (V), such as tissue maintenance and locomotive power, and factors related to surface area (SA), such as resource uptake or waste elimination. The relative contribution of volume or surface area-related factors alter as the metabolic level changes. Metabolic level (*L*) increases with overall energy use, and is often quantified as the mass-specific metabolic rate at the geometric mid-point of the mass range covered by the metabolic scaling relationship (Glazier, 2010). According to the MLBH, for organisms that conserve body shape as they grow, *b* should approach 2/3 (Rubner, 1883) if SA-related processes through external exchange surfaces predominate, but should approach 1 if V-related processes predominate (proportional to body mass or volume). According to the MLBH, the amount of locomotor activity and increased environmental temperature, which both increase *L*, can change the slope *b* (Glazier, 2010) by changing the relative contributions of SA *versus* V-related processes.

The MLBH predicts that increased active movement and associated energy demands of locomotor musculature, whose mass is typically proportional to whole body mass (Glazier, 2005, 2008, 2010), will increase the metabolic scaling slope relative to that at rest. During bursts of strenuous activity (maximal *L*), metabolic rate should be mainly driven by resource demand (m^1; Fig. 2.1), rather than by surface-dependent resource supply or waste removal (see Weibel & Hoppeler, 2005). This extreme response is only possible because of short-term

storage of oxygen and energy in muscles and their temporary tolerance to accumulation of wastes, such as lactic acid (Glazier, 2009c).

Temperature appears to affect metabolic scaling in more complex ways. Contrary to influential models that assume that temperature affects only metabolic level and not b (e.g., Gillooly et al., 2001), the MLBH predicts changes in b. As temperature increases, resting metabolic demands increase; consequently, the mass-scaling of metabolic rate may decrease if it is increasingly dictated by fluxes through external exchange surfaces ($m^{2/3}$ in isomorphic growers), as limits on resource supply become more influential (Fig. 2.1). Glazier (2020) observed such a predicted negative relationship between temperature and b in 10 of 13 species of sedentary ectothermic animals and one plant. However, warming not only increases maintenance demands in ectotherms, but accelerates other energy-demanding processes such as growth, even in resting individuals (Parry, 1983; Rosenfeld et al., 2015). Importantly, although whole-body growth has been described as a V-related process (Glazier, 2010, 2014, 2020), its contribution to metabolic scaling will depend on whether mass-specific growth rate remains constant as the organism gets bigger. Exponential growers continue to add new growth in direct proportion to body mass (i.e., $\propto m^1$), which some species achieve by changing shape, thereby maintaining a high ratio of SA for resource uptake relative to body mass, as in various pelagic invertebrates (Hirst et al., 2014). But more generally, mass-specific growth rates decline during ontogeny, as is generally observed in vertebrates and several benthic invertebrates (von Bertalanffy, 1951, 1957; Lee et al., 2020). Therefore, increasing growth rate, and its attendant costs, in most animals is expected to contribute to lowering b below 1. Another effect of temperature on metabolic scaling depends on how it affects locomotor activity. Glazier (2020) found that in contrast to 71% of 14 sedentary species that showed a negative relationship between b and temperature, significantly fewer (18% of 165) mobile species showed a negative relationship, which supports the idea that warming-enhanced locomotion, which includes contribution of muscular output (and is considered approximately proportional to body mass) mostly countered SA-influenced reduction in b. Clearly, therefore, the mass-scaling of metabolic rate predicted by the MLBH depends on the relative influence of different processes that scale differently with body mass (e.g., SA- *versus* V-related processes). A major challenge for predictive ecology is to identify situations when particular influences on metabolic scaling predominate.
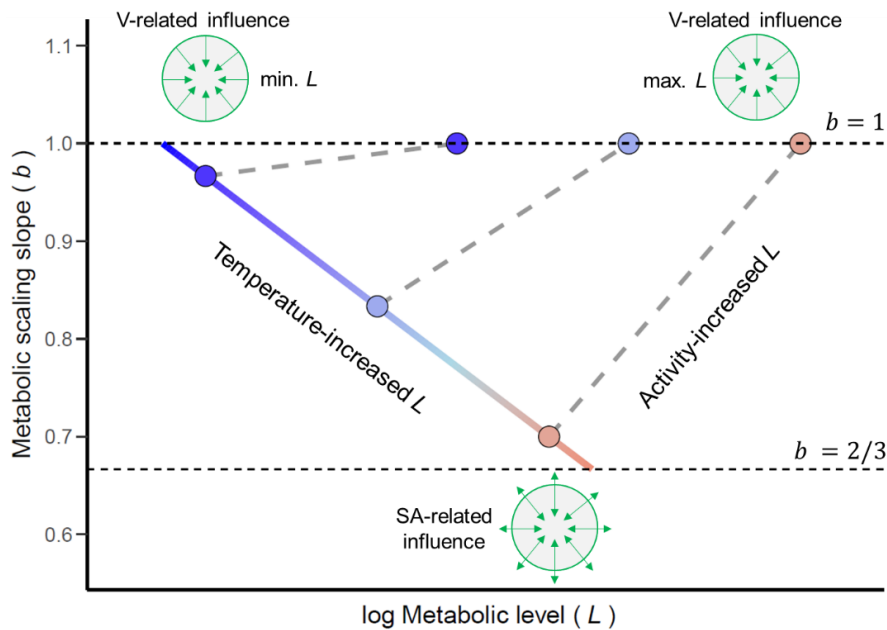
Figure 2.1. Graphical model of the expected relationship between the metabolic scaling slope (*b*) and the metabolic level (*L*, the mass-specific metabolic rate at the geometric mass midpoint of the scaling regression), according to the 'Metabolic-Level Boundaries Hypothesis' (Glazier, 2010). Over the range of metabolic states, *b* varies with *L* following a convex relation viewed from below within the limits set by volume-related (V ~ m^1) and surface-area related (SA ~ $m^{2/3}$) resource demand, denoted here by dashed horizontal lines. In cold temperatures (deep blue), the energy demand of resting organisms is low and sufficiently met by SA-related processes (minimal *L*), so body maintenance dictates metabolic rate (*b* ≈ 1). As temperature rises (from blue to red), resting metabolic rates relatively increase and so *L*, becoming more influenced by fluxes through exchange surfaces, which causes *b* to approach 2/3. Activity, conversely, leads *b* to increase and ultimately approach 1 during strenuous exercise (maximal *L*), since metabolism is driven temporarily by demands of muscular mass, proportional to body mass (m^1) when growth is isomorphic. Note that *L* increases here exponentially (or linearly if log-transformed) with temperature and activity. The shape of the relationship between *b* and log *L* will depend on the predominant influence of each contributing process under specific temperatures and activity levels.

I propose that combining a second theoretical approach with the MLBH may help to identify when particular processes with particular mass-dependences (e.g., SA-related *versus* V-related) predominate. Specifically, the effects of temperature and activity on metabolic scaling may differ between aquatic and terrestrial organisms due to different physical properties of the environments they inhabit. Water is 800-fold denser, 60-fold more viscous

and contains 43-fold less oxygen than air, making breathing in water more energy-costly than breathing in air (Dejours, 1981; Makarieva et al., 2008; Gillooly et al., 2016). Moreover, the ability of water-breathers to increase their oxygen bioavailability tends to be less sensitive to warming (Einum et al., 2021; Deutsch et al., 2022) than does oxygen demand (metabolic rate), which typically doubles with 10 °C of warming in both water- and air-breathers (Seebacher et al., 2015). For water-breathers, warmer temperatures and larger sizes are expected to combine to place a greater challenge on supplying sufficient oxygen, as the ratio of surface area for respiratory exchange relative to body mass is reduced (Atkinson & Sibly, 1997; Rubalcaba et al., 2020). Aquatic ectotherms whose ancestors have experienced oxygen limitation at large sizes in the warm (the 'Ghost of Oxygen Limitation Past'; Verberk et al., 2021; Atkinson et al., 2022) are predicted to have evolved adaptations that enable them to avoid oxygen shortage as size and temperature both increase. Such avoidance strategies could include reduction in growth and metabolic rate as size and temperature both increase, and hence reduce *b*.

Here, I combine these two theoretical approaches to quantitatively investigate impacts of temperature and activity on intraspecific metabolic scaling in ectothermic vertebrates. Ectothermic vertebrates are ideal to test the MLBH predictions quantitatively because they comprise various lineages in which changes in metabolic scaling have been observed, thereby alleviating some of the confounding effects of phylogeny. Furthermore, since all species belong to a monophyletic clade (Subphylum Vertebrata), the comparison is more restricted to a set of common biological traits that if a more phylogenetically diverse range of species were examined (e.g., Ehnes et al., 2011): (*i*) near-isomorphic and indeterminate (continuous post-maturational) growth in most species, with body masses spanning over 10 orders of magnitude; (*ii*) closed circulatory systems and specialised respiratory organs, such as lungs or gills, facilitating the comparison between water- and air-breathing species (Shelton et al., 1986); and (*iii*) physiological performance and body temperature intrinsically linked to ambient temperature (Angilletta et al., 2002), making it easier to control for temperature when examining the effect of activity alone. Ectothermic vertebrates inhabit a wide range of environments and temperatures, from deep-sea to desert habitats, and from below 0°C to above 40°C. By studying vertebrates rather than the phylogenetically diverse invertebrates with varied respiratory and circulatory systems, I avoid complications arising from profound and variable body-shape changes over ontogeny that affect surface area for respiratory exchange,

hence metabolic scaling, observed in diverse aquatic zooplankton and cephalopods (Hirst et al., 2014).

A key feature of this investigation is to quantify how the relative importance of two influences on energy use – temperature and locomotor activity – on the metabolic scaling slope b, depend on whether animals are air-breathers or water-breathers. I first hypothesise that b decreases more steeply with warming in water-breathers, which are influenced by (SA-related) avoidance of oxygen shortage. Secondly, I expect that b increases more steeply with activity level in air-breathers due to increasing metabolic contributions from (V-related) musculature, whereas the muscular contribution in water-breathers may be countered by pressures to reduce oxygen consumption. Through a meta-analysis that compares water- and air-breathing vertebrates, I test whether, and the degree to which, b changes as metabolic level (L) increases within species: (1) with warming of inactive individuals and (2) with increasing activity. I, therefore, comprehensively quantify for the first time the intraspecific change in b with L. As predicted, my findings show that b decreases with temperature-increased L only within water-breathers, whereas b increases consistently with activity-increased L only within air-breathers. My conceptual advance contrasts relative influences of SA- and V-related processes between different modes of respiration (water-, air-breathers), and under different influences on metabolic level (temperature, activity). My findings highlight the value of integrating more than one theoretical approach to increase the predictive potential of ecological theory.

2. Materials and Methods

2.1 Data collection

To test the relationship between the slope (b) and metabolic level (L) with increasing temperature, I searched the literature for studies that measured metabolic scaling during ontogeny in at least two temperature treatments of the same species, complementing the intraspecific datasets of Glazier (2005, 2020). Searches were carried out with Google Scholar, Web of Science and OATD (Open Access Theses and Dissertations), using the names of the target taxa (i.e., 'fish', 'amphibian' or 'reptile') followed by terms such as '<name of taxon> + metabolism', '+ metabolic + rate', '+ respiration + rate', '+ oxygen + consumption', all including 'temperature'. Finally, I checked the reference lists and citations of all relevant papers (i.e., those including the search terms in the title) for related studies. Here, I only included estimated parameters from scaling regressions in non-active and unstressed animals

(i.e., showing no or minimal locomotion), to minimise the effects of muscular activity on metabolic scaling (Glazier, 2020). Sets of regressions from studies were grouped by experimental conditions (e.g., metabolic states, such as resting or routine metabolism, if different states were measured) in the same species.

Second, to test the relationship between b and L with increasing locomotor activity, I searched the literature for studies that measured ontogenetic metabolic scaling in at least two activity levels in the same species at the same temperature, complementing the dataset of Glazier (2009c). The literature search was identical to that above but replacing 'temperature' with 'activity'. Again, I grouped regressions according to experimental conditions, into single studies, and the same species. Active metabolic rates here were usually measured during continuously sustained activity, including freely moving animals (e.g., Wood et al., 1978; Du Preez et al., 1988), measurements of active (e.g., Brett & Glass, 1973) and maximum metabolic rate through experimentally forced exercise at peak locomotory performance (e.g., Rao, 1968; Garland, 1984), as well as activity sustained to near or complete exhaustion (e.g., Brett, 1965; Walton, 1988), or immediately after (e.g., Killen et al., 2007).

Species were grouped into their principal respiration modes (water- vs. air-breathers). For air-breathing fish, I preferred regressions based on bimodal respiration (i.e., aquatic + aerial) when available, as this is their normal behaviour in nature (Graham & Wegner, 2010). I excluded regressions measured in fish larvae only, given that this life stage exhibits different metabolic influences from those on non-larval stages (Glazier, 2005), related to exponential growth and high surface-area of respiratory organs (Post & Lee, 1996). All regressions of amphibian species were based on aerial respiration. I disregarded non-statistically significant regressions ($p \geq 0.05$, which excluded only 6). When equation parameters or body mass ranges were missing in a study, data were extracted from figures using WebPlotDigitizer v4.4 (Rohatgi, 2020), performing regressions, if needed, through ordinary least squares models of log-log data. Metabolic levels were calculated as the mass-specific metabolic rate at the geometric mass-midpoint of the mass range of each regression, and converted to mg O_2 g wet mass^{-1} h^{-1}. No weighting method was applied here because many studies lacked uncertainty information of estimated slopes b.

2.2 Data analyses

I assessed data comparability by checking for systematic differences between datasets (Appendix 2.1 – 2.2). Specifically, I checked whether scaling regressions covered similar body mass ranges in water- and air-breathing species, and whether experiments measured comparable increases in metabolic level by either temperature or activity, as differences in these factors might influence the change in slope *b* (Glazier, 2020). I also checked that acclimation duration showed no obvious influence on *b*. Moreover, to minimise the variation in metabolic level due to variation in mass between regressions within experiments, I excluded regressions whose mass-midpoints were too dissimilar (i.e., differing by > 0.5 orders of magnitude) to the rest of the set (Appendix 2.3).

I determined whether temperature and activity underpin the intraspecific variation in slopes *b* of ectothermic vertebrates through their effects on metabolic level (*L*), and whether these effects differ between air- and water-breathers, using Bayesian phylogenetic multilevel models. I used linear models with *b* as the response variable and $\log_{10} L$ as an explanatory variable because: (*i*) the MLBH predicts a linear relationship between *b* and log-transformed *L* (Glazier, 2010) when only one of temperature or activity is varied (Fig. 2.1); (*ii*) the change in *b* is expected to be mediated through the change in *L*, but not the opposite; and (*iii*) these models allow the estimation of variance in *b* within species and experiments (Bürkner, 2018). Moreover, using $\log_{10} L$ as an explanatory variable enable me to examine the increase in metabolism with warming or activity in a continuous manner, and hence quantify and compare the effects of these influences on *b*.

To determine the effect of temperature-increased *L* on *b,* and whether this effect differs between water and air-breathers, I fitted a regression model with a global intercept (β_0), and the fixed effects of $\log_{10} L$ (β_L), animal group according to respiration mode (air- or water-breather, β_g) and the interaction between $\log_{10} L$ and group (β_{Lg}), as described in the Appendix (2.4). I used a Student's *t* distribution to describe errors in *b*, since this distribution is robust against outliers (Gelman & Hill 2006). I included two random effects: species relatedness with a variance-covariance matrix estimated from a phylogenetic tree (with species-specific intercepts ψ_k) and an experiment effect (with experiment-specific intercepts ϕ_{0j} and slopes ϕ_{Lj}). I included the phylogenetic relationship among species as a random effect because evolutionary history may influence differences in physiological traits (Verberk et al., 2022). I

searched species names in the Open Tree of Life (OTL, https://tree.opentreeoflife.org) and built phylogenetic trees through package 'rotl' (Michonneau et al., 2016). Polytomies (> 2 species sharing a direct ancestor) were resolved using the function *multi2di* in package 'ape' (Paradis & Schliep, 2019), which transforms polytomies into a series of random dichotomies with one of several branches of length close to 0 (Appendix 2.5). Variance-covariance matrices on these trees were calculated following Grafen's method (Grafen, 1989) using the 'ape' package. By allowing experiment-specific slopes, I accounted for variation in the strength of the relationship between b and $\log_{10} L$ (Harrison et al., 2017), which is expected under varying experimental conditions (Glazier, 2020). To analyse the effect of activity-increased L on b, I fitted a similar model but also including the effect of experimental temperature (in °C, β_T), since temperature and activity exert opposite effects on b according to MLBH predictions (Fig. 2.1).

I used a mix of weakly informative and informative priors. I applied an empirical estimate of the effect of $\log_{10} L$ between species (Killen et al., 2010) and MLBH predictions of the intercept (Glazier, 2010), as means of the normal prior distributions for β_L, and β_0, respectively. I fitted models using the package 'brms' (Bürkner, 2017, 2018) in R v. 4.2.0 (R Core Team, 2022), with the NUTS algorithm and four chains of 3000 warm-up and 16000 sampling iterations (Hoffman & Gelman, 2014). Convergence was checked through potential scale reduction factors ($\hat{R}$, Gelman et al., 2003). Residuals and trace plots were inspected using packages 'ggmcmc' (Fernandez-i-Marin, 2016), 'bayesplot' (Gabry et al., 2019), and 'tidybayes' (Kay, 2022). I checked that I could recover known parameters by simulating 10 data sets under the temperature-effect model, with posterior mean parameter values and the same structure as the real data, and fitting the model to these simulated data sets (Appendix 2.4).

2.3 Extending the MLBH: quantifying effects of increased L on b

The MLBH does not quantitatively predict influences of activity on the metabolic scaling slope b except at the boundaries. To quantitatively extend the MLBH, I calculated active metabolism by adding a term $a'm$ to the inactive metabolic rate, as $R + a'm$. By increasing a' values, this formula recreates how muscular work elevates metabolic rate, assuming that this component of metabolism is proportional to body mass. I then estimated activity-increased L and b through linear regressions of $\log (R + a'm)$ *vs.* $\log m$, using a standard body mass range

for ectothermic vertebrates (0.1 g to 1 kg). Observed changes in b with activity-increased L were then compared with those predicted from this quantification of the MLBH.

3. Results

I collected 523 metabolic scaling regressions for 68 water-breathing species (65 teleost fish and 3 elasmobranchs) at temperatures between -1.8 °C and 37 °C, and 43 air-breathing species (4 amphibians and 39 reptiles) at temperatures between 4 °C and 45 °C (Table S2.1). These experiments covered, on average, similar increases of metabolic level (L) in inactive water- and air-breathers (0.12 $vs.$ 0.19 mg O_2 g^{-1} h^{-1}, respectively). Moreover, I compiled 281 scaling regressions at different activity levels, from inactive to maximal metabolic rates, for 37 aquatic species (35 teleost fish and 2 elasmobranchs), and 10 terrestrial species (4 amphibians and 6 reptiles) (Table S2.2). The latter experiments comprised, on average, smaller increases in L due to locomotor activity in water- than in air-breathing species (0.24 $vs.$ 0.90 mg O_2 g^{-1} h^{-1}, respectively). This is partially because only a third of experiments measured minimal and maximal L in water-breathers, whereas all but one experiments included both measures in air-breathers. Additionally, the difference in activity-increased L may be due to water-breathing species exhibiting lower mean aerobic scopes (i.e., the difference between max. and min. L) than air-breathing species (0.34 $vs.$ 1.35 mg O_2 g^{-1} h^{-1}). Last, mass-midpoints of regressions varied over 4 orders of magnitude across species in the datasets, whereas mass ranges covered by the regressions were similar between water- and air-breathers, spanning on average over one order of magnitude.

Our models showed that the slopes b values were not different between water- and air-breathing species, as 95% equal-tailed credible intervals (CI) of the effect of groups overlapped 0 (Table 2.1), under both warming ($\beta_g = -0.03$, CI: (−0.20, 0.16)) and increasing activity ($\beta_g = -0.11$, CI: (−0.44, 0.23)). However, the effect of increasing $\log_{10} L$ by warming and by increasing activity on b did vary between water- and air-breathers (Table 2.1). Under warming conditions (Fig. 2.2A, B), water-breathers showed strong evidence of a negative relationship between b and $\log_{10} L$ ($\beta_L + \beta_{Lg} = -0.09$, CI: (−0.13, −0.05)), yet this coefficient was strongly centred on zero in air-breathers ($\beta_L = -0.002$, CI: (−0.04, 0.04)), which showed a species' mean $b = 0.74$ (±0.14 standard deviation). Conversely, under increasing activity (Fig. 2.2C, D), b showed a positive relationship with $\log_{10} L$ in air-breathers ($\beta_L = 0.19$; CI: (0.09, 0.30)), but

no consistent increase in *b* was found in water-breathers ($\beta_L + \beta_{Lg} = 0.04$; CI: (−0.02, 0.10)). Furthermore, the mean estimate of global intercept (i.e., predicted *b* at *L* of 1 mg O_2 g^{-1} h^{-1}) fell between 2/3 and ¾ in the model for temperature-increased *L* ($\beta_0 = 0.73$; CI: (0.58, 0.87)), whereas this estimate was close to 1 in the model for activity-increased *L* ($\beta_0 = 0.98$; CI: (0.68, 1.27)).
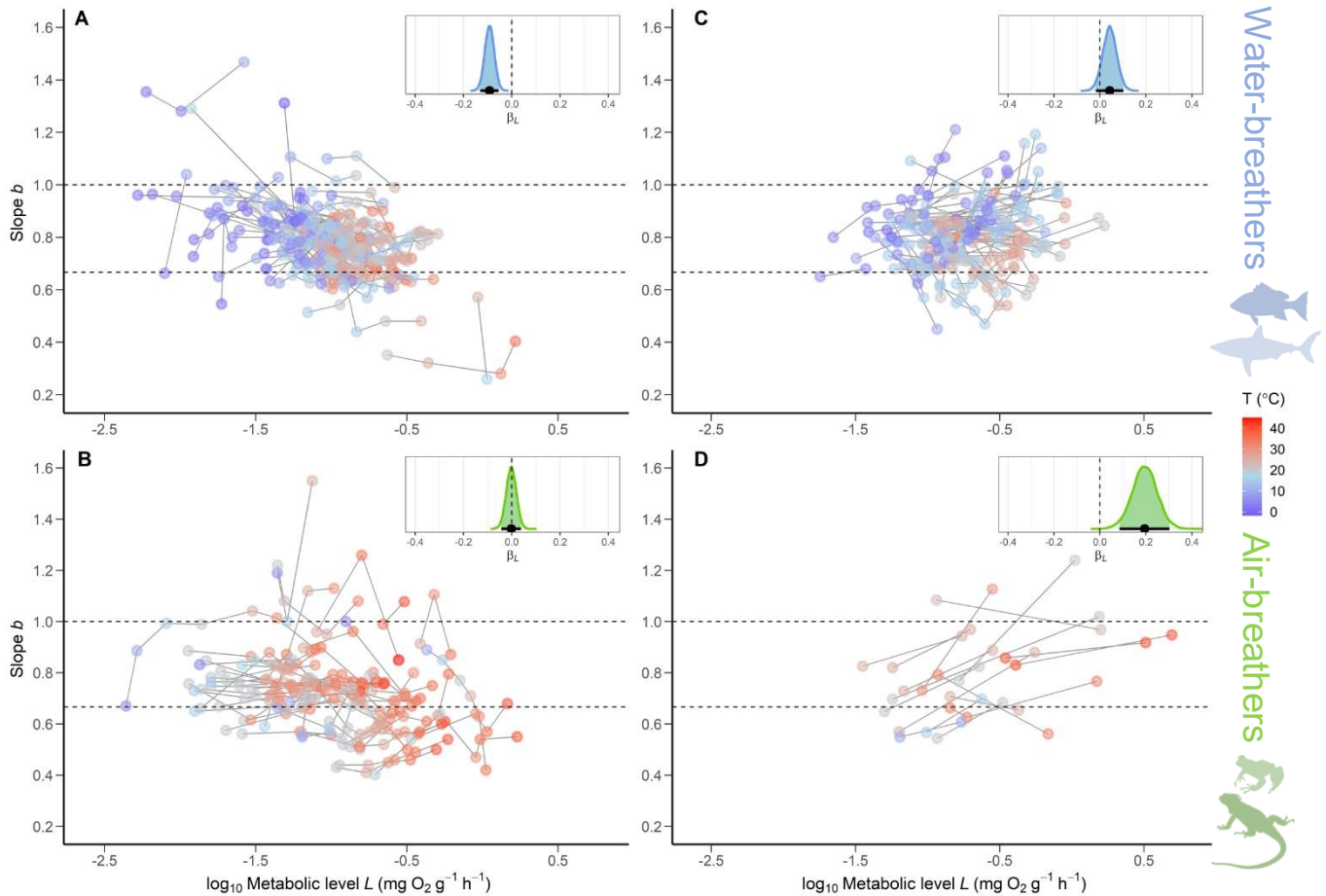
Figure 2.2. The relationship between the metabolic scaling slope *b* and $\log_{10}$ metabolic level *L* within species of ectothermic vertebrates. Left panels show measurements in inactive animals of water- (**A**) and air-breathing (**B**) species, where lines join measurements made at different temperatures of single experiments in the same species. Right panels show values for animals under different activity levels of water- (**C**) and air-breathing (**D**) species, where lines join measurements made at a single temperature and species (temperature of treatments is indicated by colour). Inset plots show posterior kernel density estimates of the effect of $\log_{10} L$ on *b* (β_L) for each group (water- or air-breathers), with means (dots) and 95% credible intervals (horizontal bars and shaded areas) from Bayesian models (see Table 2.1). Experimental temperature (T) is shown by a colour scale, and dashed horizontal lines indicate the typical metabolic scaling boundaries under the MLBH.

Table 2.1. Posterior mean estimates, 95% credible (equal-tailed) intervals and effective sample size of posterior distributions for the fitted parameters of the model examining the variation in slopes b with $\log_{10}$ metabolic level (L, in mg O_2 h^{-1} g^{-1}) as temperature or activity level increase. These models incorporated the respiration mode (water or air) and the interaction effect with $\log_{10} L$, to test whether b changes differently with L between water- and air-breathers under warming conditions or increasing locomotion. Experimental temperature (°C) was included as an additional covariate in the model analysing the effect of activity, as temperature and activity-increased L are expected to show opposite effects on b (Fig. 2.1)

Dataset	Parameter	Posterior mean estimate	Credible interval 2.5%	97.5%	Effective sample size
Increasing temperature (n = 523)	Random effects				
	Experiment (n = 149)				
	Intercept, ϕ_{0j}	0.122	0.091	0.157	2,590
	Slope, ϕ_{Lj}	0.096	0.061	0.135	1,073
	Phylogeny, ψ_k (n = 111 spp.)	0.065	0.003	0.153	1,293
	Fixed effects				
	Intercept, β_0	0.725	0.581	0.873	8,649
	$\log_{10} L$, β_L	-0.002	-0.043	0.038	6,182
	Group, β_g	-0.027	-0.198	0.160	8,600
	$\log_{10} L \times$ Group, β_{Lg}	-0.090	-0.145	-0.035	5,883
Increasing activity (n = 281)	Random effects				
	Experiment (n = 56)				
	Intercept, ϕ_{0j}	0.103	0.044	0.157	1,804
	Slope, ϕ_{Lj}	0.141	0.092	0.194	3,438
	Phylogeny, ψ_k (n = 47 spp.)	0.136	0.041	0.247	1,367
	Fixed effects				
	Intercept, β_0	0.978	0.679	1.273	10,953
	$\log_{10} L$, β_L	0.194	0.085	0.302	6,758
	Group, β_g	-0.111	-0.438	0.225	8,481
	$\log_{10} L \times$ Group, β_{Lg}	-0.152	-0.274	-0.029	11,530
	Temperature, β_T	-0.002	-0.004	0.001	6,639

The quantitative prediction of changes in b associated with activity-increased L, utilising an assumption that muscular demands were proportional to body mass (see Methods: (c) Extending the MLBH), predicts well the changes seen in air-breathing herptiles, but not for fish (Fig. 2.3A *vs*. 3B): the mean b and its standard deviation for fish at maximal activity fall below the predicted value for a given increase in L.
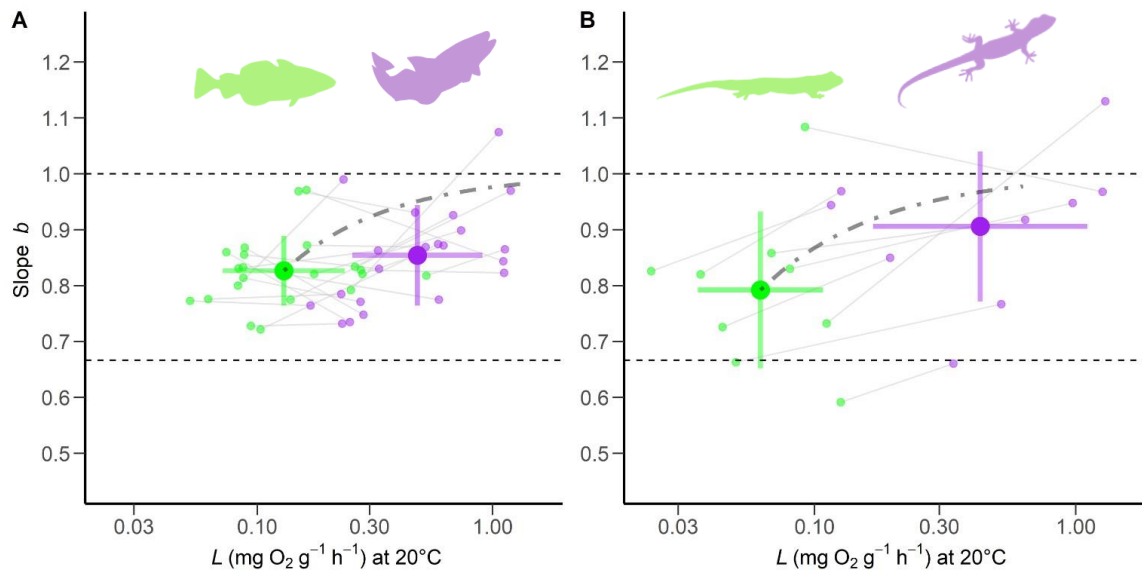
Figure 2.3. The mean slope b and metabolic level (L) ± standard deviation in water- (**A**) and (**B**) air-breathing species at minimal (in green) and maximal activity (purple). L values are adjusted to 20 °C for comparison (see Appendix 2.6). Dash-dotted lines show the expected relationship between b and L, if muscular work scales as m^1, and gradually increases by an order of magnitude from minimal activity (see discussion). Species' data are shown to illustrate variation between species, with a line joining each pair of measurements, i.e., at minimal and maximal activity. Mean values were used when more than one pair of measurements was available for a species. Dashed horizontal lines indicate the typical boundaries proposed by the MLBH.

4. Discussion

By combining two theoretical approaches – from the MLBH and the Ghost of Oxygen Limitation Past – I was able to extend predictions of metabolic scaling beyond those of either hypothesis individually. Increased locomotor activity is predicted by MLBH to increase metabolic scaling slope b towards a value of 1, whereas the Ghost of Oxygen Limitation Past predicted that warming – beyond any increase in b due to locomotor activity (Glazier, 2020) –

contributes to a reduction in b in water-breathers only, as expected from an evolved avoidance of oxygen limitation at large sizes.

My analysis, using a diverse set of ectothermic vertebrates, temperatures, and activity levels, supported these predictions (Fig. 2.2; Table 2.1). I showed that intraspecific metabolic scaling slopes (b) decreased as the $\log_{10}$ metabolic level L increased with temperature only within water-breathing vertebrates (teleosts and elasmobranchs). Conversely, b values increased consistently as $\log_{10} L$ increased with locomotor activity only within air-breathers (amphibians and reptiles). Specifically, b decreased by ca. 0.1 as L increased from 0.01 to 0.1 mg O_2 g^{-1} h^{-1} with warming in water-breathers), whereas b increased by ca. 0.2 when locomotion increases L to the same extent within air-breathers.

4.1 The effect of temperature

To explain why metabolic scaling slopes decrease consistently with warming in fish but not in air-breathing herptiles (Fig. 2.4A *vs*. B), I focus on the greater risks in water-breathers of oxygen becoming limiting at increased temperatures as individuals grow: I am unaware of other parsimonious mechanisms that would explain different responses among these vertebrate groups. I suggest that metabolic rates of water-breathers at increased temperatures are influenced to a greater extent than for air-breathers by surface area for oxygen uptake, because the energetic costs of increasing water flow over respiratory surfaces to meet increased demand is higher (and oxygen-demanding) (Verberk et al., 2021; Atkinson et al., 2022). Indeed, given the much higher density and viscosity of water than air, and the ca. 43-fold higher oxygen concentration in air than in water, air-breathers can increase metabolic rates ca. 280-fold above that of water-breathers for the same ventilation cost (Makarieva et al., 2008). Oxygen is thus hypothesized to become limiting in fish when respiratory SA, hence oxygen-supply capacity, is unable to satisfy the increased demand with increasing temperature and body size (von Bertalanffy, 1964; Pauly, 2021), providing there are no physiological or behavioural adjustments that avoid oxygen shortage (Atkinson et al., 2006; Verberk et al., 2021; Atkinson et al., 2022). However, if increased temperature is associated with increased risks of oxygen shortage at large body sizes in a predictable manner, such adjustments are expected to evolve as adaptive plastic responses to warming such that water-breathers avoid insufficient oxygen ('gasping for breath'; Pauly, 2010), especially under conditions of low exertion and non-extreme warming (Verberk et al., 2021; Atkinson et al., 2022). Apart from measures to improve

oxygen supply capacity at increased temperatures as water-breathers grow (e.g., Nilsson et al., 2012; Funk et al., 2021; Woods et al., 2022), oxygen demands may be reduced. Metabolic costs are not just from tissue maintenance, but also include overhead costs of growth, which contribute strongly to metabolic rate (Parry, 1983), even in resting individuals (Rosenfeld et al., 2015). From cold to optimal temperatures, growth rate and its metabolic costs increase mostly in young and small individual fish, but barely change in large and old ones (Imsland & Jonassen, 2001; Barneche et al., 2019), which would lead to lower slopes b with warming. Air-breathing species, by contrast, do not seem to show such abrupt deceleration of growth rates over ontogeny with increasing temperature (e.g., Rhen & Lang, 1995; Roosenburg & Kelley, 1996; Steyermark & Spotila, 2001). Moreover, body size reductions associated with increasing rearing temperature are also stronger in aquatic ectothermic species in comparison to air-breathing species (Forster et al., 2012). The increasingly steep reduction in both mass-specific growth and mass-specific metabolic rates over fish ontogeny with warming may thus have evolved as a plastic response to maintain a safety margin for oxygen uptake (i.e., aerobic scope; Atkinson et al., 2006; Verberk et al., 2021), thus avoiding oxygen shortage under specific conditions (Jutfelt et al., 2021).

Fast-growing fish in warm waters are therefore expected to show lower b values than slow-growing fish in cold waters, as the latter exhibit slower but generally more sustained growth throughout ontogeny (reviewed in Imsland & Jonassen 2001; e.g., Björnsson & Steinarsson, 2002; Árnason et al., 2009; Lefébure et al., 2011). Indeed, a recent study demonstrated that optimum temperature for growth generally decreases with fish size (Lindmark et al., 2022). Thermal effects on the mass-scaling of growth can hence explain why b decreases at rest (Tan et al., 2019; Glazier, 2020), sometimes below 2/3 (Fig. 2.2A). Complementarily, high slopes b in cold, viscous waters may result from large fish experiencing less drag and smaller boundary layers than small individuals, hence improved oxygen-uptake capacity (Verberk & Atkinson, 2013). In resting, slow-growing individuals at cool water temperatures, b would thus approach 1 following predominant V-related influences from body maintenance.

Conversely, the absence of a general relationship between b and temperature-increased L within air-breathing amphibians and reptiles (Fig. 2.4B), support the prediction from the metabolic theory of ecology that warming affects only metabolic level but not the predicted ¾-

power scaling (Gillooly et al., 2001; Brown et al., 2004), albeit within a specific set of species and conditions. This lack of relationship between *b* and *L* with temperature in herptiles could be attributed to a balance between influences from SA-related processes (e.g., water loss avoidance or heat conservation) and V-related maintenance (discussed in Glazier, 2020). Complementarily, the absence of warming-induced growth deceleration at large sizes in herptiles, unlike in fish, may explain the absence of an imbalance of processes that increase *b* (maintenance) *versus* those that decrease it (growth costs).

4.2 The effect of activity

Following the MLBH prediction that increased muscular activity during locomotion increases the relative influence of V-related over SA-related processes (Glazier, 2008, 2009c), I found that slopes *b* increased with *L* as activity increases in air-breathing amphibians and reptiles. However, no consistent effect of activity on *b* was observed within fish species (Fig. 2.4C *vs*. D). Moreover, the predicted quantitative effect of activity on *b*, based on an assumed metabolic cost of locomotor activity proportional to body mass, was consistent with observed *b* values in these air-breathing herptiles, but not in fish (Fig. 2.3A *vs*. 2.3B). This difference between air-breathing herptiles and fish suggests an influence that prevents *b* from increasing during muscular power production in fish. Again, I propose that evolved avoidance of oxygen shortage in water-breathers may explain this finding. I posit that the oxygen costs of aerobically fuelled locomotion will not generally be proportional to body mass (or V) in water-breathers, but will be disproportionately less at larger sizes, following selection against large individuals that over-exert themselves to the extent that oxygen shortage reduces fitness.

High activity and warm temperature would therefore be expected to combine to lower *b* in water-breathers, but increase it in air-breathers. Indeed, warming-induced reductions in mass-specific aerobic scope were predicted in a recent quantitative model and supported by empirical data on 286 teleost species (Rubalcaba et al., 2020), suggesting that larger, active individuals may be more susceptible to oxygen limitation in warmer water. In contrast, mass-specific aerobic scopes exhibit no such decrease with warming in air-breathing herptiles (e.g., Wright, 1986; Gifford et al., 2013).
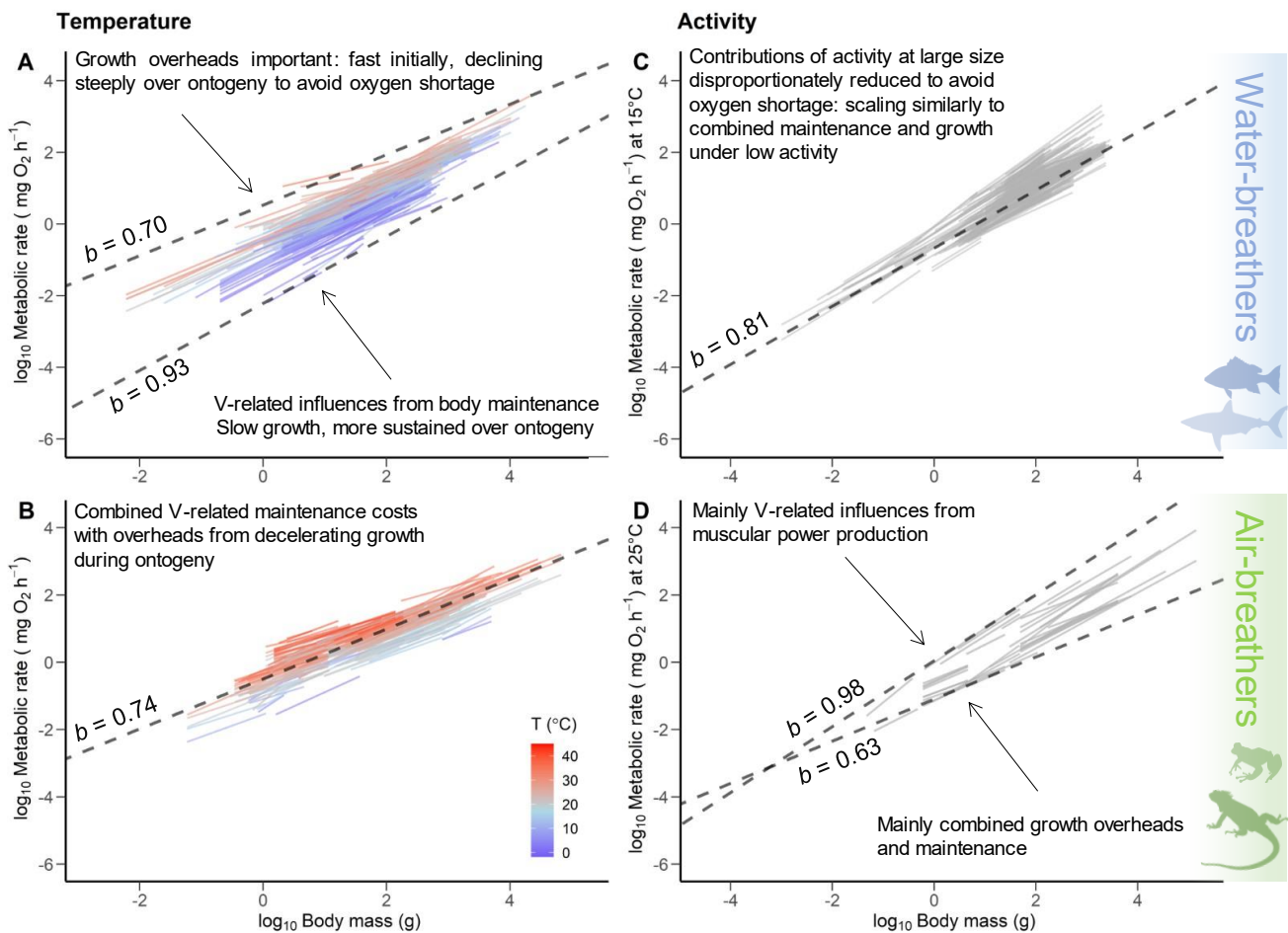
Figure 2.4. Comparison of the intraspecific metabolic scaling with body mass in ectothermic vertebrates. Left panels show scaling regressions performed at various temperatures in inactive individuals of water- (**A**) and air-breathers (**B**). Right panels show regressions for individuals under different activity levels of water- (**C**) and air-breathers (**D**), adjusted to the approximate mean temperature of each dataset (Appendix 2.6). Dashed lines denote the upper and lower metabolic scaling slopes (*b*) as metabolic level (*L*) increases with temperature (A, B) or activity (C, D). These slopes were predicted through model estimates, by using values of the minimal and maximal *L* values calculated at the geometric mass-midpoint of the range reported for water- and air-breathing species in each dataset. B and C show mean *b* and *L* values, as the estimated change in *b* overlapped 0, indicating no consistent variation with *L*. The explanation proposed here for these changes in *b* is shown on each panel.

4.3 Intraspecific variation in metabolic scaling: Improving explanatory power

Theory to explain and predict variation in ecological energetics in general, and metabolic scaling in particular, needs to account for context, which includes: metabolic state or activity level; body and ambient temperature; and selection pressures on resource supply, demand and allocation among metabolic activities (Glazier, 2014). For example, Glazier (2020) partly explained why thermal effects on metabolic scaling in ectotherms were not uniform, because of their dependence on activity level, consistent with expectations from the MLBH. I have further extended explanatory power by incorporating the idea of evolved avoidance of oxygen limitation in warm, large, and active water-breathers. I found that responses of intraspecific metabolic scaling to warming and activity did indeed differ as predicted between air-breathing herptiles and fish. I have also presented new quantitative predictions and tests of the effects of locomotor activity on metabolic scaling, assuming locomotor costs were proportional to body mass.

Finally, I caution against considering the effects of metabolic level on the slope b as just a balance between SA- and V-related processes. Instead, I encourage expectations from evolved size-, temperature-, and activity-related avoidance of oxygen shortage. Even when muscular mass is proportional to body mass, the costs of locomotion may not be proportional to body mass if locomotor effort is dependent on size- or age-related pressures on resource allocation. Larger water-breathers, with greater selection pressures on maximum oxygen consumption because of lower exchange surface:mass ratio, may have evolved a lower maximum sustainable locomotor metabolism (i.e., lower than isometric investment in musculature and organs servicing locomotion), thereby providing enough aerobic scope for other activities whose variation is not necessarily included in measures of aerobic scope (e.g., digestion of large meals, fighting disease, or predator avoidance; Jutfelt et al., 2021). Likewise, the extent to which growth rates, hence overhead growth costs on resting metabolism, decelerate during ontogeny in response to warming would protect aerobic scope to enable other activities in large individuals at high temperatures (Atkinson et al., 2006). Such thermal plasticity may be also influenced by factors not SA-related, as mortality affecting timing of maturation, or allocation from growth to reproduction (Marshall & White, 2019a). Overall, this new theoretical approach to understanding intraspecific variation in metabolic scaling combines extrinsic (temperature) and intrinsic (activity) influences on organismal physiology, together with different respiration modes and their evolutionary pressures.

Chapter 3: Understanding the adaptive significance of metabolic scaling: interspecific variation in mass-scaling slopes may reflect different growth demands among teleost fish

Parrotfish (*Sparisoma cretense*) during daily routine on the reef

Understanding the adaptive significance of metabolic scaling: interspecific variation in mass-scaling slopes may reflect different growth demands among teleost fish.

Abstract

Metabolism fuels growth and self-maintenance functions in all living organisms. The extent to which metabolic rates change as organismal size increases (i.e., metabolic scaling) is important in ecology because this relationship describes, among other things, how energy use varies over ontogeny. Yet, the mechanism(s) underlying the differences in metabolic scaling between species remain under debate. Among teleost fishes, while some species show a near constant metabolic rate per gram as they grow, others show a marked reduction in mass-specific metabolic rates over ontogeny. Such reduction in metabolic scaling slopes has been explained by a predominant influence of surface-area over volume-related processes on resource supply of species occurring in warm temperatures and with active lifestyles. In this study, I investigate an alternative hypothesis based on changes in growth and its metabolic demands over ontogeny. Through a meta-analysis, I showed that metabolic scaling slopes decrease with maximum growth rates, supporting that growth contributes to the variation in mass-scaling of metabolic rates across species, as an alternative (or complementary) explanation to surface-area related influences on resource supply. Moreover, using a theoretical model, I estimated the overhead costs of growth and maintenance metabolism in the species compiled here, and show that the thermal sensitivities of these metabolic demands are similar. Lifestyle is shown to affect only maintenance metabolism, which was higher for pelagic fishes than for less athletic species. Finally, I found that net growth efficiency shows relatively small variation and is largely independent of body size at maximum growth rate, ecological niche, and evolutionary history. Overall, these results suggest that whole-body demands from growth and body maintenance may explain interspecific differences in metabolic scaling, and highlight the importance of accounting for such differences to estimate energetic demands in fish.

Keywords: Metabolic rate; Body mass; Allometric scaling; Biomass production; Growth performance; Ecophysiology; 'Growth Scaling Hypothesis'

1. Introduction

All organisms use metabolic energy to transform materials from the environment into new tissue and to power self-maintenance functions (Wieser, 1994; Brown et al., 2018). Because the energy that organisms are able to obtain from the environment and use for metabolism is limited, the rate and cost of biomass production can influence the metabolic energy available for survival, and ultimately affect fitness (Lindeman, 1942; Brown et al., 1993). The allocation of metabolic energy between growth and self-maintenance is thus important for adapting to various ecological pressures, yielding a restricted range of life-history outcomes over the evolution of a wide variety of species for which fitness is expected to be equal (Ricklefs & Wikelski, 2002). This equal fitness is necessary for the persistence of such diversity (Brown et al., 2018; Burger et al., 2021). Given the relevance of energetics and trait diversity in ecology (Brandl et al., 2023), it is important to understand and quantify how metabolic demands are related to specific ecological factors and life-history traits.

Metabolic rate is linked to body size (*m*) by a relationship (often termed scaling) typically described as a power equation $R = am^b$, where *a* is the scaling coefficient and *b* is the exponent, or slope in the linear regression between log *R* and log *m*. Understanding the extensive variation in metabolic scaling has been a long-standing challenge in ecology (Glazier, 2022a), where the emphasis has gradually shifted from physical constraints of resource supply (e.g., Rubner, 1883; Kleiber, 1932; West et al., 1997; Brown et al., 2004) to evolutionary adaptations of resource demand (e.g., Agutter & Wheatley, 2004; Glazier, 2005; da Silva et al., 2006; White et al., 2022). Among the most influential explanations, the 'Metabolic-Level Boundaries Hypothesis' (MLBH; Glazier, 2005, 2010, 2014) proposes a multi-mechanistic approach, whereby metabolic scaling is affected by the relative influence of surface-area (SA) and volume (V) related processes in organismal physiology. According to the MLBH, when growth is isomorphic (i.e., body shape invariant throughout ontogeny), the body mass-scaling of metabolic rates in organisms with high energy demands should be strongly influenced by resource supply and waste removal through exchange surfaces (which scales as $m^{2/3}$), thus resulting in shallow slopes (*b* ≈ 2/3). Conversely, organisms with low energetic demands are likely not so influenced by SA-related processes, and metabolic rate is dominated by minimal tissue maintenance that is proportional to body V or mass (m^1), thus leading to steep slopes (*b* ≈ 1). The combination of SA- and V-related processes would produce an approximation to a power relationship between metabolic rate and body mass with a *b* value somewhere between

1 and 2/3.The MLBH therefore provides a mechanistic link between ecology, life-history traits, and metabolic scaling, because any factor influencing resting or routine metabolism, whether extrinsic (e.g., temperature, predation pressure) or intrinsic (e.g., maintenance, growth), may affect its relationship with body mass. For instance, how SA of respiratory organs such as gills varies as body mass increases is thought to greatly influence growth rate, adult size, and lifestyle in water-breathing animals (Pauly, 2010; Gillooly et al., 2016; Bigman et al., 2018). Indeed, the MLBH has received empirical support in ectotherms such as spiders, snakes, and fish (Glazier, 2008, Killen et al., 2010). Specifically, Killen et al. (2010) found a decline in allometric slopes of ontogenetic metabolic scaling across 89 species of teleost fish with increasing environmental temperature and more active lifestyles, both associated with elevated energetic demands.

While the MLBH mechanism invoking SA-related influences on resource supply can apply to intraspecific variation in metabolic scaling (Glazier, 2020; Rubalcaba et al., 2020; see also Chapter 2 in this thesis), the same mechanism may not extend to interspecific comparisons of resting organisms at a standardized size and near their optimum conditions (Jutfelt, 2021). Indeed, species adapted to high energy demands and hence high metabolic rates will have evolved to obtain resources quickly and efficiently (Anderson, 1994; Glazier, 2009b; Killen et al., 2016), and so they may not be nearer to SA limitation than are their sluggish counterparts, which are adapted to a slower rate of resource acquisition. For instance, among ectotherms, species with more active foraging behaviours generally show higher resting metabolic rates (Glazier, 2008; Killen et al., 2010; Tan et al., 2019). Hence, instead of limitations or influences on resource supply, differences in interspecific metabolic scaling may be explained by resource demands of fitness-related processes that have adapted to certain ecological pressures (Glazier, 2022a).

Alternatively, Glazier (2005, 2015) proposed that the interspecific variation in metabolic scaling could also be related to the different growth trajectories among animals. This explanation was more recently developed and termed the 'Growth Scaling Hypothesis' (GSH; Tan et al., 2019), which argues that differences in the mass-scaling of whole-body energetic demands, such as organismal growth or maintenance, may lead to differences in mass-scaling of resting or routine metabolic rates across species. This hypothesis is based on the influence of overhead costs of growth, i.e., the metabolic energy needed for synthesis of new tissue, which contribute strongly to metabolic rate, even at resting levels (Parry, 1983; Rosenfeld et

al., 2015). Specifically, the GSH predicts that a decrease in mass-specific growth rate, and so the metabolic cost of growth as body size enlarges, will lead to shallower scaling slopes (lower *b*). Hence, in species whose mass-specific growth rate declines with increasing mass at a similar rate during ontogeny (von Bertalanffy, 1938, 1957; Froese & Pauly, 2010), rapid-growing species will have a higher proportion of metabolism determined by growth costs than their slow-growing counterparts, and hence be predicted to have lower *b* at rest. In contrast, resting metabolic rates in slow-growing species will be dictated by maintenance demands such as protein turnover and regulation of electrochemical gradients (Wieser, 1994; Verberk et al., 2021), which are proportional to body mass, and hence *b* will approach 1 in these species.

Although the energy required to synthesize macromolecules (e.g., proteins or polysaccharides) seems similar among taxa, the associated costs of growth, such as the transport of monomers and ATP to production sites (i.e., the 'growth machinery'; Clarke, 2017, 2019), may vary between organisms. Indeed, Barneche & Allen (2018) found that the overhead costs of growth increased with temperature and level of activity within 13 families of teleost fishes, suggesting that warm-water fishes with active lifestyles will require a greater fraction of their assimilated energy per unit growth than cold-water and sluggish fishes. Following the GSH, the decline in metabolic scaling slopes *b* with increasing metabolic rates observed across teleost species (Killen et al., 2010) could be underpinned by the increasing contribution of overhead costs of growth relative to resting metabolism with temperature and more active lifestyles (Barneche & Allen, 2018). This GSH prediction assumes that maintenance demands are additional to growth costs and similar among species with varying growth rates (Wieser, 1994; Clarke, 2017, 2019). Conversely, growth and metabolism may be co-adjusted over long evolutionary times (Brandl et al., 2023), so the resulting metabolic costs of growth are conserved across species adapted to different temperatures and lifestyles.

Combining theory and empirical data can help to understand how metabolic energy is allocated into various fitness-related processes (Sibly et al., 2015; Barneche & Allen, 2018), and how these energetic demands may change with ecological factors such as temperature or lifestyle. For this purpose, the Ontogenetic Growth Model (OGM; West et al., 2001, Moses et al., 2008; Hou et al., 2008) offers a useful tool to integrate the main components of resting metabolic rate, comprising organismal growth (dm/dt) and its overhead costs (C_g), as well as maintenance metabolism ($R_m m$). In agreement with current theory (von Bertalanffy, 1957,

Glazier, 2005; Kooijman, 2010), the OGM assumes that mass-specific maintenance demands (R_m) remain constant over ontogeny, so that total maintenance scales isometrically with body mass (m). Hence, in this model, the relative contribution of supporting a certain growth rate and body mass to resting metabolism is respectively determined by C_g and R_m. Furthermore, the OGM assumes that the relationship between metabolic rates and body mass follows a general ¾ power scaling due to limitations of fractal-like resource transport networks (i.e., $b = 0.75$; West et al., 1997), whereas deviations from this general scaling are explained as statistical noise (Moses et al., 2008).

This study explores the interspecific variation in ontogenetic metabolic scaling of teleost species, and whether this variation may reflect differences in the energetic demands of growth and body maintenance. Teleost fish are ideal to investigate the extensive variation in metabolic demands of growth and body maintenance because all species belong to a monophyletic group that comprises half of all extant vertebrates (ca. 33,000 species), cover a vast functional and body size range (ca. 10^9-fold variation), and occur in a variety of environments with temperatures from below 0 °C to 40 °C (Froese & Pauly, 2010). Moreover, although most species start life at a similar size (~1 mg hatchlings), growth rates and final body sizes differ enormously between species (Pauly, 2010; Sibly et al., 2015). Indeed, while some species produce less than a gram of body mass during their lifetime (e.g., zebrafish), others must attain the energy to grow by over half a tonne (e.g., giant tuna) (www.fishbase.org). Remarkably, field data have shown that juveniles of large species grow generally faster (in length per time) than juveniles of small species, regardless of their initial size (Winemiller & Rose, 1992; reviewed in Sibly et al., 2015), indicating differences in energy allocation between maintenance and growth among species (Sibly et al., 2015). Despite such variety of life-histories, growth efficiency seem to be unchanged with species body size among fishes (Hatton et al., 2019). This similar growth efficiency may be possible if energy gains and expenditures are co-adjusted among species, which evolved under certain ecological pressures to maximise fitness (Glazier, 2018b; Tan et al., 2019).

Here, I compiled data on growth and metabolic scaling in teleost species, and used the OGM to characterise the metabolic demands of growth and maintenance. Through this meta-analytic approach, I investigate the GSH (Glazier, 2005; Tan et al., 2019) by testing three hypotheses: the metabolic scaling slope (*b*) decreases as maximum growth rate and its energy

demands increases across species (H1); both overhead costs of growth per gram of new tissue (C_g) and mass-specific maintenance metabolism (R_m) have similar, relatively low temperature sensitivities due to long-term evolutionary adaptation (Clarke, 2004; Juftlet, 2020)(H2); and athletic fishes exhibit higher C_g and R_m than other species with more sluggish lifestyles (H3). Moreover, I test whether net growth efficiency varies systematically with species body size, ecological niche, and evolutionary history (H4). In agreement with the GSH, my findings show a negative correlation between *b* and maximum growth rates across teleost species, yet the relative contribution of growth costs to resting metabolism seems unchanged with environmental temperature. Overall, my results indicate that growth demands are conserved over evolution, whereas athletic fishes possess higher maintenance demands, reflecting the cost of sustaining high locomotory capacities. Finally, this study shows that overlooking the interspecific variation in ontogenetic metabolic scaling may yield unrealistic estimates of energetic demands in teleost fish, highlighting the importance of incorporating the variation in slopes *b* to quantify species performance.

2. Material and methods

2.1. Collection of metabolic scaling relationships

The literature was searched for scaling regression parameters of the relationship between metabolic rate and body mass within teleost fish species, supplementing with additional regressions from the sets compiled in Glazier (2005) and Killen et al. (2010). Searches were carried out with Google Scholar, Web of Science and OATD (Open Access Theses and Dissertations), searching for terms as 'fish + metabolism', 'fish + metabolic + rate', 'fish + respiration + rate', 'fish + oxygen + consumption', '<taxon name> + metabolism', which were also translated to German, Portuguese, Spanish and French. The search was completed by looking for related studies through the list of references and citations of all relevant papers, i.e., those including the search terms in the title.

Measurements were only accepted when taken on non-active, non-stressed, post-larval and post-absorptive animals. A single study was used per species to avoid over-representation of species with more data available (Clarke & Johnston, 1999; Killen et al., 2010). When multiple scaling regressions were available for a species, measurements of the lowest metabolic state (e.g., resting over routine) were preferred, followed by regressions covering the widest

body mass range, and last, measurements made at the closest to the species' optimal or highest preferred temperature (according to available literature or FishBase.org, respectively). For regressions performed at various temperatures and including both body mass and temperature term, metabolic rates were estimated at the closest temperature to the thermal optimum from the studied range. Regressions based on wet body mass were also preferred, to avoid variation due to water content of species (Yeannes & Almandos, 2003), as different mass types may lead to differences in the scaling regression (e.g., Moran & Wells, 2007). In two cases where exclusively dry mass was used, conversion to wet mass was calculated as described in the original study (Mitz & Newman, 1989) or assuming dry mass is 20% of wet mass (Horn & de la Vega, 2016). When regression parameters or body mass ranges were missing in a study, data were extracted from figures using WebPlotDigitizer v4.4 (Rohatgi, 2020), performing regressions if needed through ordinary least squares (OLS) regressions using log-log data.

2.2. Estimating overhead costs of growth and maintenance metabolism

This approach is guided by the OGM, which is based on mass-scaling of biological rates and organismal energy balance (Moses et al., 2008; Barneche & Allen, 2018). Following this model, the resting metabolic rate R (mg O_2 d^{-1}) for an organism of body mass m (g), and growth dm/dt (g d^{-1}) can be described as:

$$R = C_g \left(\frac{dm}{dt}\right) + R_m m, \qquad [1]$$

where $C_g \left(\frac{dm}{dt}\right)$ is the metabolic energy invested in biosynthesis (mg O_2 d^{-1}), and C_g is the overhead cost of growth (i.e. the energy needed per unit growth, mg O_2 g^{-1}), whilst $R_m m$ is the metabolic energy allocated to self-maintenance (mg O_2 d^{-1}), and R_m is the mass-specific maintenance metabolism (mg O_2 g^{-1} d^{-1}). In agreement with current theory (Glazier, 2005; Kooijman, 2010; Clarke, 2019), the OGM assumes that R_m remains constant over ontogeny. By eq. [1], the extent to which growth rate contributes to resting metabolic rate is determined by C_g. The metabolic rate of a resting (i.e., non-active, non-reproductive and post-absorptive) organism, on the other hand, can be approximated by the metabolic scaling equation:

$$R = am^b, \qquad [2]$$

where a (mg O_2 g^{-b} d^{-1}) is the normalisation constant, and b is the dimensionless mass-scaling exponent. Since growth theoretically ceases when the organism reaches the asymptotic or final mass M_∞ (von Bertalanffy, 1938, 1957), the resting metabolic rate of an organism at M_∞ is therefore entirely allocated to body maintenance:

$$R = R_m M_\infty \qquad [3]$$

and hence R_m can be calculated as:

$$R_m = a M_\infty^{b-1} \qquad [4]$$

Note that eq. [4] predicts that mass-specific maintenance metabolism decreases with final body size for $b < 1$. Last, when R, R_m, and dm/dt are known, the overhead cost of growth (C_g) can be calculated through eq. [1] as:

$$C_g = \frac{(R - R_m m)}{dm/dt} \qquad [5]$$

2.3. Comparing growth rate across species

Growth was compared across fish species by the inflection point in the von Bertalanffy growth model (VBG; von Bertalanffy, 1938, 1957), which is an estimate of the species' maximum growth rate (g_{max}, g d^{-1}). This estimate provides an objective standard to compare growth performance among species and prevents the problems of comparing size-at-age data (Pauly, 2010). The calculation of g_{max} was done using the classical VBG equation, which describes fish growth in the form:

$$\frac{dm}{dt} = \alpha m^h - \beta m \qquad [6]$$

According to the OGM (Moses et al., 2008; Barneche & Allen, 2018), eq. [1], [2] and [6] simply represent statements of energy balance in organisms, and can be simultaneously true if: $\alpha = \frac{a}{C_g}$, $\beta = \frac{R_m}{C_g}$, and $h = b$. Whereas the OGM assumes a general $b = 3/4$ for mass-scaling of metabolic rates (West et al., 1997, 2001), this study uses actual b values from species-specific relationships (see previous section). Using eq. [6], the body mass at which maximum growth rate is achieved (m_{gmax}, g) can be estimated by taking the second derivative of mass with respect to time, and setting this expression equal to 0, which yields:

$$m_{gmax} = \left(\frac{h\alpha}{\beta}\right)^{\left(\frac{1}{1-h}\right)} = M_\infty \left(\frac{h}{1}\right)^{\left(\frac{1}{1-h}\right)} \qquad [7]$$

Length-based growth data in FishBase were converted to mass values using parameters of the length-weight relationships for species from the same website, which describe body mass as:

$$m = a_L l^{b_L}, \qquad [8]$$

where a_L (g cm$^{-b_L}$) and b_L (dimensionless) are the scaling coefficient and exponent respectively, that describe the change in body shape over ontogeny, while l is body length (cm). According to the VBG, $h = 1 - \frac{1}{b_L}$ (see Appendix 3.1); hence, using species-specific length-weight parameters of eq. [8] and replacing h in eq. [7], yields:

$$m_{gmax} = a_L L_\infty{}^{b_L} \left(1 - \frac{1}{b_L}\right)^{b_L} \qquad [9]$$

where L_∞ is the final or asymptotic body length (i.e., the length at an infinitely old age, in cm). Finally, the corresponding maximum growth rate g_{max} is calculated by replacing m_{gmax} (eq. [9]) in eq. [6]:

$$g_{max} = a_L K L_\infty \left(L_\infty \left(1 - \frac{1}{b_L}\right)\right)^{b_L - 1} \qquad [10]$$

where K is a factor of dimensions time $^{-1}$ (d^{-1}) by which body length approaches L_∞ (obtained from $\frac{\beta}{b_L}$ in eq. [6]; see Appendix 3.1). The values of the VBG parameters K and asymptotic length (L_∞) were extracted from FishBase.org (March 26, 2022; only 'non-questionable' records) for those species included in the metabolic dataset, together with data on temperature when available. Mean values were used when multiple data were available for a species, so that each species was only represented by a single datapoint.

The values of m_{gmax} and g_{max} have been shown to be largely invariant whether these are calculated using VBG or OGM assumptions (Barneche & Allen, 2018). While the VBG typically expects that $b_L = 3$ due to isomorphic growth (i.e., invariant body shape over ontogeny) of organisms like fish, and hence $h = 2/3$ (though variation around this value is expected; von Bertalanffy, 1938, 1957), the OGM predicts that $h = 3/4$, following the general

¾ metabolic scaling proposed for all life forms (West et al., 1997). Using either VBG or OGM, the m_{gmax} of a species will be reached in any case at about 1/3 of its final mass M_∞ ($0.30M_\infty$ and $0.32M_\infty$, respectively). Likewise, the estimation of m_{gmax} here by either $h = b$, using species-specific b values as for the estimation of metabolic rates (see section 2.2), or by $h = 1 - 1/b_L$, using species-specific b_L following VBG, would result respectively in m_{gmax}= 0.318 ($\pm$ 0.0029 s.e.) M_∞ *vs.* 0.298 ($\pm$ 0.0002 s.e.) M_∞. The calculations of m_{gmax} and g_{max} are therefore expected to be almost identical if the length-based data from FishBase are used following either VBG or the present approach, thus supporting the use of these data to compare growth and metabolic rates among the compiled species.

2.4. Linking metabolic and growth rates

To link growth and metabolism at species level, metabolic rates R were first calculated through metabolic scaling relationships (eq. [3]) at the body mass corresponding to the species' maximum growth rate ($m_{g_{max}}$). Metabolism and growth are therefore estimated at a physiologically comparable mass across species. Species whose scaling relationships showed $b \geq 1$ were excluded because $b < 1$ is a necessary condition in this approach, yet this screening step excluded only 3.39% (4 species) of the total 118 species collected here. Because mean temperatures reported in FishBase and experimental temperatures from metabolic studies were already highly correlated [Pearson correlation, $r = 0.83$, 95% CI (0.74, 0.89), df = 74, $p < 0.001$; Appendix 3.2], no temperature correction was made to link growth and metabolism of these species. Growth and metabolic data were thus considered as reliably thermally linked values within the species' thermal ranges.

2.5. Further predictors of metabolic scaling

The metabolic scaling slopes b are expected to vary not just with growth rate, but also with temperature and metabolic level (Killen et al., 2010; Glazier, 2010, 2015), and with the mass-scaling of respiratory organs, as an indicator of the influence of surface area-related processes (Glazier, 2020). To investigate the possible effect of metabolic level L on b, L (in mg O_2 g^{-1} d^{-1}) was calculated as the mass-specific metabolic rate at the geometric mass-midpoint of the metabolic scaling relationships. Likewise, to account for the influence of SA-processes, data on the mass-scaling of gill SA was searched for the compiled species. As for metabolic rate, the relationship between gill SA (G) with body mass (m) in fish is generally described by

a power equation of the form $G = a_G m^{b_G}$, where a_G and b_G are respectively the scaling coefficient and exponent (Pauly, 2010; Pauly & Cheung, 2018). The literature was searched for gill SA scaling exponents (b_G) as above for metabolic scaling relationships, but using terms as '<taxon name>' + 'gill + surface-area', 'gill + scaling', and 'gill + body mass', and including exclusively measurements in post-larval fish.

2.6. Statistical analysis

(a) The relationship between scaling slopes *b* and maximum growth rates (H1)

Statistical analyses were performed using R v. 4.2.0 (R Core Team, 2022). Except for metabolic scaling slopes (b), all metabolic traits, as well as maximum growth rates and body mass were $\log_{10}$ transformed to account for the wide allometric variation among species in these variables, and because the relationships are expected to be linear after transformation (Hatton et al., 2019; Glazier, 2010, 2021). Firstly, the relationship between scaling slopes (b) and $\log_{10}$ maximum growth rates was investigated through a Reduced Major Axis (RMA) regression using package 'smatr' (Warton et al., 2012), assuming both variables have similar measurement error. A further screening step was used to exclude species with sparser data, i.e., whose mass ranges in scaling relationships covered less than 5% of ontogenetic mass range (*cf.* Killen et al., 2010; see Appendix 3.3), as well as less than 3 records of growth parameters in FishBase. Second, Ordinary Least Squares (OLS) regressions were performed to explore the variables that best predict the variation in slope b, assuming that b is dictated by growth rate (Glazier, 2005, 2015; Hatton et al., 2019), metabolic level, temperature (Glazier, 2005, 2010), or mass-scaling of gill SA (Glazier, 2020). These OLS models also enable the assessment of the individual effects of these variables on the slopes b and allow comparison between models including different explanatory variables. The variables that best predict b were thus investigated by incorporating the possible linear effects of $\log_{10}$ maximum growth rate, $\log_{10}$ metabolic level, temperature, and gill SA scaling exponent (b_G) as explanatory variables in an OLS model. This analysis was repeated excluding gill SA scaling exponents, as data on b_G were scattered and reduced substantially sample size to 21 species. Comparison between candidate models to best predict the variation of slopes b across species was made using package 'MuMIn', which is based on Akaike's Information Criterion corrected for small samples (AICc) (Barton, 2018). Model averaging was used to identify the best explanatory variables across the candidate models and determine their relative importance, calculated as

the sum of Akaike weights of each variable from all models in which they are incorporated. All possible combinations of variables included in these models were compared using the function 'dredge', identifying the best model as that with the lowest AICc value.

(b) Variation in C_g and R_m with temperature and among lifestyles (H2-H3)

Further OLS models were used to investigate the effect of temperature (β_T) and lifestyle on the overhead costs of growth (C_g, mg O_2 g^{-1}) and maintenance metabolism (R_m, mg O_2 g^{-1} h^{-1}) across species. These regressions incorporated either C_g or R_m as response variables, with explanatory variables temperature, lifestyle, and body mass (to account for the effect of body size, β_m). The temperature recorded in metabolic studies was used in these analyses because these values were close to temperatures recorded for growth data (see section 2.2), but also precisely measured, and available for all compiled species. Lifestyle groups followed the classification in FishBase: 'demersal' (i.e., living near the bottom), 'benthopelagic' (i.e., between the bottom and the surface), 'pelagic' (i.e., near the surface), and 'reef-associated' (i.e., on coral reefs). One species (*Sebastolobus altilevis*) was excluded from the categorical analyses because it was the only representative of the bathy-demersal lifestyle.

For comparison of temperature effects only, the residuals of OLS models for C_g and R_m were expressed relative to the fitted regression values at 1 g of body mass. The Q_{10} value was then calculated for each variable, using the equation:

$$Q_{10} = (k_{30}/k_0)^{(10/(30-0))}$$ [11]

where k_{30} and k_0 are either C_g and R_m estimated at 30 and 0 °C using the fit of OLS regressions to the mass-corrected data. Likewise, for further comparisons of lifestyle effect alone, C_g and R_m were corrected at 15°C and 1 g (using residuals of OLS regressions as described above). The differences in these mass- and temperature-corrected values between lifestyles were then analysed through *post hoc* comparisons using Tukey's 'Honest Significant Difference' tests (HSD), which account for multiple pairwise comparisons (Abdi & Williams, 2010). Furthermore, to explore how predictions may change by overlooking the variation in slopes *b* between species, the latter analyses were repeated with estimates obtained using the general ¾ metabolic scaling approach (*b* = 0.75), instead of the actual *b* values of species.

(c) Variation in net growth efficiency across species (H4)

To calculate net growth efficiency of species, both resting metabolic rates and maximum growth rates were firstly transformed into energy units (Joules) using a general oxyjoule conversion of 14.14 J mg^{-1} O$_2$ consumed (Elliot & Davison, 1975; often applied in fish, e.g., Navarro et al., 2019; Dawson et al., 2020) and 6,276 J g^{-1} wet mass (i.e., 1500 calories g^{-1}, as approximated mean value for teleosts; Cumminns & Wuycheck, 1971). The net growth efficiency was then calculated as $\frac{g_{max}}{(R + g_{max})}$, i.e., the proportion of energy stored by growth per total assimilated energy at body mass $m_{g_{max}}$ (Angilletta & Durham, 2003). A Beta regression model (BRM) was performed using package 'betareg' (Cribari-Neto & Zeileis, 2010) similar to the OLS above, including net growth efficiency as response variable and temperature, lifestyle and log$_{10}$ body mass as explanatory variables. The BRM was used here because it accounts for the right skewed distribution of the growth efficiency data, which comprises proportions ranging from more than 0 to less than 1 (Cribari-Neto & Zeileis, 2010). Finally, the variation in the estimates of net growth efficiency obtained using either actual *b* values or the general ¾ scaling were compared among lifestyles and thermal regimes. Species were then grouped into climate zones, again following FishBase: 'tropical' (i.e., preferring temperatures > 20°C), 'subtropical' (i.e., tolerating minimum temperatures of 10 – 20°C), 'temperate' (i.e., tolerating temperatures < 10°C), and 'polar' or 'boreal' (i.e., adapted to temperatures < 5°C).

(d) Model checking and phylogenetically informed comparisons

The outputs of OLS models are presented through ANOVA tables for model objects to examine the significance of each independent variable. Following Zuur & Ieno (2016), these models were validated by visually checking the normality of model residuals, the plot of residuals versus fitted values, normal Q–Q plots, and Cook's distances, using the R package 'performance' (Lüdecke, 2021). Furthermore, OLS analyses as well as the BRM for growth efficiency were repeated using phylogenetic generalised least squares (PGLS) in the 'caper' package (Orme et al., 2018) to account for phylogenetic non-independence of species. Phylogenetic information was obtained from The Fish Tree of Life using the package 'fishtree' (Chang et al., 2019), which contains a phylogeny of 11,638 teleost species estimated from genetic data and dated using 139 fossil calibrations. The phylogenetic correlation between C_g,

R_m or net growth efficiency and the linear predictors (i.e., temperature, lifestyle, $\log_{10}$ body mass) was tested through Pagel's λ (Freckleton et al., 2002). The value of λ ranges from 1, meaning a strong phylogenetic signal when model residuals are best described by species phylogeny, to $\lambda = 0$, when species traits can be considered statistically independent (i.e., all species equally distant in the phylogeny). For comparability between BRM and PGLS, net growth efficiencies were used in the PGLS regression after logit transformation. Since PGLS and phylogenetically non-informed models yielded very similar outputs, only the latter results are reported in the text. Last, the variation in net growth efficiency across the fish phylogeny was visualised using package 'ggtree' (Yu et al., 2017), where the state transition of efficiency from ancestral to offspring nodes was represented in the phylogenetic tree using the function 'fastAnc' in package 'phytools' (Revell, 2012).

3. Results

3.1. Growth rate covaries inversely with metabolic scaling slope across species (H1)

Metabolic scaling relationships and growth parameters were obtained for 118 teleost species comprising 23 orders (plus *Incertae sedis*), spanning over 6 orders of magnitude in body mass at which maximum growth rate was derived ($m_{g_{max}}$) across species (21 mg – 241 kg), occurring from polar to tropical zones, and covering from demersal to pelagic lifestyles (Table S3.1). Across these species, metabolic scaling slopes (b) showed a weak yet significant, negative relationship with $\log_{10}$ maximum growth rates (g_{max}) (Figure 3.2). The resulting RMA regression was defined as: $b = 0.72 - 0.12 \log_{10} g_{max}$ [95% CIs (0.69, 0.75) and (-0.15, -0.10) for slope and intercept respectively; $R^2 = 0.07$, $p = 0.003$]. The latter regression was repeated including only species for which metabolic scaling regressions covered $\geq 5\%$ of the species' ontogenetic mass range (Killen et al., 2010), and growth rates were calculated from $\geq$ 3 records in FishBase. This further screening step kept just 54 species in the analysis, though yielded a very similar yet stronger relationship between b and $\log_{10}$ maximum growth rates [RMA: $b = 0.70 (0.66, 0.74) - 0.13 (-0.17, -0.10) \log_{10} g_{max}$; $R^2 = 0.41$, $p < 0.001$]. Moreover, the best model (i.e., with the lowest AICc score) for the variation in slopes b across all sampled species incorporated $\log_{10}$ maximum growth rates and temperature as predictors, yet the latter variable showed no significant effect on b (OLS: $p = 0.267$; Table A3.1-2, see Appendix 3.4). Likewise, $\log_{10}$ maximum growth rate was included as the only predictor in the best model for the subset of 21 species for which data on gill SA scaling slopes (b_G) were available (Table

A3.3-4). Moreover, the PGLS analysis of the latter OLS regressions showed no phylogenetic signal (i.e., λ was not significantly different from 0) and so yielded nearly identical results for the species with phylogenetic data available in The Fish Tree of Life (see Appendix 3.5; Table A3.5-6).
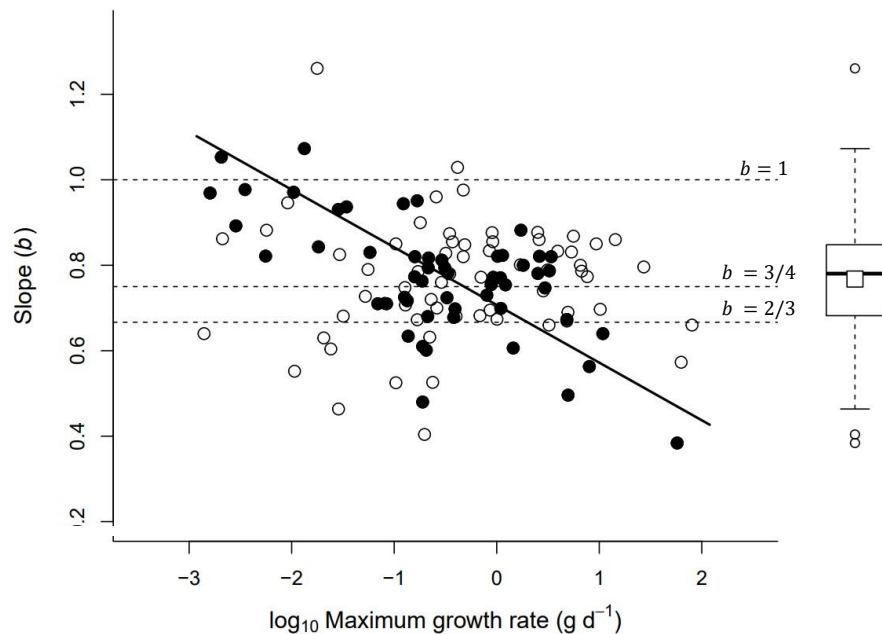
Figure 3.1. The relationship between ontogenetic metabolic scaling slopes (b) and maximum growth rates (g_{max}) across the 118 species of teleost fish compiled in this study. The line denotes the regression line of the Reduced Major Axis regression [RMA: $b = 0.72$ 95% CI (0.69, 0.75) $-$ 0.12 (-0.15, -0.10) $\log_{10} g_{max}$; $R^2 = 0.07$, $p = 0.003$]. By including only species for which metabolic scaling regressions covered $\geq 5\%$ of the ontogenetic mass and growth rate data from ≥ 3 records in FishBase (filled points, n = 54), the regression yielded a stronger relationship between b and $\log_{10}$ maximum growth rates [RMA: $b = 0.70$ (0.66, 0.74) $-$ 0.13 (-0.17, -0.10) $\log_{10} g_{max}$; $R^2 = 0.41$, $p < 0.001$]. The boxplot shows the distribution of b: mean (white square, $b = 0.756$), median (solid line within the box), 25th and 75th percentiles (box boundaries), and whiskers indicate the largest and smallest value within 1.5 times the interquartile range beyond either box boundary. Horizontal dashed lines indicate the slope b assumed in the 'Ontogenetic Growth Model' ($b = \frac{3}{4}$), as well as the upper ($b = 1$) and lower ($b = 2/3$) boundaries of b predicted by the 'Metabolic Level Boundaries Hypothesis'.

3.2. The overhead costs of growth and maintenance metabolism exhibit similar temperature sensitivity (H2)

The overhead cost of growth (C_g, mg O_2 g^{-1}) and maintenance metabolism (R_m, mg O_2 g^{-1} d^{-1}) were calculated for 114 of the total 118 sampled species, whose slopes b were less than 1 and hence fitted into the current approach (see Methods). One of the latter species (*Sebastolobus altilevis*) was excluded from the analyses due to it being the only representative of the bathy-demersal lifestyle. Among the remaining 113 species, the variation in both C_g (mean 458.50 ± 48.9 standard error, mg O_2 g^{-1}) and R_m (mean 1.52 ± 0.11 s.e., mg O_2 g^{-1} d^{-1}) covered a similar range of ca. 2 orders of magnitude.

The OLS models showed that both temperature and body mass ($m_{g_{max}}$) had significant effects on the overhead cost of growth (C_g) and maintenance metabolism (R_m) across species (Table 3.1). As expected by this approach, $\log_{10} R_m$ decreased with $\log_{10}$ body mass [β_m = -0.145, 95% CI (-0.192, -0.099), $p < 0.001$]; conversely, $\log_{10} C_g$ showed a small yet significant increase with $\log_{10}$ body mass [β_m = 0.074 (0.013, 0.135), $p = 0.018$]. Temperature exhibited similar effects on $\log_{10} C_g$ [β_T = 0.015 (0.008, 0.022), $p < 0.001$] and $\log_{10} R_m$ [β_T = 0.018 (0.013, 0.024), $p < 0.001$]. After correction at 1 g of body mass (Fig. 3.2A), C_g and R_m increased respectively with a Q_{10} value of 1.42 (1.21, 1.67) and 1.53 (1.34, 1.73) from 0 to 30 °C. Moreover, while the thermal effect was nearly identical for C_g values obtained by using actual b values and by using the general ¾ metabolic scaling [β_T = 0.015 *vs.* 0.018 (0.010, 0.026), respectively], the effect of temperature was almost doubled for R_m estimates obtained using actual *versus* $b = 0.75$ [β_T = 0.018 *vs.* 0.029 (0.022, 0.037)].

Table 3.1. Ordinary least squares models to describe the variation in the overhead costs of growth (C_g) or maintenance metabolism (R_m), as explained by body mass ($m_{g_{max}}$, g), temperature (°C), and lifestyle across the sampled species of teleost fish. All metabolic costs as well as body mass were $\log_{10}$-transformed. Results are reported as analysis of variance tables including R^2 for each model, whereas significant effects ($p < 0.05$) are shown in bold.

variable	predictor	df	*F*-value	*p*	R^2
Overhead cost of growth (C_g, mg O$_2$ g^{-1})	Body mass	1	10.865	**0.001**	
	Temperature	1	17.809	**<0.001**	0.19
	Lifestyle	3	0.844	0.473	
Maintenance metabolism (R_m, mg O$_2$ g^{-1} d^{-1})	Body mass	1	23.206	**<0.001**	
	Temperature	1	45.544	**<0.001**	0.40
	Lifestyle	3	3.672	**0.015**	

The PGLS models included 109 of the latter 113 species for which phylogenetic data were available in The Fish Tree of Life (Fig. 3.3). This model showed a negligible phylogenetic signal (i.e., λ was not significantly different from 0) for C_g, yielding nearly identical results to those from the OLS models (Table A3.7). Conversely, the PGLS analysis of maintenance metabolism did exhibit a significant phylogenetic signal (λ = 0.544), meaning that R_m tends to be similar between closely related species.

3.3. The overhead costs of growth are similar but maintenance metabolism varies among lifestyles (H3)

Lifestyle showed a significant effect only on maintenance metabolism ($p = 0.014$). After correcting for both temperature and mass (Fig. 3.2B), $\log_{10} R_m$ was significantly higher for pelagic species than for benthopelagic (HSD: $p = 0.024$) and demersal species (HSD: $p = 0.011$). Indeed, the mean maintenance metabolism of pelagic species (3.78 ± 0.42 s.e., mg O$_2$ g^{-1} d^{-1}) was ca. 1.6-fold higher than that of benthopelagic (2.39 ± 0.19 s.e., mg O$_2$ g^{-1} d^{-1}) and demersal species (2.38 ± 0.24 s.e., mg O$_2$ g^{-1} d^{-1}). In contrast, by using the general ¾-power scaling, pelagic species exhibited significantly higher $\log_{10} C_g$ and $\log_{10} R_m$ than benthopelagic (HSD: $p = 0.004$ and $p < 0.001$, respectively) and demersal species (HSD: $p = 0.01$ and $p < 0.001$). Furthermore, the PGLS model showed that lifestyle was only marginally significant ($p = 0.053$, Table A3.7), indicating that the differences between lifestyles found in the OLS model

might be influenced by closely related species sharing similar levels of maintenance metabolism.
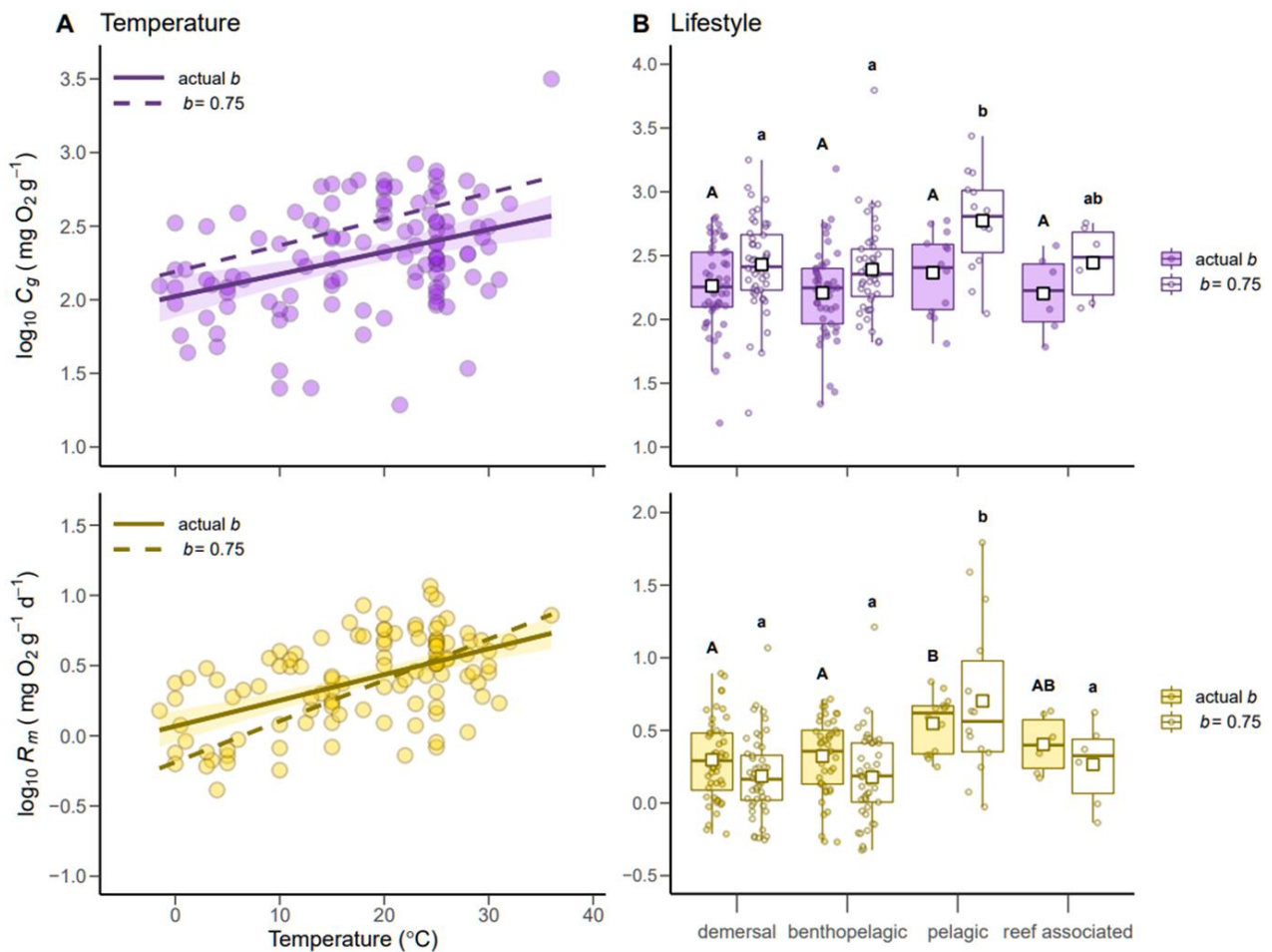
Figure 3.2. The variation in metabolic cost of growth (C_g, upper panels) and maintenance metabolism (R_m, lower panels) with: (**A**) temperature, after body mass correction at 1g; and (**B**) lifestyle, after correction at a temperature of 15°C and body mass of 1g. In A, lines and colour bands denote regression lines and 95% confidence intervals of the OLS models. Thick and dashed lines respectively indicate model predictions using either actual slopes b from species-specific scaling relationships, or a general ¾ metabolic scaling ($b = 0.75$) for all species. In B, boxplot symbols as in Fig. 3.1. Filled and empty boxes respectively indicate whether C_g and R_m were calculated using actual b values or the general ¾ scaling. Significant differences between lifestyles using either actual b values (upper case) or a general $b = 0.75$ (lower case) are indicated by different letters (Tukey's HSD, $p < 0.05$).

3.4. Net growth efficiency is independent of body size, lifestyle, and phylogenetic relatedness (H4)

The net growth efficiency averaged, in percentage, 25.20 ± 1.21 % and varied ca. 17-fold among teleost species (Fig 3.3). Temperature only showed a weak negative effect on growth efficiency [BRM: $t = -2.96$, $\beta_T = -0.019$ (-0.032, -0.0065), $p = 0.003$, pseudo-$R^2 = 0.09$], which decreased 11.69% from 0 to 30 °C, according to this model. As for C_g, the PGLS model showed no phylogenetic signal (i.e., $\lambda = 0$) for net growth efficiency (Table A3.8). Last, while the estimates obtained using actual slopes b and the general ¾ scaling were overall similar for demersal, benthopelagic and reef-associated species along climate zones, the estimates for pelagic species showed opposite trends from cold to warm climates between these methods. This difference was especially pronounced for tropical, pelagic species, whose growth efficiencies were on average ca. 4.7 times lower when using the general $b = 0.75$ instead of the actual b of species.
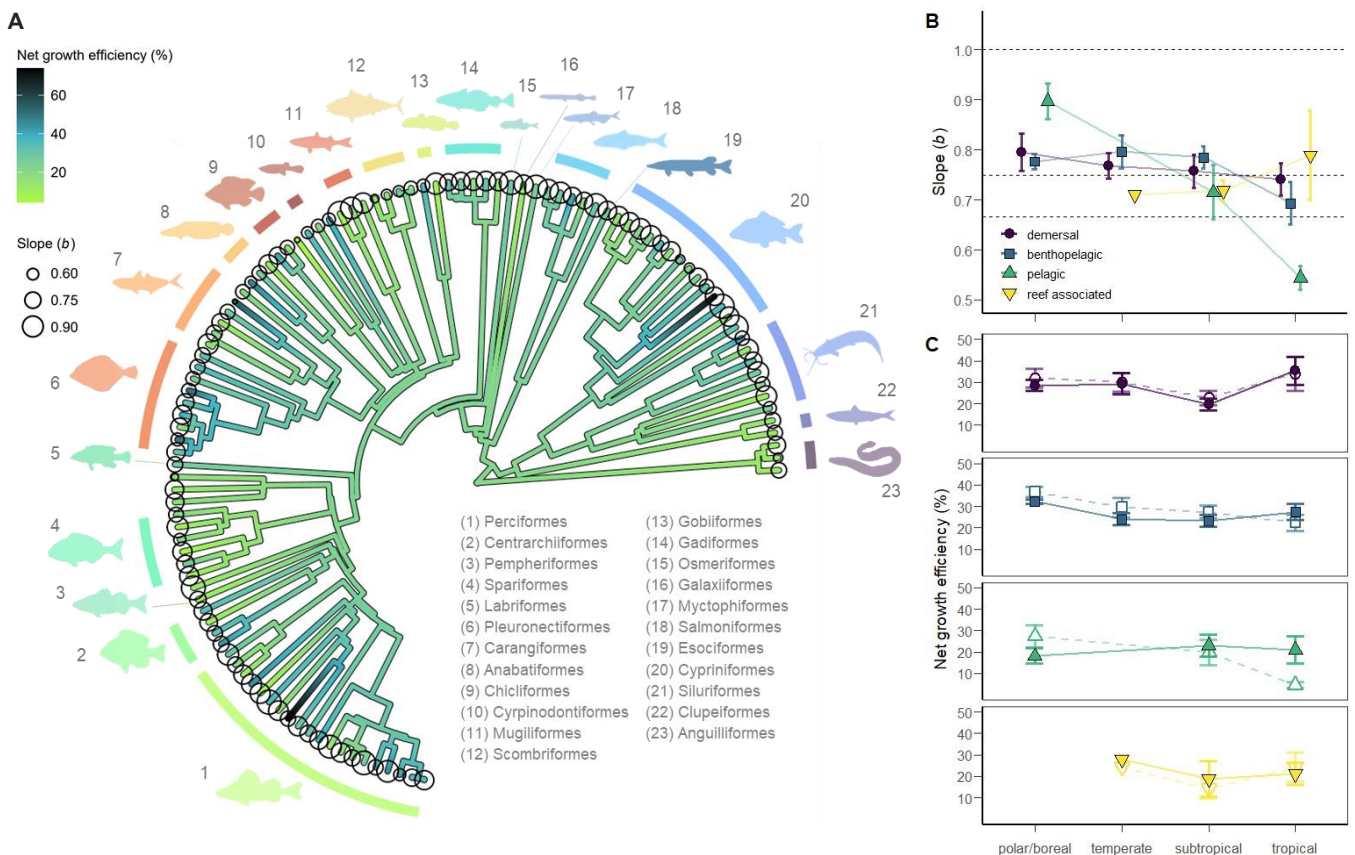
Figure 3.3. The phylogeny of teleost fish used in this study (**A**), comprising species from 23 orders (plus *Incertae sedis*), spanning over 6 orders of magnitude in body mass, exhibiting lifestyles from demersal to pelagic, and occurring from polar to tropical waters. Four species are missing in this tree due to lack of phylogenetic data. Point size shows the ontogenetic

metabolic scaling slope *b* of species. Branches are coloured by gradient projection from ancestral nodes to offspring nodes, whereas colours reflect the variation in net growth efficiency, from light (low efficiency) to dark green (high efficiency). Right panels show the variation in mean (± s.e.) slopes *b* (**B**) and net growth efficiency (in percentage) (**C**) between lifestyles and climate zones. Horizontal dashed lines in B are as in Fig. 3.1. In C, two sets of growth efficiencies are shown for each lifestyle, indicating whether estimates were obtained using actual slopes *b* (filled symbols and thick lines) or the general ¾ metabolic scaling for all species (empty symbols and dashed lines).

4. Discussion

Across a variety of teleost fish with widely different thermal preferences and lifestyles, the ontogenetic mass-scaling of metabolic rates decreased with maximum growth rates (Fig. 3.1). This supports the GSH prediction that differences in resource demands of growth may underpin the interspecific variation in metabolic scaling (Tan et al., 2019). This hypothesis may be considered an alternative or complementary explanation to the surface-area related influences on resource supply proposed by the MLBH (Glazier, 2005, 2010, 2014; Killen et al., 2010). Moreover, the overhead costs of growth and maintenance metabolism exhibited similar thermal sensitivities (Fig. 3.2A), suggesting that the relative contributions of these two energetic demands to resting metabolism remain invariant within the temperature range studied here across species. Maintenance demands, by contrast, were higher in pelagic species than in more sluggish lifestyles (Fig. 3.2B). Finally, my results indicate that net growth efficiencies are relatively conserved among teleost fishes living under extremely different ecological pressures (Fig. 3.3), but also highlight the importance of the interspecific variation in metabolic scaling to quantify energy requirements in these species.

4.1. Metabolic scaling slopes decrease with growth rates across teleost fishes

As expected by the GSH, the scaling slopes *b* showed a downward trend from 1.07 to 0.48 as maximum growth rates increased ca. 5 orders of magnitude across 118 teleost species (Fig. 3.1), revealing that mass-specific metabolic rates at rest decrease more steeply over ontogeny in species that achieve faster growth. The wide variability observed in the latter relationship ($R^2 = 0.07$) was substantially reduced after excluding species with sparser data ($R^2 = 0.41$). This further screening step yielded an almost identical trend between *b* and growth rates, thus supporting the slope of this relationship (Fig. 3.1). Besides effects of data quality, the extensive variation in slopes *b* here may be related to differences in mass-scaling of growth

rates between species (Glazier, 2020), which were not considered here. Indeed, according to the GSH (Tan et al., 2019), not only the variation in relative contribution of growth demands to metabolism, but also in the mass-scaling of these demands may underpin differences in metabolic scaling. Mass-specific growth rates tend to decline linearly with body mass when plotted on a log-log scale, whereas the negative slope of this relationship usually ranges between -0.3 and -0.5 in teleost fishes (reviewed in Imsland & Jonassen, 2001), but stark differences in this slope also occur between co-occurring species. For instance, in the bluefish *Pomatomus saltatrix*, mass-specific growth rates exhibit a much steeper decline during ontogeny than in flounders *Platichthys flesus* (slope: -0.88 *vs*. -0.29, respectively; Buckel et al., 1995; Fonds et al., 1992), which may lead to differences in mass-scaling of metabolic demands and hence slopes *b*, even if the relative contribution of growth demands at $m_{g_{max}}$ to metabolism was the same in both species.

Furthermore, I found that the variation in scaling slope (*b*) among species was better explained by maximum growth rate, rather than by temperature, metabolic level, or mass-scaling of gill SA, as evidenced by the best OLS models that always incorporated maximum growth rates as predictor of *b* (Appendix 3.4). Altogether, these results suggest that growth rates and so final sizes have adaptively co-adjusted to different environmental pressures in teleost fish (Winemiller & Rose, 1992; Sibly et al., 2015), which led to various patterns of metabolic scaling between species (Glazier, 2015). In effect, large species in this dataset (i.e., upper quartile of body mass at maximum growth, mean = 15,643 g) exhibited on average the highest maximum growth rate and the lowest slope *b* (12.22 ± 3.69 s.e. g d^{-1}; *b* = 0.74 ± 0.02), whereas small species (lower quartile, mean = 30 g) exhibited the slowest maximum growth rate and highest *b* (0.05 ± 0.01 g d^{-1}; *b* = 0.82 ± 0.03). All else being equal (e.g., resource availability, predation pressure), a relatively higher growth investment might explain shallower metabolic scaling in large species, according to the GSH. However, a complementary explanation may be possible if growth rate, and so its metabolic demands, are more surface area-related than maintenance, due to the influence of exchange surfaces on the mobilisation of body reserves needed for growth (Kooijman, 2010, Maino et al., 2014). In such case, large species allocating greater fractions of metabolic energy into growth would be more influenced by SA-related processes than small species, thus leading to lower slopes *b* as expected by the MLBH.

4.2. Temperature affects similarly the costs of growth and maintenance metabolism

According to my second prediction (H2), the overhead costs of growth (C_g) and maintenance metabolism (R_m) showed similar increases with temperature after accounting for body mass (Q_{10} = 1.42 and 1.53, respectively; Fig. 3.2A). These metabolic demands showed lower Q_{10} values than those previously found for resting metabolic rates among teleost fishes (Q_{10} = 1.83 – 1.91; Clarke & Johnston, 1999; Killen et al., 2010). Moreover, the similar thermal sensitivity between costs of growth and maintenance indicates that the relative contribution of these demands to metabolism would remain unchanged in species with identical growth rate and body mass, regardless the temperature they live at. Hence, the argument that C_g is disproportionally higher in warm-water species compared to R_m could not explain the decrease in scaling slopes (*b*) with temperature observed across species in teleost fish (Killen et al., 2010). Interestingly, Barneche & Allen (2018) reported a similar range of overhead costs of growth for teleost fishes to this study, yet they estimated a 22-fold increase in C_g from 0 to 30 °C within fish families, whereas C_g here only increased ca. 3-fold over the same temperature range across species. This contrasting result may be due to the different taxonomic levels at which these comparisons were made, as increasing evolutionary time – from variation within families (Barneche & Allen, 2018) to across species (this study) – implies that fishes may have diverged more independently of temperature (Clarke, 2004; Jutfelt, 2020). Additionally, although both studies are based on similar data and methods, Barneche & Allen (2018) applied a general ¾ mass-scaling of metabolic rates to obtain C_g, which may also affect the estimation of growth demands (see discussion below).

4.3. Lifestyle shows no effect on the costs of growth, yet pelagic fishes exhibit higher maintenance metabolism

In contrast with H3, I found that C_g was largely independent of lifestyle (Fig. 3.2B), after accounting for both mass and temperature. Overall, the results for C_g suggest that differences in growth rate and its energetic demands among species, rather than other costs related to thermal regime or lifestyle, contribute to the interspecific differences of slopes *b* seen in resting fish. This finding also agrees with empirical evidence of similar overhead costs of growth among species at comparable life stages (Wieser, 1994; Clarke, 2017). Conversely, the mass- and temperature-corrected maintenance metabolism (R_m) for species with pelagic lifestyles was significantly higher than for benthopelagic and demersal species. These results

suggest that, while the metabolic costs of achieving certain growth rates are adapted to specific selective pressures (Brandl et al., 2023), increased maintenance demands may have evolved in species with higher activity levels.

In effect, fish living in sunlit, pelagic zones experience stronger selective pressures from predation than other species, which requires faster and more sustained swimming to capture prey. Hence, pelagic fishes may have adapted to sustain high locomotory capacities (Killen et al., 2010, 2016). The athletic performance of these species involves energy-costly organs, such as protein-rich muscles, as well as large hearts and gill surface-area (Muir & Hughes, 1969; Brill, 1996; reviewed in Killen et al., 2016), whose maintenance requirements are higher than in more sluggish counterparts, even when fish are compared at rest. Likewise, athleticism implies higher mitochondrial densities (Hoppeler et al., 1987; Johnston et al., 1998; Burpee et al., 2010) and increased proton leakage across mitochondrial membranes (Brand, 1990), which can decrease ATP synthesis relative to oxygen consumption by the mitochondria (Koch et al., 2021). Although this might be seen as low metabolic performance, high proton leakage can decrease protonmotive forces and hence reduce the production of reactive oxygen species by mitochondria, thus reducing oxidative stress (Koch et al., 2021), which might be advantageous in open, well-oxygenated waters (Verberk & Atkinson, 2013). Moreover, as occurs in endotherms, increased proton leak can also produce metabolic heat (Koch et al., 2021), which may be useful for pelagic fishes (Carey et al., 1971; Block, 1991; Block & Finnerty, 1994), as in dolphinfish or some scombrids included in this dataset, to maintain the temperature of specific organs (e.g., locomotory muscles or brain) above water temperature, thus enhancing swimming and response capacity (Killen et al., 2016).

4.4. Growth efficiency is conserved across teleost species

According to the prediction (H4) that species possess equivalent growth performance at steady state (Brandl et al., 2023), I found that net growth efficiency was largely independent of body size, lifestyle, and phylogenetic relatedness, yet efficiencies decreased slightly with temperature. These results indicates that growth efficiency may have converged within a narrow range over teleost evolution, as it varied ca. 17-fold compared to the ca. 60,000-fold variation in maximum growth rates among species with widely different body sizes, ecological niches, and taxonomic affiliations (Fig. 3.3). A similar independence of growth efficiency from species body size has been observed within other major taxa, including protists, ectotherms,

mammals, and plants (Banse, 1979; Hatton et al., 2019). However, for the range of net growth efficiencies observed here in teleost fishes (congruent to previous estimates in aquatic ectotherms, including fish; Welch, 1968), the declining trend with temperature suggests that, even after long-term evolutionary adaptation (Clarke, 2004), warm-water species require more assimilated energy than cold-water species to produce a gram of body mass.

4.5. The adaptive significance of interspecific variation in metabolic scaling

The mean metabolic scaling slope across all teleost fishes compiled here ($b = 0.77 \pm 0.01$ s.e.; Fig. 3.1) was very close to the predicted ¾ power scaling in the OGM (West et al., 1997, 2001). However, systematic deviations from this average slope do occur among climate zones and lifestyles (Killen et al., 2010; Fig. 3.3B), where b tends to decrease from cold to warm waters. Consequently, when these differences in metabolic scaling are ignored and $b = $ ¾ is assumed, the mass-corrected maintenance metabolism (R_m) is expected to increase with temperature about twice as much as when actual, species-specific b values are used to estimate R_m (Fig. 3.2A). In other words, the maintenance demands of cold-water fishes could be underestimated when their relative steep slopes b compared to their counterparts in warmer climates are overlooked (mean $b = 0.81 \pm 0.02$ *vs*. 0.76 ± 0.01, respectively). Following reasoning from the GSH (Tan et al., 2019; see also Glazier, 2005, 2015), not only slow growth, but also relatively large contributions of maintenance metabolism can lead to steep metabolic scaling when self-maintenance functions are a major part of total metabolism. I here argue that such high b values in cold-water fish are not just statistical noise (Glazier, 2022a) but may indeed reflect a greater contribution of tissue maintenance to the resting metabolism in these species.

Similar to pelagic species, cold-adapted fishes possess high mitochondrial densities (Johnston et al., 1998; Pörtner, 2002), as well as highly duplicated genes for antifreeze glycopeptides compared to other fish (Clarke & Johnston, 1996; Peck, 2020). In effect, among the highest mitochondrial volume densities in vertebrates are observed in nototheniids, a family of cold-adapted fishes that radiated in the Antarctic Ocean (Clarke & Johnston, 1996), and whose representatives in this study exhibited relative high scaling slopes ($b = 0.83 \pm 0.05$). Moreover, many of the duplicated protein-coding genes in cold-water species are involved in protein folding, which seems especially difficult in fish living at low temperatures, as reflected

by the low fractions of newly synthesised proteins retained relative to warm-water fish (Clarke, 2017). The high turnover of misfolded proteins should thus require a major fraction of metabolic energy available in these organisms, at the expense of energy needed for synthesis of new tissue (Clarke, 2017; Peck, 2018). A neat example of this energy trade-off hypothesis may be seen among the pelagic species studied here. Whereas the Antarctic silver fish *Pleuragramma antarctica* and the Atlantic bluefin tuna *Thunnus thynnus* exhibited similar costs of growth (mass- and temperature-corrected C_g = 270.28 *vs.* 239.62 mg O_2 g^{-1}, respectively), the maintenance metabolism for silver fish was twice as high as that for bluefin tuna (mass- and T-corrected R_m = 4.48 *vs.* 2.13 mg O_2 g^{-1} d^{-1}). Consistent with the GSH, silver fish and bluefin tuna showed stark differences in mass-scaling of metabolic rates (b = 0.93 *vs.* 0.66), which may reflect the different energy allocation between tissue maintenance and growth in these species (Tan et al., 2019).

Remarkably, despite the considerable variation in b between species (b = 0.38 to 0.98), their estimated overhead costs of growth (C_g) and net growth efficiencies were generally similar, whether these were obtained using the actual b values or the general ¾ -power scaling, except in pelagic species. Indeed, excluding the wide variation in slopes b among pelagic fish (b = 0.38 to 0.94), the average C_g appears to be significantly higher for these species than for other lifestyles (Fig. 3.2B), whereas net growth efficiency declines from cold to warm climates (Fig. 3.3B), being especially low in tropical species. Overall, the differences arising from using actual b values or a general b = 0.75 reveal the importance of accounting for the variation in metabolic scaling (as seen in pelagic or cold-water fish), especially in quantitative models aiming to describe the energetic requirements of species.

Chapter 4: The cost of biomass production changes during ontogeny and between reproductive modes in a model crustacean

The cost of biomass production changes during ontogeny and between reproductive modes in a model crustacean

Abstract

The relationship between metabolic rate and body mass (often termed metabolic scaling) describes the change in energy use with organismal size, and varies widely across all levels of organisation. Within species, metabolic scaling usually shifts during ontogeny and differs between sexes. To explain such variation, the emphasis has been placed on changes in rates of biomass production with body mass, whereas the metabolic costs of synthesising new tissue are generally assumed invariant. Concomitantly, the cellular mode of growth of organisms, generally dictated by cell multiplication early in ontogeny and later by cell expansion, may influence either resource-supply capacity per cell or the costs of supply to cells, thus affecting the costs of production. Using a well-known model crustacean, *Artemia franciscana*, I here investigate how the relationships between rates of metabolism and biomass production during ontogeny and reproduction may align with changes of cellular growth seen in this species. My findings show synchronous shifts in metabolic scaling and growth trajectory over ontogeny. Moreover, the cost of growth increased between larvae and post-larval individuals, which may reflect the transition from predominant cell multiplication to expansion during *Artemia* growth. Metabolic scaling differed between single males and females, likely due to steep mass-scaling of developing eggs and longer post-maturational growth in females, yet no sexual difference in metabolic scaling was found in reproductive individuals. My results suggest that reproduction demands and their mass-scaling may converge between reproductive individuals due to increased activity of mating, but also due to the ability of females to switch reproductive mode and so change offspring production costs. Overall, these results indicate that biomass production as well as its associated costs can vary between ontogenetic phases and during reproduction, and hence lead to different metabolic scaling patterns.

Keywords: Metabolic rate; Body mass; Allometric Scaling; Ontogeny; Arthropods; Growth; Reproduction; Physiology; Costs of Production; Cellular Mode of Growth

1. Introduction

All life forms depend on metabolism to transform energy and materials into new biomass (Gillooly et al., 2001). Metabolic rate is strongly associated with body size (M), whose relationship can be described as a power function, $R = am^b$ (Kleiber, 1932; Bertalanffy, 1957), where a is the scaling coefficient, and b is the scaling exponent, or allometric slope in a linear regression between log R vs log M. The existence of a universal slope value of ¾ (Hemmingsen, 1960; West et al., 1999; Savage et al., 2004) has been increasingly challenged by growing evidence of variation in the scaling exponent (e.g. White et al., 2007; DeLong et al., 2010; Glazier, 2022a), particularly within species (Bokma, 2004; Glazier, 2005). Indeed, metabolic scaling generally changes over ontogeny and between sexes, yet the underlying mechanism(s) of this variation remain under debate (Wieser, 1984, Glazier, 2005, 2020; Somjee et al., 2022). Understanding how and why intraspecific metabolic scaling varies is crucial in ecology, since this variation is intrinsically linked to changes in organismal physiology, biomass production, and ecological energetics (Gould, 1966; Glazier, 2005; Glazier et al., 2015).

Metabolic scaling slopes shift over ontogeny in many diverse species, from copepods to humans (Wieser, 1984; Glazier, 2005, 2014; Glazier et al., 2015). These shifts generally entail steep metabolic scaling (i.e., high slope b) during early postembryonic (e.g., larval) ontogeny and shallow scaling (low b) later in ontogeny (Glazier, 2005). Since maintenance costs such as tissue turnover or regulation of ion gradients are typically assumed to be constant on a mass-specific basis over ontogeny (Glazier, 2005; Moses et al., 2008; Kooijman, 2010; see empirical evidence, e.g., Vahl, 1984; Nielsen et al., 1995; Rombough, 2006), these energetic demands are not expected to underpin ontogenetic changes in slopes b. Building new mass, by contrast, requires a substantial amount of metabolic energy that varies following changes in biomass production as organisms enlarge (Parry, 1983; Wieser, 1994); hence, these costs have been hypothesised to explain shifts in metabolic scaling over ontogeny (Glazier, 2005). Rapid and accelerating mass-specific growth as size increases during early ontogeny is therefore linked to steep increases in metabolic rate with body mass (e.g., Kamler, 1992; Sears et al., 2012), whereas slower, declining growth later in ontogeny is associated with shallower increases of metabolic rate with size (Riisgård, 1998; Glazier, 2005, 2014, 2022). The production of offspring in adults, on the other hand, may also lead to differences in slope b between sexes (Somjee et al., 2022). Although the overall energy contribution towards

reproduction (i.e., mating, egg production, etc.) has been shown to be similar between sexes (Parker et al., 2018), the energy invested by females in offspring production (e.g., egg production or brooding) can scale particularly steeply with body mass (Barneche et al., 2018). Despite the considerable contribution of growth and reproduction to energy expenditure of organisms (Marshall & White, 2019b), metabolism and biomass production are rarely studied simultaneously during ontogeny or in different sexes, hindering a mechanistic explanation of intraspecific variation in metabolic scaling.

The cellular mode of growth (i.e., cell multiplication *versus* expansion) may underpin changes in biomass production by influencing either resource supply or cost per unit supply to cells, which is hypothesised to ultimately affect metabolic scaling (Kozłowski et al., 2003; Glazier, 2022b) (Fig. 4.1). Developing embryos generally grow by cell multiplication with reduction in cell size (Wesley et al., 2020), producing smaller cells with greater surface-area (SA) relative to body volume (V) or mass, which may underpin hyper-allometric increases in metabolic rate with body mass ($b > 1$; Oikawa et al., 1991; Rombough, 2006; Gaitán-Espitia et al., 2013). During postembryonic development, rapid, often exponential growth is generally associated with a greater contribution of cell multiplication relative to cell expansion (i.e., hypertrophy) (Goss, 1966; Alami-Durante et al., 1997; Arendt, 2000). Compared with growth by cell enlargement that reduces total cell SA/V ratio, multiplication of cells of similar size maintains total cell SA/V as organisms enlarge, hence enabling faster cell (and organismal) growth per unit resource supply to the cell exterior, which could explain metabolic rate increasing exponentially (i.e., isometrically with body mass; $b = 1$). Body shape change can also support fast growth during early ontogeny in some skin-breathing organisms that flatten or elongate as they grow, keeping high SA/V and hence resource supply (Glazier, et al., 2015). Conversely, declining growth later in ontogeny, generally by cell expansion (Goss, 1966; e.g., Higgins & Thorpe, 1990), implies a decrease in cell SA/V and greater intracellular transport of resources, associated with a declining cell and organismal growth rate per unit of resource supply, or greater cost of supplying sufficient resources to maintain a given growth rate. A deceleration in organism growth rate associated with a shift to relatively more cell expansion could therefore contribute to a deceleration in metabolic rate with body mass ($b < 1$) (Arendt, 2007). Arguably, cell multiplication can increase intercellular (or extracellular) transport; yet the absolute intercellular transport will be also greater in large, adult individuals with similar

amount (yet larger size) of cells in comparison to small, juvenile organisms. After growth ceases (or is replaced by reproduction as a dominant energetic cost), the slope *b* can also vary between sexes due to differences in reproductive investment (Somjee et al., 2022). Females continue producing biomass as ovarian tissues and offspring, involving again increases in cell density during embryo formation (Fig. 4.1), which may elevate *b* in gravid individuals (Moffett et al., 2022). Therefore, I examine here the relationships among rates of biomass production and metabolic rate during juvenile ontogeny and reproduction, to see how they align with changes in cellular growth mechanisms.

While the energetic costs involved in the bond formation of macromolecules seem largely invariant across life forms (ca. 0.08 Joules of metabolic energy are needed for 1 J of protein), the associated costs with building those macromolecules and assembling new tissues may vary among organisms (Wieser, 1994; Clarke, 2017, 2019). These associated costs of biosynthesis generally exceed by 3-fold the costs of bond formation, and comprise actions such as RNA processing or the transport of monomers from reserves to cells, and of ATP within these cells. Because biomass production entails many processes for which energy requirements are unknown, the cost of production can currently only be estimated empirically. This estimation is generally achieved by determining the relationship between the mass-specific rates of production (on the x-axis) and metabolism (on the y-axis) (both in energy units), and assuming that production costs are additional to other metabolic costs, such as body maintenance or routine activity (Rombough, 2011; Clarke, 2017). For instance, this relationship showed a slope of ~ 0.32 across a variety of ectotherms, indicating that in the synthesis of 1 J of new mass approximately 0.32 J of energy is dissipated as heat through respiration, so the total energy needed to produce that mass is 1.32 J (Wieser, 1994; Clarke, 2017, 2019).

Because the production of new mass involves the energetic demands of transporting materials within the organism, sustaining rapid growth might be less energetically costly during early ontogenetic phases than in late juveniles and adults, whose lower cell SA/V and longer intracellular transport distance in larger cells, may require more metabolic energy to achieve the same growth rate. Indeed, within early life-stages, the fastest growing phases exhibit

generally the lowest costs of growth (i.e., energy demands per unit of new tissue), as observed in insect larvae like caterpillars (Sears et al., 2012; Ferral et al., 2020). Likewise, the metabolic demand per unit growth in fast-growing fish larvae is lower than in larger, older juveniles (Kiørboe et al., 1987; Conceição et al., 1998), whereas these costs are sometimes unaltered with further increases in growth rate in larvae (Wieser, 1994; Rombough, 1994, 2011). Conversely, during metamorphosis in flatfish, growth rates are substantially reduced but energetic costs increase, whereas fish grow by cell expansion throughout this process (reviewed by Geffen et al., 2007). Sustaining high growth rates after post-larval ontogeny can therefore increase steeply the costs of growth, yet rapid growth can be crucial for fitness of young individuals, so they can overcome early mortality, mature, and reproduce sooner (Dmitriew, 2011).

The cost of offspring production in adults, on the other hand, may differ not with the mechanism of adult growth, but with mode of reproduction, as viviparity (embryos develop inside females body) entails greater energetic demands than oviparity (embryos develop externally inside eggs) (Angilletta & Sears, 2000). Whereas developing embryos require high resource supply from females that increases steeply as embryos grow, egg production is considered as the encapsulation and release of body reserves with low metabolic activity (Kooijman, 2010; Maino et al., 2017), and hence is much energetically cheaper than the production of embryos.

The well-studied crustacean genus of *Artemia* provides an ideal model to explore the variation in metabolic rates with biomass production because (*i*) the cellular mode of growth changes from cell multiplication to cell differentiation and expansion during development (Manzanares et al., 1993; Freeman, 1986, 1995, 2005); (*ii*) mass-specific growth rates shift over ontogeny from increasing to then declining with body size (Evjemo & Olsen, 1999); (*iii*) reproductive investment differs between sexes, and (*iv*) females can switch from oviparity to ovoviviparity, producing either cysts or larvae during their lifetimes. This group comprises continuous filter-feeding species that inhabit salt marshes and lakes, where individuals experience major morphological and ecological changes during ontogeny (Provasoli & Shiraishi, 1959; Reeve, 1963; Gajardo & Beardmore, 2012). Larvae possess only one or two undeveloped segments at hatch, and start feeding using antennae (Barlow & Sleigh, 1980)

forming swarms near the surface, and are thus exposed to predators (Gulbrandsen, 2001). Throughout nineteen postembryonic stages, the remaining body segments and limbs develop and take over feeding (Schrehardt, 1987; Evjemo et al., 2000), whilst developed individuals migrate to deeper waters during daytime (Bradley & Forward, 1984; Britton et al., 1986). Moreover, to ensure offspring survival, females switch reproductive mode following environmental cues (Versichele & Sorgeloos, 1980; Gajardo & Beardmore, 2012). Under favourable conditions, fertilised eggs predominantly develop into swimming larvae; but under extreme conditions, early embryos are surrounded by a thick shell and enter a dormant state as a cyst that withstands such conditions (Stappen, 1966). Therefore, as in other organisms that live in changing environments, differences in metabolic costs of biomass production during development or between reproductive modes possess a high adaptative relevance in *Artemia*.

Here, I investigate whether variation in biomass production rates and its associated costs during ontogeny and between sexes may lead to changes in metabolic scaling (Glazier, 2005). Using a model crustacean, *Artemia franciscana*, I measure the rates of biomass production and metabolism at high resolution over ontogeny and between sexes. Specifically, I formulate two main hypotheses. First, the metabolic scaling of individuals growing exponentially during postembryonic ontogeny (i.e., larvae) may be steeper (higher *b*) than that of post-larval individuals, whose mass-specific growth and associated metabolic costs decline with body size (H1a). This change in slope *b* during ontogeny of *A. franciscana* may be associated with a shift from relatively fast but less energy expensive growth by cell multiplication during early ontogeny to slower but more costly growth involving relatively more cell differentiation and expansion as body structures develop. Consequently, I expect that the energy cost per Joule of new tissue produced may increase between early (larval) and later (post-larval) phases (H1b), as cell expansion in the latter should involve higher metabolic demands to supply and transport resources during growth. Second, I hypothesise that females possess steeper *b* than males, as the former develop eggs and offspring, whose energetic demands may increase steeply with body mass (H2a). Moreover, I expect that metabolic costs differ depending on reproductive mode, as producing larvae involves the high energy demands of developing embryos compared with releasing dormant cysts (H2b). My findings show a synchronous shift in metabolic and growth rates during ontogeny, where the cost of growth is higher after the juvenile phase than during the earlier larval and juvenile periods, as expected

from the ontogenetic change in cellular mechanisms of growth and their associated costs. I also find that females exhibit higher metabolic scaling slope *b* than males in single individuals (i.e. those not in a reproductive pairing), likely reflecting the steep mass-scaling of energetic demands from developing eggs and longer post-maturational growth. However, allometric slopes *b* in reproductive individuals are similar, suggesting that costs associated with reproduction, such as increased activity during mating as well as the ability to swift between reproductive modes with variable costs in females, may affect *b* similarly between sexes. Indeed, I finally show that the costs of offspring are dictated by larval production but not by cysts, revealing an energetic trade-off between reproductive modes.
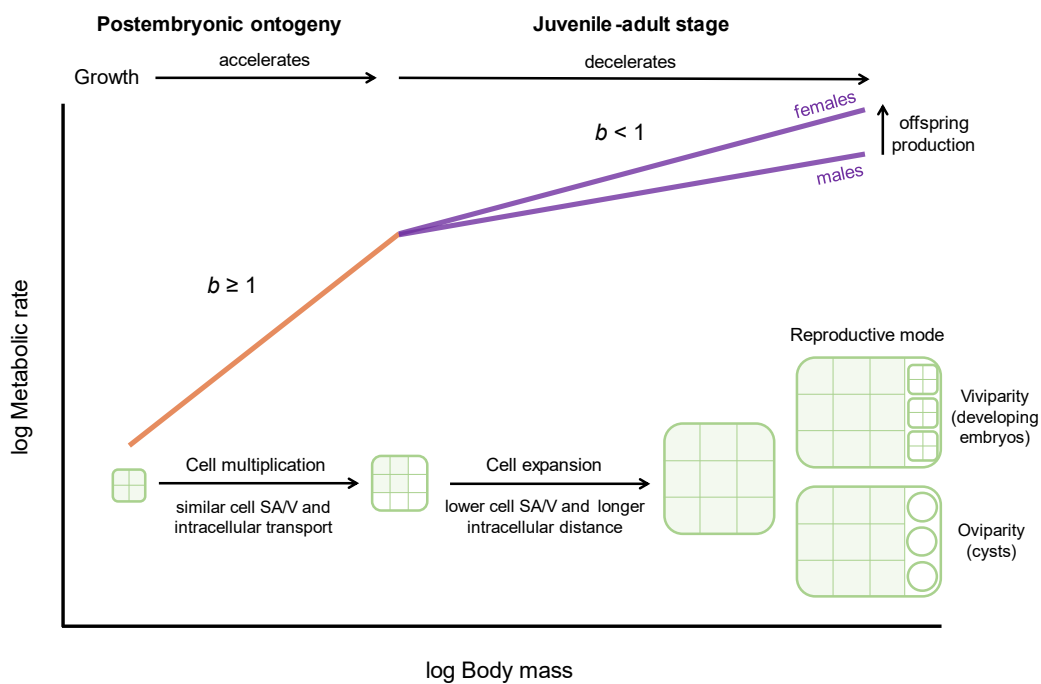
Figure 4.1. Schematic of the variation in metabolic scaling with body mass during ontogeny and between sexes. Steep, often hyper-allometric metabolic scaling ($b \geq 1$; red) typically occurs during postembryonic ontogeny, and is thought to fuel rapid, accelerating growth rates with body size. Conversely, hypo-allometric scaling (low $b < 1$; purple) tends to occur later in ontogeny, when growth declines with body size in juveniles and adults. The cellular mode of growth is hypothesised to underpin this shift in metabolic scaling (Glazier, 2022b), by influencing either average resource-supply capacity per cell or cost per unit supply to cells, hence organismal growth. During postembryonic ontogeny, a greater contribution of cell multiplication relative to cell expansion facilitates maintaining total cell surface-area (SA) relative to body volume (V) and similar intracellular transport distances, keeping high resource supply to cell growth with increasing size, and may result in higher *b* than later in ontogeny (H1a). Later in ontogeny, by contrast, growth involves greater cell differentiation and expansion that leads to lower SA/V and longer intra-cellular transport distances, thereby either decreasing resource supply or potentially increasing costs of maintaining a given resource

supply per cell V as cells and individuals enlarge (H1b). Among juveniles and adults, *b* may also differ between sexes due to the energetic costs of developing eggs in females, which are expected to increase steeply with body mass (H2a). Moreover, reproductive mode can influence offspring costs (H2b), as the increase of cell density in developing embryos (viviparity) would entail higher resource demands in gravid females than releasing eggs or cysts (oviparity).

2. Material and Methods

2.1. Animal rearing

Batch cultures of *Artemia franciscana* were set up using decapsulated cysts collected from the Great Salt Lake (Utah, USA), provided by Waterlife ®. A total of ca. 3000 cysts were placed in 1L beakers containing artificial seawater with salinity 33 ppt (Tropic Marin® PRO-REEF) at 26 °C and constant illumination. Experimental water was treated with pH buffer (Easy Life®) to maintain pH and alkalinity conditions over time in the cultures. Air stones in each beaker gently mixed and aerated the water. Experimental temperature was controlled using a water bath (Grant SUB Aqua 26) held within $\pm$ 0.2 °C. After hatching (day 0), 600 nauplii (stage 0 and 1) were transferred into separate 1L beakers (batch cultures). Animals were fed an algal blend for *Artemia* (RG Complete, Reef Nutrition ®) *ad libitum*, by supplying daily 0.5 mL of blend mixed with 10 mL of water, such that a green colour was always sustained in the Cultures. Cultures were grouped into three phases following distinct periods in the ontogenetic development of *A. franciscana* (Weisz, 1946): (1) torathic phase (stages 0 to 11), when thoracic segments and their limbs are formed; (2) abdominal phase (stages 12 to 18), when abdominal segments and limbs are developed; and (3) post-larval phase (stage 19), when larval development is completed and individuals mature sexually. To keep water conditions and food concentration nearly constant (Evjemo & Olsen, 1999), culture densities were decreased to 0.3 individuals mL^{-1} when animals reached phase 2, and further reduced to 0.08 – 0.1 ind. L^{-1} in phase 3. Water was replaced on day 3, 7 and 10 coinciding with the start of each culture dilution in phases 1 and 2, and then weekly during phase 3. Measurements of individual animals (described below) were taken from at least two different beakers in each of the three developmental phases, totalling 5 batch cultures from independent starts.

Individuals were monitored for 1 to 5 days (depending on body size) to capture growth and development in animals of a wide size range, by using cylindrical cages made of plankton

net mesh, which floated in the cultures (Fig. 4.2A). These cages allowed water and food to move through the mesh but prevented individuals from escaping (see Appendix 4.1). Cage sizes were matched to accommodate the range of body sizes, ensuring that animals could swim and forage naturally during the monitoring periods. Body length and developmental stage were recorded before and after this period during which metabolic rates were measured; these animals were not returned to the culture so that each individual was measured only once. Development stage (from 1 to 19) was determined according to the method of Weisz (1946), using the number of mature segments and mobility of their limbs (Forster & Hirst, 2012).

2.2. Growth rate

Animals were photographed under a stereomicroscope for length measurements before and after the monitoring period using the Motic Images Plus 2.0 software. Body length was measured from the anterior tip of the head to the base of the caudal furcae (Reeve, 1963). Length measurements were then converted into dry mass using the empirical scaling equation between body length (mm) and dry body mass (µg) given in the Appendix. Similar to Forster & Hirst (2012), the potential breakpoints at which the relationship of length *vs.* mass might change over ontogeny were estimated using piece-wise regression analysis (Appendix 4.2). The specific growth rate of individuals (in d^{-1}) was hence calculated as:

$$SGR = \frac{\ln(m_{t1}) - \ln(m_{t_0})}{t_1 - t_0},$$

where m_{t_0} and m_t are the initial and final body mass (µg) of an individual before (t_0) and after the monitoring period (t_1).

2.3. Metabolic rate

Metabolic rate was measured as oxygen consumption per unit time, in µg O_2 h^{-1}. All monitored individuals were fed at the same time of day and then fasted for 3 hours in beakers separated from the culture prior to measurements, thus reducing the influence of variation in food processing or digestion costs (Evjemo et al., 2000). All measurements were carried out from 13:00 to 15:00 pm. Since *A. franciscana* is a planktonic filter feeder that swims continuously in the water column, the metabolic rate measured here can be considered aerobic

energy expenditure during routine activity. Oxygen consumption was measured in a sealed glass microplate equipped with planar oxygen sensor spots with optical isolation on the bottom of wells (Loligo Systems ®), integrated with a fluorescence-based respirometry system (SDR SensorDish ® Reader, PreSens). Well volumes of 80 and 1700 mL were used for small (stage 1 to 10) and large individuals (stage 11 to adults), respectively, to accommodate animals of different size. Single individuals were introduced into wells with air-saturated seawater, which were sealed afterwards using PCR film (Thermo Scientific ®), ensuring that no air bubbles were trapped in the wells. The preparation of the plate was conducted in the same temperature-controlled room containing the cultures, and plates were then placed in the reader inside an incubator (JUMO Dtron 316, LEEC), keeping experimental temperature (26 °C) constant throughout. Prior to measurements, individuals were allowed to acclimatise to the wells for 10 min. Oxygen concentration inside the wells was measured in the dark every 3 minutes for 10 – 60 min depending on animal size. Oxygen consumption rate was estimated from the decrease in oxygen concentration during the time interval in which this decrease was linear. Four blank measurements (i.e., wells with only seawater and no animals) in each reading were used to control for oxygen diffusion from outside or background microbial respiration in experimental wells.

2.4. Offspring production rate

Mating adults form male-female pairs, in which males clasp females and swim together during reproduction (Tapia et al., 2015). These pairs generally last longer than the time needed for copulation (Wolfe, 1973). Single pairs of *A. franciscana* from 5 batch cultures were placed in 250 mL beakers to track offspring production (Browne & Wanigasekera, 2000) (Fig. 4.2B). Females in these pairs were already ovigerous, i.e., their broodsacs were visibly full of eggs. All experiments were maintained for a minimum of a week because this is the average time that females of *A. franciscana* remain with the same male (Rode et al., 2011). To account for variation in mating time and brood production among females (Browne et al., 1984), experiments were maintained until individuals of each pair were found swimming separately for more than a day. Experimental duration, however, showed no correlation with the number of cysts and larvae produced by females in these pairs (Pearson test, $r = 0.17$, 95% CI (-0.33, 0.60), df = 15, $p = 0.504$). Water was changed once a week, though the time varied depending on when individuals of the pair were separated, thus avoiding any disturbance that might affect the mating process (Rode et al., 2011). Offspring production by females in these pairs, i.e.,

cysts and larvae, were removed and counted when water was changed and at the end of each experiment. The metabolic rate of females and males from each pair was measured immediately afterwards. All females were developing new eggs in their brood sacs at the time of these measurements, and hence their metabolic rates reflect the demands of offspring production. Offspring count was converted into dry mass by assuming 3 μg per cyst or larvae based on empirical measurements (see Appendix 4.2), and the production rate was calculated as μg h^{-1}.
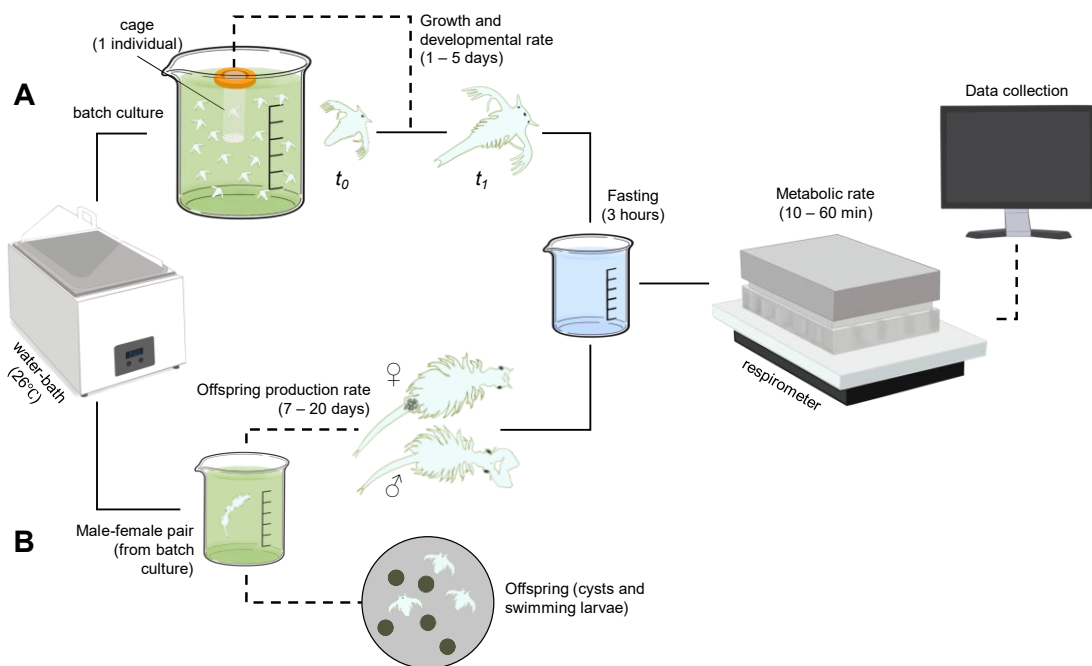
Figure 4.2. Schematic of the experimental design. Cultures of *Artemia franciscana* were kept in water-baths at 26 ± 0.2 °C and *ad libitum* food. Dashed lines indicate data collection events. (**A**) Growth and developmental rates were measured throughout the ontogeny of *Artemia* in the batch cultures. Individuals were introduced in cages of plankton mesh immersed in the culture water during a time interval. Mesh size of cages permitted free flow of water and food, allowing animals to swim naturally inside. Body length and developmental stage of these individuals were recorded before (t_0) and after (t_1) the monitoring period. (**B**) Male-female pairs were taken from main cultures and placed into separate beakers, where reproduction was monitored. Once mating was finished, offspring production (i.e., cysts and swimming larvae) was recorded, and body length of males and females from pairs were measured. After measurements in (A) and (B), and prior to measuring metabolic rates, all sampled individuals were fasted in separate beakers to reduce the energetic costs of food processing and digestion costs. Last, individual metabolic rates were measured in the respirometer placed in an incubator at experimental temperature in darkness. Body length was later converted into dry mass by the empirical length-mass equation given in the Appendix 4.2.

2.5. Energy conversion of biomass production and metabolic rates

Individual rates of growth in body mass (i.e., mass gain per unit time, in µg dry mass h^{-1}) and aerobic metabolism were converted to J g^{-1} dry mass h^{-1} by using respectively a factor of 22 kJ g^{-1} dry mass (Caudell & Conover, 2006) and a general oxyjoule equivalent of 14.14 J mg^{-1} O$_2$ consumed (Elliot & Davison, 1975), suitable for herbivorous animals with carbohydrate-rich diets such as anostracans (e.g., Marchant, 1978; Glazier & Calow, 1992). A single mass-energy conversion factor was applied for all individuals because body composition shows little variation during ontogeny in *Artemia*, i.e., protein plus lipid proportion vary between 71-68% from larvae to adults (Léger et al., 1987), ranging 21-23 kJ g^{-1} dry mass in the population from the Great Salt Lake (Vanhaecke et al., 1982; Caudell & Conover, 2006). Offspring production was converted from dry mass into energy by using the same factor of 22 kJ g^{-1} for larvae, and 23.5 kJ g^{-1} for cysts (Vanhaecke et al., 1982). Biomass production was equal to growth in body mass for single individuals, or to offspring production for reproductive females, as growth was expected to be negligible in reproductive individuals from mating pairs (see details in Appendix 4.3).

2.6. Estimating metabolic costs of biomass production and maintenance metabolism

The cost of biomass production, i.e., energy needed to synthesise a unit of body or offspring mass, can be estimated empirically using the relationship between the rates of metabolism and production, when both are expressed in energy units and on a mass-specific basis (Wieser, 1994; Clarke 2017, 2019):

$$R_g = c\,P \qquad\qquad [1]$$

where R_g is the metabolic energy dissipated during mass production, P is the energy deposited in new mass (both in J g^{-1} h^{-1}), whilst c is the slope of the relationship between R_g and P, which is a dimensionless estimate of the cost of production. The value of c reflects the overhead energetic demands of building new mass, such as the associated costs of transport from reserves and within the cell (Risgaard, 1998; Wieser, 1994; Clarke, 2019). Importantly, this model relies on the assumption that the metabolic energy allocated to production (R_g) is additional to that invested in body maintenance (R_m, J g^{-1} h^{-1}), i.e., the demands of non-growth, life-sustaining

functions. Summing both terms give the mass-specific metabolic rate (R') of inactive organisms (Rombough, 2011):

$$R' = R_g + R_m \qquad [2]$$

In agreement with current theory (Moses et al., 2008; Kooijman, 2010), this model also assumes that mass-specific maintenance R_m, remains constant over ontogeny, and hence that absolute maintenance demands increase isometrically with body mass ($R_m \times m^1$), and independently of production rate (Wieser, 1984; 1994; Clarke, 2019). Therefore, when energetic demands from other activities are negligible (e.g., foraging, food processing), both R_g and R' would increase with P by the same proportion and hence exhibit the same slope in this relationship, whereas the intercept term (i.e., R' at $P = 0$) in the former relationship may denote the non-growth metabolic demands (i.e., maintenance; Wieser, 1994). In pelagic continuous-feeding invertebrates such as *Artemia*, maintenance metabolism (R_m) is complicated to quantify compared to other animals that are able to rest naturally or tolerate starvation (e.g., Jorgensen, 1988). I thus obtained the dimensionless cost of production (slopes *c*) from the relationship between the mass-specific rates of (non-feeding and low activity) routine metabolism R' and production P.

To complement the estimates of production costs, and compare with previous values in the literature, the overhead costs of production were also calculated as the net metabolic energy invested in biosynthesis per unit of mass production (i.e., R_g/P, in J g^{-1} new mass). Maintenance metabolism (R_m) was first obtained following Glazier et al. (2020), as the mass-specific metabolic rate at the body mass at which growth is expected to cease (*M*). Firstly, *M* was estimated from the relationship between final (t_1) *vs.* initial (t_0) dry mass (both log$_{10}$-transformed), as the body mass at which $m_{t1} = m_{t0}$. Given that *A. franciscana* exhibits a biphasic growth trajectory during ontogeny (Evjemo & Ojsen, 1999), only data on post-larval and non-reproductive individuals were used in these calculations, since specific growth rates decline with mass in these individuals. Second, the metabolic rate at this non-growing nor reproducing *M* was obtained from the relationship between log$_{10}$ metabolic rate vs. log$_{10}$ body mass in the latter individuals, and then divided by *M* to get R_m (J g^{-1} body mass h^{-1}). Absolute values of individual maintenance demands (J h^{-1}) were calculated as $R_m\, m$ (see assumptions

above) and subtracted from routine metabolic rates (R) of animals, thus yielding the net metabolic energy allocated to biosynthesis. The overhead costs of growth were finally obtained by dividing this fraction of metabolic rates (J h^{-1}) by mass production rates (g h^{-1}).

Last, I investigated the alternative hypothesis that overhead costs of mass production remain invariant among individuals, regardless of ontogenetic phase or reproductive mode. Based on empirical estimates across ectotherms (Clarke, 2019), R_g was first calculated from mass production rates using a fixed value of $c = 0.32$ in eq. [1], and then individual R_m values were obtained through eq. [2]. Contrary to my main premise, I here assumed that a constant fraction of routine metabolic rate is allocated to production. Thus, in contrast with current theory, I explore the possibility that mass-specific maintenance demands vary during ontogeny. I finally discuss the plausibility of this alternative assumption in the light of supporting evidence in the literature.

2.7. Statistical analysis

Statistical analyses were performed using R v. 4.2.0 (R Core Team, 2022). Data were log$_{10}$ transformed to explore the allometric relationships between metabolism and body mass. The potential change in metabolic scaling slope during the ontogeny of *A. franciscana* (H1a) was investigated by a piece-wise regression model for the relationship between log$_{10}$ metabolic rate and log$_{10}$ body mass with package 'segmented' (Muggeo, 2008). This method firstly requires performing a generalised linear model, and a broken-line relationship is then added by re-fitting the overall model to account for a piece-wise linear relationship (Muggeo, 2008). This piece-wise regression was finally compared with the generalised linear model without breakpoints through Bayesian Information Criterion (BIC; Aho et al., 2014), where the best model to describe the metabolic scaling with body mass was that with the lowest BIC value (Gkioulekas & Papageorgiou, 2019). The starting breakpoint value in the latter model was selected by exploring visually the variables using 'loess' method in the package ggplot2 (Wickham et al., 2016).

Non-linear least squares models (NLS) were used to analyse the variation in specific growth rates and log$_{10}$ body mass, as specific growth rates describe a concave (downward)

curve with body mass over ontogeny in *A. franciscana* (Evjemo & Olsen, 1999). The maximum specific growth rate over ontogeny was then estimated by function 'optimize' in R, which searches for the maximum value of specific growth rates in the NLS equation with respect to body mass (Brent, 1973). Second-, third-, and fourth-degree polynomial equations were fitted to specific growth rates *vs.* $\log_{10}$ body mass. As above, the best model to describe the growth trajectory over ontogeny in *A. franciscana* was chosen as that with the lowest BIC value.

Ordinary least squares regressions (OLS) were used to analyse the mass-scaling of metabolic rates in adult individuals, as well as the mass-scaling of offspring production rates (all $\log_{10}$-transformed) of reproductive adults from sexual pairs. A further OLS was used to test whether the metabolic scaling slope differs between females and males (H2a), incorporating body mass, sex, and the interaction term between the latter variables in the model.

The dimensionless costs of biomass production, i.e., the slope (*c*) of the relationship between the mass-specific rates of production, either in body mass or offspring, *vs.* metabolism (all in J g^{-1} h^{-1}; Wieser, 1994; Clarke, 2019) were similarly calculated using OLS regressions. These models incorporated metabolic rates as dependent variable and either growth or offspring production as independent variable, since mass production dictates metabolic demands but not the opposite (Hatton et al., 2019), and thus higher production rates result in increased metabolic rates. The possible difference in the cost of growth between larvae and post-larval individuals (H1b) was analysed using an OLS model that incorporated mass-specific growth rate, the ontogenetic phase (stages < 19, *vs.* stage 19 individuals), and the interaction term between them. I used a similar OLS model to test whether the cost of production in females varies following differences in reproductive mode (H2b), by incorporating mass-specific metabolic rate of reproductive females as dependent variable, and their mass-specific offspring production rate as well as the proportion of larvae produced (i.e., number of larvae per total offspring) as explanatory variables. Finally, to explore how production costs in these females differ between ovi- and ovoviviparous reproduction, the associated cost of each reproductive mode was analysed by separate regressions of either cysts or larvae production rate *vs.* mass-specific metabolic rate (in J g^{-1} h^{-1}).

Last, the differences in overhead costs of growth, i.e., the net metabolic energy needed per unit of mass production (J g^{-1}), were investigated among the larval phase, post-larval phase,

and reproductive females. Comparisons between groups were performed using pairwise non-parametric Wilcoxon tests, as these data were not normally distributed (Shapiro-Wilk test = 0.35; $p < 0.001$). As above, OLS regressions were performed to estimate final mass (M) and its expected metabolic rate, which was used to obtain mass-specific maintenance metabolism (see section 2.6). This approach (i.e., assuming invariant mass-specific maintenance) was then compared to the alternative assumption of constant cost of production, whereby differences in maintenance demands among ontogenetic phases and reproductive females were investigated using pair-wise t-test comparisons.

3. Results

3.1. Growth

The rates of growth, development and metabolism were obtained for 103 individuals throughout the ontogeny of *A. franciscana*, from stage 1 nauplii to adults with body sizes spanning 2.62 orders of magnitude (3 – 1241 µg) (Table S4.1). The relationship between $\log_{10}$ metabolic rate (R, µg O_2 h^{-1}) and $\log_{10}$ body mass (m, µg) varied during ontogeny, as denoted by the piece-wise model, which showed better fit for these data than the non-segmented model (BIC: -205.41 and -96.83, respectively). This change in b was estimated to occur at a dry body mass of 55.73 (95% confidence intervals: 42.93, 72.35) µg, coinciding with the start of the post-larval phase (stage 19). According to the piecewise regression model (Fig. 4.3A), the ontogenetic metabolic scaling of *A. franciscana* could be hence described as:

$\log_{10} R = -2.12 + 1.36$ (95% CI: 1.28, 1.43) $\log_{10} m$, for individuals from 2.99 to 55.73 µg, and

$\log_{10} R = -0.73 + 0.56$ (95% CI: 0.48, 0.64) $\log_{10} m$, for individuals larger than 55.73 µg

The variation in specific growth rates (SGR, d^{-1}) with $\log_{10}$ body mass over ontogeny was best described by a third-degree polynomial equation, based on the lowest BIC value (Table A4.2), as:

$$SGR = -0.52 + 1.59 \log_{10} m - 0.81 \log_{10} m^2 + 0.12 \log_{10} \log_{10} m^3$$

Specific growth rates increased with body mass early in ontogeny, reaching maximum values at the end of larval development (maximum of 0.53 d^{-1}), and then declining with mass as individuals become large adults (Fig. 4.3B). The maximum growth rate was estimated at a body mass of 24.15 µg, coinciding nearly with the end of juvenile development (after stage 17). The three smallest individuals in this experiment (2.99 – 3.50 µg) exhibited negative growth rates, corresponding to adjustments in yolk and structural mass that take place early in ontogeny of *A. franciscana* (Weisz, 1946; Barlow & Sleigh, 1980; see Appendix 4.2).

The cost of growth (Fig. 4.3c), as reflected by the slope of the relationship between mass-specific rates of metabolism and growth, was $c = 0.35$, 95% CI (0.22, 0.47), when considering all individuals in the model (OLS: df = 101, $t = 5.38$, $R^2 = 0.22$, $p < 0.001$). However, the cost of growth varied when developmental stage and its interaction term with growth rate were incorporated in the model (Table 4.1), showing a lower cost during larval development ($c = 0.20$ (0.05, 0.36)) than in post-larval individuals ($c = 0.87$ (0.68, 1.07)).
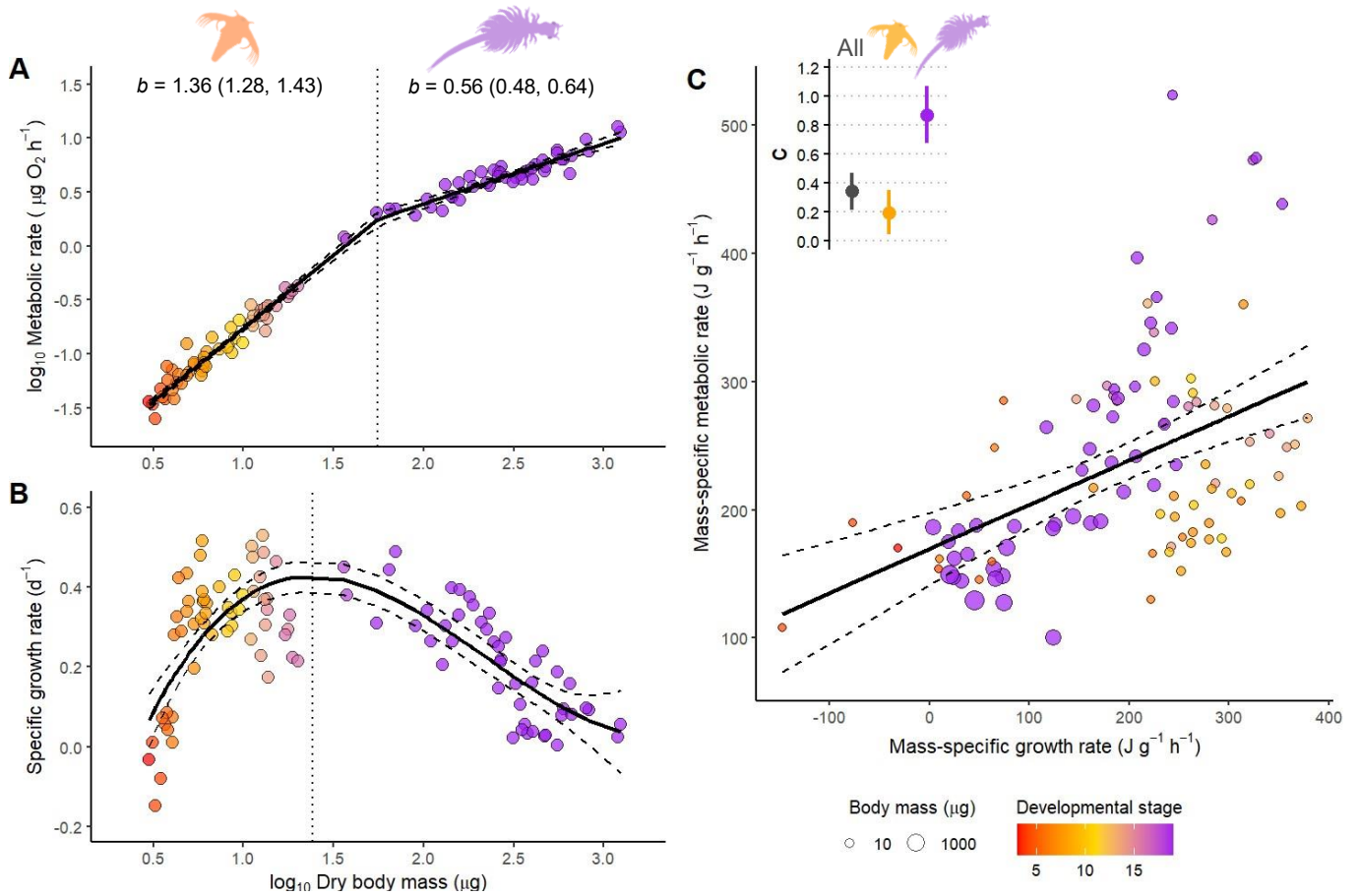
Figure 4.3. The relationship of metabolic and growth rates with body mass over the ontogeny of *A. franciscana* at 26 °C: **A**, the mass-scaling of individual metabolic rates, showing the mass breakpoint (dotted line) where metabolic scaling shifts according to the piece-wise regression model, at a dry body mass of 55.73 μg. The slopes and 95% CI of scaling slopes *b* are indicated in the upper part of the panel. **B**, the variation in specific growth rates as $\log_{10}$ body size increases, which was best described by a third-degree polynomial regression. Dotted line shows the body mass at the estimated maximum specific growth rate in this regression. **C**, the relationship between mass-specific rates of metabolism and growth from larvae to adults, whose slope represents the metabolic cost of growth. Inset plot shows *c* values and 95% CI from OLS models using all data (black), only larvae and juveniles (i.e., stage < 19, orange), or pre-adults and adults (stage 19, purple). Developmental stages are coded through a colour gradient from red to purple, and point size in C denotes body mass (μg). Thick and dashed lines denote regression lines and 95% CI from models.

Table 4.1. Results of the ordinary least squares (OLS) models for the relationship between the mass-specific rates of metabolism and growth (both in J g^{-1} h^{-1}) of 103 individuals of *A. franciscana*, incorporating the ontogenetic phase (0 for larvae, 1 for post-larval individuals), and the interaction between the latter variables. Significant effects ($p < 0.05$) are shown in bold.

variable	estimate	Standard error	*t*-value	*p*	*R²*
Intercept	187.132	18.265	10.245	**< 0.001**	
Growth rate	0.202	0.072	2.796	**0.006**	0.41
Ontogenetic phase	-75.801	25.799	-2.938	**0.004**	
Growth rate × Ontogenetic phase	0.674	0.130	5.182	**< 0.001**	

3.2. Reproduction

The metabolic rates and offspring production were obtained from 17 male-female pairs (Table S4.2). In these pairs, the difference in mass-scaling of metabolic rates was between males and females was not significant ($b = 0.67$, 95% CI (0.15, 1.19), *vs.* 0.76, (0.32, 1.20), respectively; Fig. 4.4A), as denoted by the interaction term between $\log_{10}$ body mass and sex (Table 4.2). Conversely, in younger, single individuals, the metabolic scaling with body mass did differ between females and males (Table 4.2), with females showing a steeper scaling slope ($b = 0.61$ (0.52, 0.69)) than males ($b = 0.46$ (0.35, 0.57)) (see Appendix 4.5). The mass-scaling of offspring production rate of these pairs was nearly isometric though with large confidence intervals for females (Fig. 4.4B), which was described as $\log_{10}$ offspring production $= -2.64 + 0.96$ (0.30, 1.63) $\log_{10}$ body mass, (OLS: df = 15, $t = 3.08$, $R^2 = 0.35$, $p = 0.007$). However, no relationship between offspring production and body mass was found for males (OLS: df = 15, $t = 0.16$, $R^2 = -0.06$, $p = 0.875$).

Table 4.2. Results of OLS models for the variation in $\log_{10}$ metabolic rates (in mg O_2 h^{-1}) of single or reproductive adults as explained by $\log_{10}$ dry body mass (in µg), sex (0 for females, 1 for males), and the interaction between the latter variables. Significant effects ($p < 0.05$) are shown in bold.

	variable	estimate	Standard error	t-value	p	R^2
Single individuals	Intercept	-0.846	0.105	-8.097	**< 0.001**	
n = 45	Body mass	0.606	0.041	14.722	**< 0.001**	
	Sex	0.362	0.165	2.195	**0.034**	0.87
	Body mass × Sex	-0.148	0.068	-2.192	**0.034**	
Mating individuals	Intercept	-1.308	0.657	-1.991	0.056	
n = 34	Body mass	0.762	0.212	3.589	**0.001**	
	Sex	0.307	0.932	0.329	0.744	0.60
	Body mass × Sex	-0.088	0.320	-0.275	0.785	

I found no significant cost of total offspring production (i.e., combined cysts and larvae, in µg h^{-1}) in reproductive females (OLS: df =15, t = 0.49, R^2 = 0.12, p = 0.092) (Fig. 4.4C). However, accounting for the proportion of larvae produced per offspring enhanced substantially the variance explained by the latter model (R^2 = 0.54), which also showed a significant cost of offspring production of c = 0.80 (0.04, 1.57) (Table 4.3), indicating that the reproductive mode of females influenced the demands of generating offspring. Indeed, while no significant cost was found for cyst production alone (OLS: df = 15, t = -0.78, R^2 = -0.02, p = 0.447), larval production did show a significant metabolic cost in these females (OLS: df = 15, t = 4.05, p = 0.001), yielding a relatively high value of c = 1.82 (0.86, 2.78) (Appendix 4.6). Finally, although the proportion of larvae per offspring generally decreased with female body size in females, no significant correlation was found between these variables (Pearson test, r = -0.41, 95% CI (-0.75, 0.08), df = 15, p = 0.094).

Table 4.3. Results of OLS models for the relationship between the mass-specific rates of metabolism and offspring production (both in J g^{-1} h^{-1}) in 17 females from mating pairs, accounting for the proportion of larvae produced per total offspring as an additional explanatory variable. Significant effects ($p < 0.05$) are shown in bold.

variable	estimate	Standard error	t-value	p	R^2
Intercept	64.426	17.383	3.706	**0.002**	
Offspring production rate	0.800	0.357	2.242	**0.042**	0.54
Proportion of larvae	75.029	19.660	3.816	**0.002**	
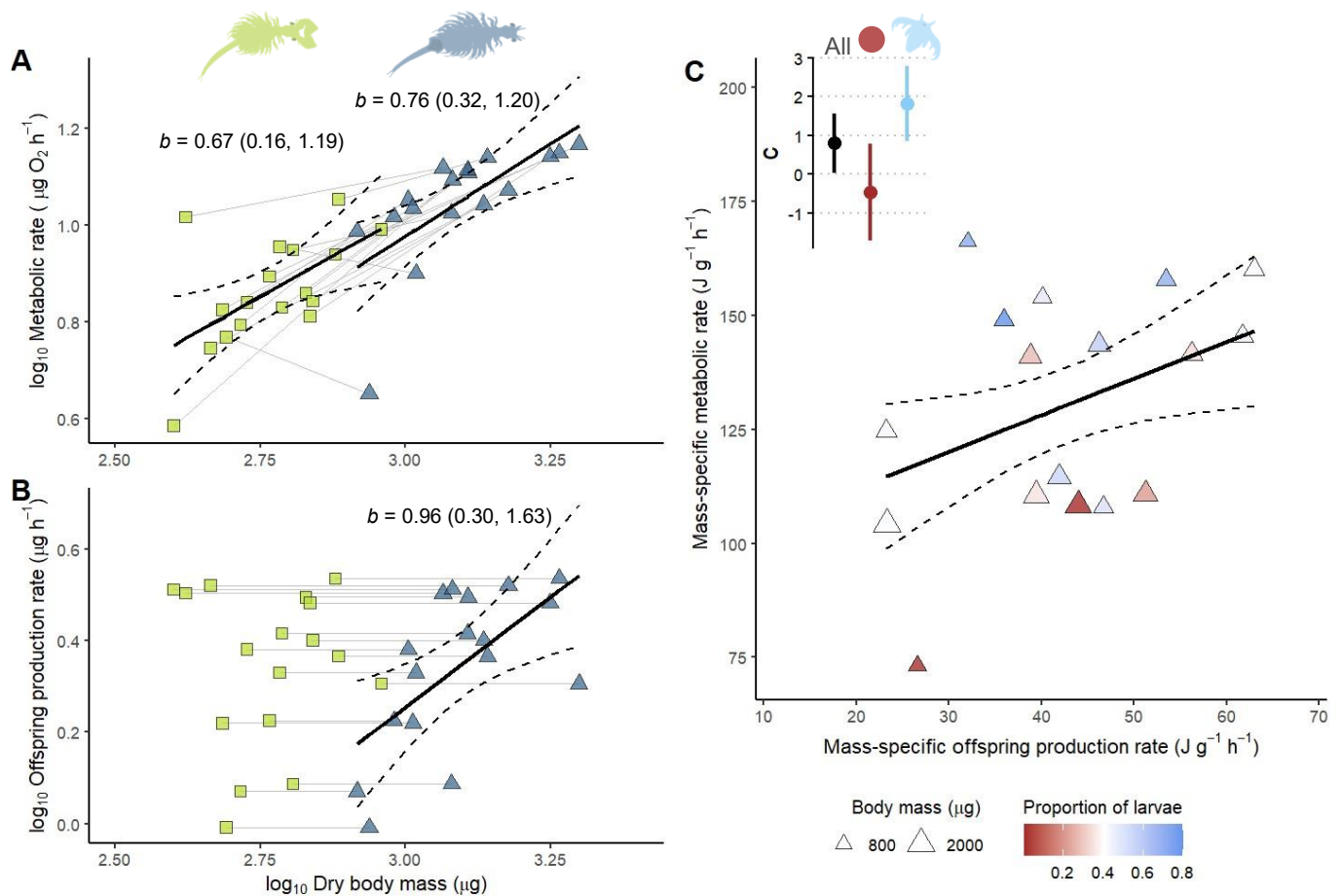
Figure 4.4. The relationship of metabolic and offspring production rates with body mass in reproductive individuals of *A. franciscana* at 26 ℃. **A**, the mass-scaling of metabolic rates of males and females in mating pairs. **B**, the mass-scaling of offspring production rates in males and females in these pairs. The slopes and 95% CI of mass-scaling relationships are indicated in the upper part of panels A and B, whereas grey lines denote a male-female pair. **C**, the relationship between mass-specific rates of metabolism and offspring production in reproductive females, whose slope represents the metabolic cost of offspring production. Inset plot shows slopes *c* and 95% CI from OLS models using overall offspring production after accounting for the proportion of offspring that are larvae (black), and using solely cysts (brown), or larvae production (blue). In A-B, point shape and colour indicate males (green squares) and females (blue triangles). In C, point size denotes body mass (μg), whereas colour gradient from brown to blue shows the proportion of larvae produced by females per total offspring. Thick and dashed lines denote regression lines and 95% CI from models.

3.3. Expectations under constant *vs.* variable mass-specific maintenance costs

Mass-specific maintenance metabolic rate was estimated as 0.007 μg O_2 μg^{-1} body mass h^{-1} (or 100.31 J g^{-1} h^{-1}), determined at a theoretical final mass (M) of 1637 μg. By assuming that these maintenance demands are invariant among different-sized individuals, the overhead metabolic costs per unit of mass production averaged 25,222 J g^{-1}, increasing from 2,902 to 50,461 J g^{-1} through development The $\log_{10}$ costs of production (Fig. 4.5A) in post-larval individuals (stage 19) were significantly higher than those in larvae (W = 661, $p < 0.001$), though the costs of none of these groups differed from the costs in reproductive females ($p > 0.1$). Five individuals were excluded from this analysis, due to either exhibiting negative growth rates (earliest larval stages; see section 3.1) or because metabolic rates fell below their expected maintenance demands (two adults).

Conversely, by assuming a constant cost of production, the mass-specific maintenance demands averaged 167.79 J g^{-1} h^{-1} (range: 58.51 – 444.91 J g^{-1} h^{-1}). The $\log_{10}$ maintenance metabolism (Fig. 4.5B) varied significantly among all studied groups, with post-larval individuals showing higher demands than larvae ($t = -3.07$, $p = 0.003$) and reproductive females ($t = 6.66$, p < 0.001).
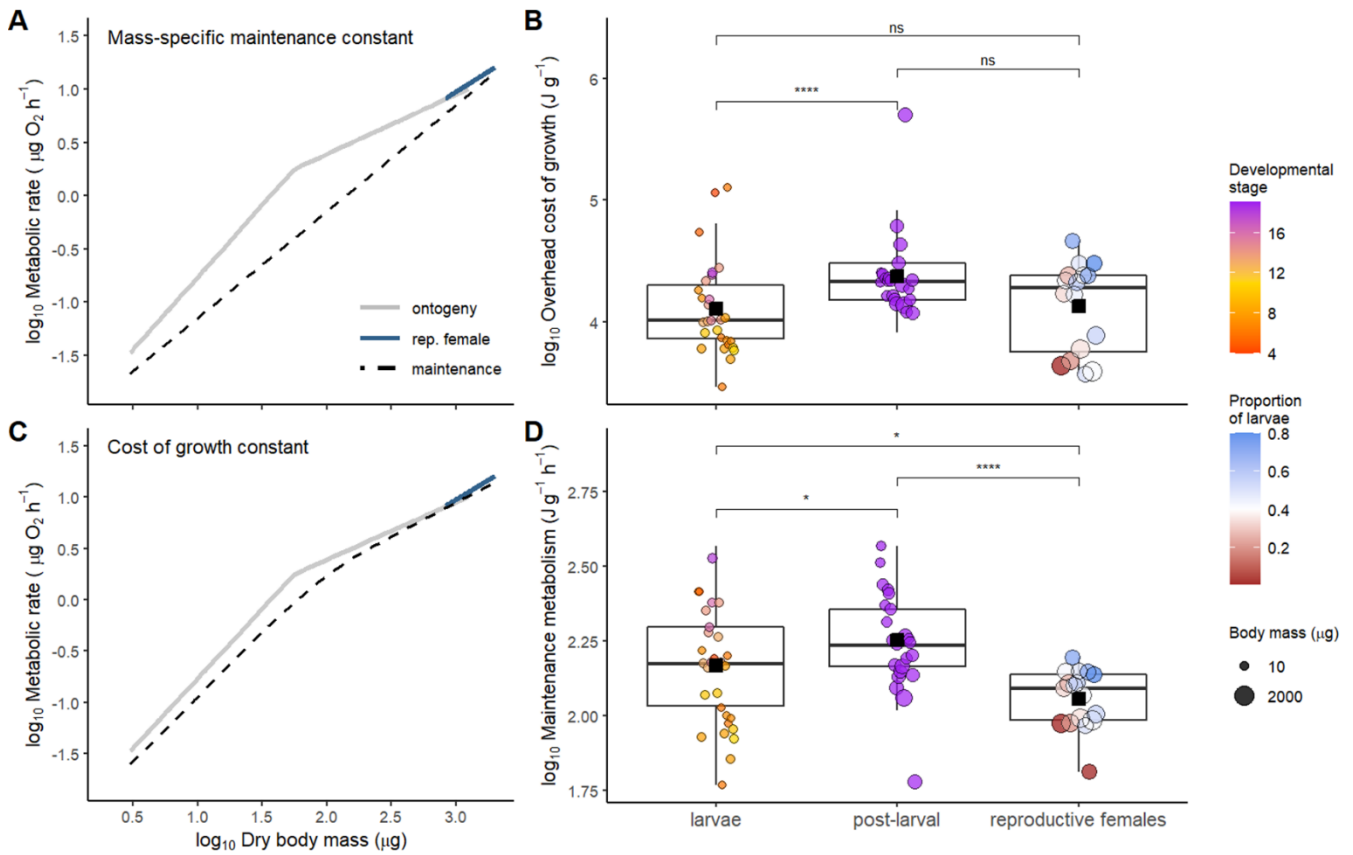
Figure 4.5. The two assumptions addressed here to explain the variation in metabolic rates with body size of *A. franciscana*: if mass-specific maintenance demands (dashed line) remain constant with body size (**A**), then overhead costs of mass production vary between larvae, post-larval individuals, and reproductive females (**B**); conversely, if overhead energetic costs per unit mass production are constant across body sizes (**C**), then mass-specific rates of remaining metabolism (non-production, or 'maintenance') vary with body size, hence ontogenetic phase and reproductive females (**D**). In A and C panels, thick lines show the observed metabolic scaling in larvae, post-larval, single individuals (grey), and reproductive females (blue). Dashed line for maintenance in C was drawn using smoothing method 'loess' in ggplot2. In B and D, black squares denote the mean, the solid line within each box marks the median, box boundaries indicate 25th and 75th percentiles, and whiskers indicate the largest and smallest value within 1.5 times the interquartile range beyond either box boundary. Significant differences between groups of individuals growing (larvae and post-larval individuals) and producing offspring (reproductive females) are indicated by asterisks (i.e., '*', $p < 0.05$; '****', $p < 0.0001$; 'ns', $p > 0.05$). Point size and colours, as shown in Figs. 4.3–4.4.

4. Discussion

I found marked, parallel shifts in metabolic scaling and growth trajectory during the ontogeny of *A. franciscana*, which reflect a change in resource-supply rates and in the metabolic cost of growth between larvae and post-larval individuals (Fig. 4.3, Table 4.1). Moreover, single individuals showed sexual differences in metabolic scaling slopes (*b*) that may be underpinned by the steep mass-scaling of egg production and longer post-maturational growth in females; in contrast, slopes *b* were similar in those paired reproductive individuals (Table 4.2), likely due to the ability of females to switch between reproductive modes with different associated costs (Fig. 4.4; Table 4.3). I next discuss these findings in detail by addressing each of the hypotheses in this study.

4.1. Metabolic scaling and growth trajectory shift during ontogeny in *A. franciscana*

As expected from my first hypothesis (H1a), metabolic rates increased steeply with body mass during larval development (*b* = 1.36, 95% CI (1.28, 1.43)) while specific growth rates accelerated as these individuals enlarged and generated new body segments (Fig. 4.3A, B). Conversely, metabolic rates showed much shallower increases with body mass during post-larval ontogeny (*b* = 0.56 (0.48, 0.64)), coinciding with a decline in specific growth rates. Similar biphasic patterns occur in many kinds of organisms, inhabiting both terrestrial (Czarnołeski et al., 2008; Gaitán-Espitia et al., 2013; Kutschera & Niklas, 2012; Hu, 2022) and aquatic realms (Risgaard, 1998). For instance, larval phases in fish and crustaceans are well-known for exhibiting higher slopes *b* than later in ontogeny (Post & Lee, 1996; Killen et al., 2007; Glazier et al., 2015), coinciding with exponential growth trajectories in these early life-stages (e.g., Kamler, 1992). I here argue that the cellular mode of growth observed in *Artemia* (Freeman 1986, 2005; Manzanares et al., 1993) may facilitate the shift in resource-supply rates to growing cells, and hence overall metabolism and organismal growth during ontogeny (Fig. 4.1). Indeed, increasing cell density with body mass in larvae support the observed hyper-allometric (*b* > 1) metabolic scaling early in ontogeny (Fig. 4.2A). During larval development, body segments and limbs elongate primarily by multiplication accompanied by reductions in cell size (Freeman, 1986; Manzanares et al., 1993), thus leading to high total cell surface-area (SA) to volume (V) ratios, which may enable exponential increases in supply rate with body mass (Kozłowski et al., 2003; Glazier, 2022b). In contrast, growth and maturation occurs by cell differentiation and expansion later in ontogeny (Freeman, 2005), presumably decreasing

cell SA/V and increasing intracellular transport distances (Glazier, 2022b). This reduced cell SA/V might slow down resource-supply rates per volume of cell, hence potentially contributing to much shallower increases of rates of metabolism and mass gain as individuals enlarge during post-larval ontogeny. Additionally, an increasing proportion of metabolically inert reserves (e.g., lipids) in larger cells may reduce mass-specific energy demand in post-larval animals, contributing to a decrease in b (Glazier, 2022b). Intracellular reserves can be crucial in organisms such as *Artemia*, whose simple hepatopancreas impedes long-term nutrient storage (Freeman, 2005). Other reductions in energy demands during post-larval ontogeny may arise from increased proportions of inert cuticle in larger *Artemia* (Criel & Macrae, 2002; reviewed more broadly in Glazier, 2022b), and possibly from the lower demands required by larger cells to maintain ion gradients across cell membranes (Davison, 1955; Kozlowski et al., 2003).

In addition to cell-size effects, other ontogenetic changes in body shape and structure may influence resource supply rates in *Artemia*. Like other aquatic skin-breathers (Glazier et al., 2015), *A. franciscana* grows mainly by elongation during early stages, (i.e., small increases in body mass m with body length L; $m \propto L^{\sim 2}$), whereas growth gradually becomes isomorphic ($m \propto L^{\sim 3}$) later in ontogeny (see Appendix 4.2). Such shape shifting maintain high body SA and so resource supply (and waste removal) in larvae (Hirst et al., 2014; Glazier et al., 2015), whereas later isomorphic growth in larger organisms decreases body SA/V and so supply rates through the cuticle. Moreover, as occurs in other arthropods such as copepods or krill (Fusco & Minelli, 2021), *Artemia* develop almost all body segments after hatching (i.e., anamorphosis), and with them thoracopods and filtering setae that gradually improve resource uptake efficiency (Schrehardt, 1987). Concomitantly, the heart enlarges and develops within these new segments, enhancing internal transport to body tissues (Spicer, 1994). Such an increase in oxygen and food supply rates with size during larval development may thus lead to high metabolic scaling slope and exponential growth, as similarly noted in copepod nauplii and fish larvae (Giguère et al., 1988; Glazier et al., 2015). Conversely, during post-larval ontogeny, resource supply capacity might be more influenced by SA-related processes with increasing body size because body shape and structure remain similar, and hence resulting in low metabolic scaling slope b and declining mass-specific growth rate (Post & Lee, 1996; Glazier et al., 2015; Glazier, 2022b). Notably, within the same order as *Artemia* (Branchipoda), cladocerans develop all segments during embryogenesis (i.e., epimorphosis), and, in contrast

with the biphasic metabolic scaling observed in *A. franciscana* and copepods, cladocerans exhibit a rather constant, nearly isometric metabolic scaling throughout ontogeny regardless food or temperature conditions ($b = 0.83 – 0.95$; Glazier & Calow, 1992; Fossen et al., 2019). Therefore, one may expect biphasic metabolic scaling (high to low *b*) in arthropods with high levels of anamorphosis (e.g., anostracans, copepods, krill) with stark changes in resource-supply rates between larval *vs*. post-larval ontogeny, though these shifts might not occur in epimorphic organisms (e.g., cladocerans, peracarids) (Fusco & Minelli, 2021).

4.2. The overhead costs of growth change between ontogenetic phases

The average cost of growth across individuals, i.e., the slope between mass-specific metabolic and growth rates, was 0.35 ($J J^{-1}$). In other words, 0.35 J of metabolic energy are needed to produce 1 J of new body mass in *A. franciscana* (Fig. 4.3C). This value is close to the costs reported among ectotherm species ($c = 0.32$; Wieser, 1994; Clarke, 2019), and falls within the range observed for single species ($c = 0.12 – 1.39$; Riisgård, 1998; Clarke, 2017). Consistent with my prediction (H1b), I found a lower cost of growth during larval development ($c = 0.20$, 95% CI (0.05, 0.36)) than in post-larval individuals ($c = 0.87$ (0.68, 1.07)). This finding challenges the current view that steep metabolic scaling early in ontogeny may result solely from greater energetic demands of rapid, accelerating growth (Riisgård, 1998; Glazier, 2022b). Instead, the lowest costs of growth have been reported in early, fastest-growing life stages of animals (e.g., Wieser, 1994; Pace & Manahan, 2007), and are particularly low in insect larvae (Sears et al., 2012; Ferral et al., 2020). Effectively, a plateau of minimum growth costs of $c \approx 0.2$ (or ~5000 $J g^{-1}$ dry mass) has been observed in the youngest individuals with highest growth rates, which sometimes show no extra costs with additional increases in growth rate (Wieser, 1994; Rombough, 2011). This value (i.e., 0.2 $J J^{-1}$) has also proved to be consistent for both protein synthesis in cultured fish cells and rapidly growing fish larvae ($c \approx 0.24$; Smith & Ottema, 2006). The low cost of growth found here in *A. franciscana* during larval development ($c = 0.20$) adds to this body of evidence.

It has been hypothesised that size-selective predation pressures favour higher growth rates, hence resource-supply capacity and metabolic rates in small, young individuals (Glazier, 2005; Glazier et al., 2015). While the ultimate causes of this rapid and energetically efficient growth early in ontogeny appear seemingly clear, the proximate mechanisms by which this is

achieved are not (Rombough, 2011). I argue that cell-size as well as whole-body shape and structure changes can contribute to the increase in growth costs and growth deceleration between early and late ontogenetic phases. Selection may facilitate rapid and accelerating organismal growth to a size at which mortality is reduced (Dmitriew, 2011) *via* cell multiplication, which is relatively fast per unit resource (or less costly per unit growth; see Goss, 1966) due to high cell SA/V and small intracellular transport distance. In zooplankton such as *Artemia*, the survival of larvae forming swarms near the water surface may indeed be favoured by rapid, low-cost growth during larval development (Gulbrandsen, 2001). This ontogenetic phase ends with the requirement for differentiation to enable a physiology suitable for changes in ecological niche associated with larger body sizes and for supporting future reproduction. Differentiation and mature structures entail high proportions of cell expansion (Arendt, 2000; Takatsuka & Umeda, 2014), which can be more energetically expensive per unit growth (or slower per unit resource input) than multiplication, due to reduced SA/V and larger intracellular transport distance as individuals enlarge. For example, during the ontogeny of *Artemia* and other crustaceans, increasing cell surface during cell differentiation and expansion involves large amounts of resources to produce proteins and phospholipids needed for biosynthesis of new plasma membrane (Freeman, 2005). Effectively, the youngest post-larval individuals in this study exhibited among the fastest mass-specific growth but also the highest metabolic rates during ontogeny (Fig. 4.3C), supporting the high costs associated with maturing structures. Instead of a single driver for the variation in growth costs during ontogeny (i.e., cellular growth or predation pressure), selection on growth trajectory and cell-size shifts might be evolutionarily co-adjusted to optimise survival of young individuals and ensure sexual maturity.

4.3. Differences in metabolic scaling between sexes

According to my second hypothesis (H2a), I found support for steep mass-scaling of offspring production rates (and so egg development rates; $b = 0.96$ (0.30,1.36); note the large CIs), though the metabolic scaling slope (b) of gravid females was not significantly steeper than that of males from sexual pairs (Fig. 4.4A, B), contrary to expectation. Indeed, the slopes b were statistically different only between single males and females ($b = 0.46$ *vs*. 0.61, respectively; $p = 0.034$), but not between reproductive adults ($b = 0.67$ *vs*. 0.76; $p = 0.785$). In single individuals, the steep mass-scaling of egg development as well as the longer post-maturational growth compared to males (Appendix 4.5) may lead altogether to steepen b in

females (Glazier, 2015). Interestingly, the opposite pattern to the observed here in *Artemia* has been recently seen in mosquitofish *Gambusia affinis* (Moffett et al., 2022), in which gravid females showed significantly steeper *b* than reproductive males, whereas *b* was similar between sexes in virgin fish. Differences in the mating process and its associated activity demands between mosquitofish (i.e., brief courting and chasing; Hughes, 1985) and *A. franciscana* (i.e., long periods of clasping and fertilisation), but also the ability of *Artemia* females to switch between reproductive modes and so change offspring production costs (discussed below), may explain to some extent the contrasting findings between these species. Complementarily, according to Glazier (2022b), a greater contribution of muscular demands to metabolism during mating might lead to higher *b* in reproductive individuals, given that muscle tissue is formed of elongated cells with high SA/V. In *Artemia*, muscular costs might be especially high and so increase *b* in reproductive males, due to the costs of hypertrophic clasping antennae and increased swimming activity during mating process, since they act as pacemakers for the pair (Lent, 1977). In any case, the underlying causes of sexual differences in metabolic scaling are still largely unexplored, which will likely provide new, fruitful research avenues (Somje et al., 2022).

4.4. The costs of offspring production vary with reproductive mode

The costs of offspring production increased with the proportion of larvae produced (Fig. 4.4C; Table 4.3), as predicted by the steep increase in cell density of developing embryos and so their aerobic demands on gravid females (H2b). These results are in line with DEB theory (Kooijman, 2010), which predicts that metabolic rate increases only slightly with mass in eggs because of the low requirements of energy reserves, whereas embryos developing body structures require steep increases in respiration as they grow (Maino et al., 2017). Indeed, while higher rates of cyst production showed no additional respiratory costs in females (Appendix 4.6), higher rates of larval production, in which embryos develop to gastrulation (i.e., rapid cell multiplication and size reduction; Crie & Macrae, 2002) and generate body structures inside brood sacs, resulted in steep increases in metabolic rates in females ($c = 1.83$). In contrast, embryo development is arrested at early gastrula states to produce cysts in *Artemia*, and despite containing a higher density of energy reserves than larvae (Vanhaeckeet al., 1982), cysts are metabolically inactive (Crie & Macrae, 2002). Moreover, differences in reproductive mode among females seem to be genetically determined, whereby more heterozygous individuals tend to produce cysts predominantly (Gajardo & Beardmore, 1989). Given the stark differences

in energy costs between producing swimming larvae *versus* dormant and resilient cysts, the variation in reproductive mode (ovi- *vs*. ovoviviparity) among *Artemia* females may have a high adaptive importance to cope with changing conditions in their ephemeral habitats.

After accounting for the contribution of reproductive modes, the costs of biomass production were similar among reproductive females and post-larval individuals ($c = 0.80$ *vs*. 0.87 respectively; Fig. 4.3C *vs*. 4.4C), reflecting a common cost after larval development. Interestingly, the cost of offspring production observed in *Artemia* was much higher than that of egg production observed in the copepod *Acartia tonsa* ($c = 0.19$; Kiørboe et al., 1985), which is close to the minimum energetic cost of synthesis (Wieser 1994). In a more detailed comparison, I found that the cost in *A. tonsa* and that of a mainly oviparous female of *A. franciscana* (99.99% cysts per total offspring) were similar (3,981 *vs*. 4,346 J g^{-1}, respectively), whereas the cost was 7-fold higher (30,262 J g^{-1}) in a mainly ovoviviparous female (80.12% larvae per total offspring). This difference of energetic costs between reproductive modes might be a widespread phenomenon across animals (Moffett et al., 2022). For instance, two closely related species of lizards (genus *Sceloporus*) with different reproductive modes exhibit strikingly different costs of litter production. Whereas for the oviparous species (*S. undulatus*) larger litter sizes involved no extra costs among gravid females (Angilletta & Sears, 2000), in the viviparous species (*S. jarrovi*) the costs of litter production for females increased by 4.16 J h^{-1} per neonate produced (Beuchat & Vleck, 1990). Moreover, the increase in metabolic rate of females in the viviparous lizard was higher than that expected by solely adding the respiration of embryos. As suggested above for the costs of growth, this additional cost of litter production in females may reflect the greater energetic demands of supplying a given rate of resource in large animals (i.e., lower cell SA/V and longer transport distances) to fuel biomass production *via* rapidly growing body tissues or embryos.

4.5. Exploring alternative explanations of metabolic scaling under constant *vs.* variable mass-specific maintenance costs

I here quantified the energetic costs of production in *A. franciscana* using a widely used additive model (i.e., metabolic activities cause proportional increases in total metabolism; Wieser, 1989), where mass-specific maintenance costs are assumed constant with body mass (Moses et al., 2008; Kooijman, 2010). After removing maintenance costs from metabolic rates

through this approach (Fig. 4.5A), the estimates of overhead costs of production, i.e., the energy needed for producing new mass (J g^{-1}), supported the predicted ontogenetic changes in the dimensionless costs of growth: individuals undergoing larval development exhibited lower growth costs than post-larval animals (Median = 10,314 *vs.* 21,437 J g^{-1}, respectively). In reproductive females, on the other hand, the cost of offspring production was close to growth costs of post-larval animals (Median = 19,077 J g^{-1}), again indicating that similar production costs are shared among large individuals. Last, I found further support for this way of estimating maintenance metabolism. Specifically, the estimated value of maintenance metabolism using final mass M (100.3 J g^{-1} h^{-1}), was within the range of the predicted metabolic rates by linear models at zero growth (168.9, 95% CI (140.82, 197.07) J g^{-1} h^{-1}; Fig. 4.3C) or zero offspring production (64.43 (27.14, 101.71) J g^{-1} h^{-1}; Fig. 4.4C). Similar maintenance demands (89 – 117 J g^{-1} h^{-1}) were observed in other anostracan species, *Daphnia magna*, whereas these costs remained similar over ontogeny (Glazier & Calow, 1992; calculations in Wieser, 1994).

Yet, this additive model of energy allocation may be challenged when energetic trade-offs between biomass production and other activities are considered (Wieser, 1994; Rombough, 2011). If the cost of biomass production is constant, higher growth rates and hence energy demands could be supported by reducing the costs of other activities, such as maintenance or activity. Here, by adopting the alternative assumption of invariant cost of production, I found that estimated mass-specific maintenance costs during larval development were significantly lower than in post-larval individuals (Fig. 4.5B). For the reasons mentioned above (e.g., higher filtering efficiencies, greater proportions of body reserves or lower demands of ion regulation), it seems unlikely that post-larval individuals possess higher maintenance costs than larvae within *Artemia* ontogeny. Instead, mass-specific maintenance costs might decrease between larvae and post-larvae (i.e., $b < 1$ for metabolism excluding production costs); in such a case, the differences in the overhead cost of growth between larvae and post-larvae could be even larger that the conservative difference presented here.

The mechanism underlying changes in metabolic scaling with increasing body mass during ontogeny possibly results from a combination of the two models discussed here, i.e.,

growth and other activities such as body maintenance or activity are co-adjusted to account for their changing costs during ontogeny. This metabolic co-adjustment may explain why rapid-growing larvae can increase growth rates with no further increases in metabolic rate (Wieser, 1994; Rombough, 2011), or how, within the same population, some individuals can sustain rapid growth rates at a lower energetic cost (Bayne, 2000). Although challenging, metabolic costs of growth and maintenance need to be partitioned to obtain accurate estimates of biomass production costs (Smith & Ottema, 2006; Rombough, 2011; Ferral et al., 2020), but also to understand the underlying mechanism(s) behind metabolic scaling shifts during ontogeny

Chapter 5: General discussion
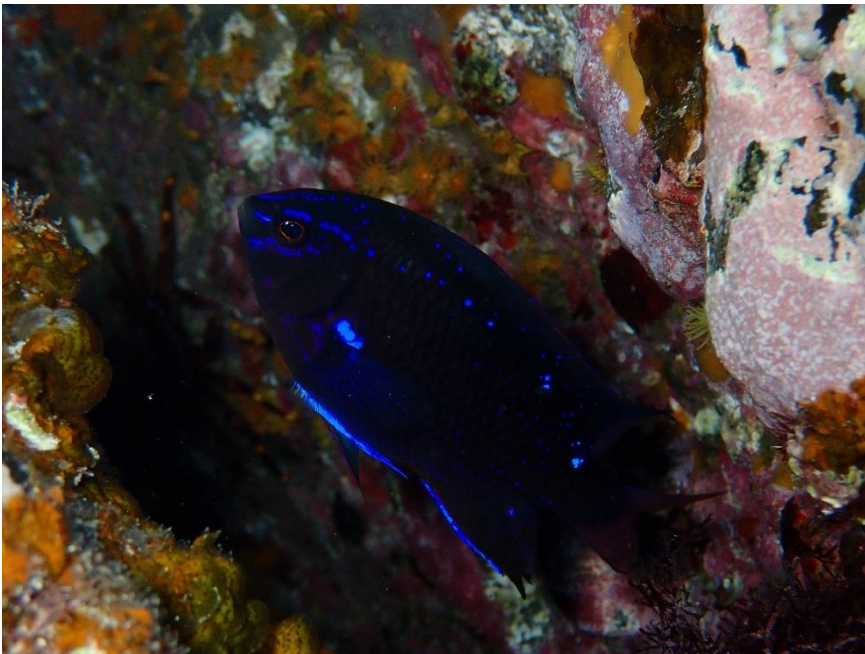
A Canary damsel (*Similiparma lurida*) guarding its house

General discussion

Metabolism supports all vital processes, and hence metabolic rate can inform about the pace at which organisms experience life (Glazier, 2005, 2014). Metabolic rate is linked to body size by a myriad of organismal traits and biological processes (Kozłowski et al., 2020; Glazier, 2022a). Among these processes, a major fraction of metabolic energy is required to produce new biomass (i.e., growth and reproduction), which influences fitness by determining the speed and size at which organisms mature as well as their offspring production (Dmitriew, 2011). Hence, understanding how and why the relationship between metabolic rate and body mass exhibits such a wide variation across and within taxa (e.g., Peters, 1983; DeLong et al., 2010; Killen et al., 2010; Tan et al., 2019), and how this relationship is influenced by environment and physiology (e.g., Glazier, 2008, 2009c; Ohlberger et al., 2012) is important to much of ecology. In this thesis, I investigated the influence of different ecological and organismal factors on the mass-scaling of metabolic rates in a diverse array of ectothermic animals occurring in extremely different environments, from deserts to the sea bottom.

Using a meta-analytic approach as well as laboratory experiments, I tested several current hypotheses that aim to explain metabolic scaling across different levels of biological organisation, performing interspecific (i.e., changes across species) and intraspecific (i.e., within-species) comparisons. My findings both challenge and support influential hypotheses, particularly predictions that underpin the 'metabolic theory of ecology' (MTE; West et al., 1997, 1999; Brown et al., 2004) and those arising from the 'metabolic-level boundaries hypothesis' (MLBH; Glazier, 2005, 2010, 2014, 2020). To explain the variation in metabolic scaling slopes observed here, I combined different perspectives, including the influence of both extrinsic (temperature) and intrinsic factors (activity, biomass production) in the energy expenditure of organisms. Complementarily, I emphasised the role of evolutionarily adaptive mechanisms to protect aerobic scope (Atkinson et al., 2006, 2022) as an alternative explanation to limitations in resource-supply capacity (e.g., Brown et al., 2004; reviewed in Glazier, 2005, 2022), and developed new hypotheses of synergistic mechanisms acting on ectotherms' metabolism. In this final chapter I will discuss the variation shown here both across and within species: first, the contrasting changes in intraspecific metabolic scaling between water- and air-breathing ectothermic vertebrates (Chapter 2); second, the variation in interspecific metabolic scaling among teleost fishes according to differences in fitness-related processes as growth and

self-maintenance (Chapter 3); last, the changes in biomass production and metabolic rates during ontogeny and between sexes in a model crustacean (Chapter 4). Furthermore, I will explore new hypotheses and reflections that emerged during the research conducted in this thesis.

1. The intraspecific variation in metabolic scaling within ectothermic vertebrates

In chapter 2, I investigated the effects of temperature and activity level on intraspecific metabolic scaling relationships in a wide range of ectothermic vertebrates, including teleost and cartilaginous fish, amphibians, and reptiles. Specifically, I tested the predictions from the MLBH that the relative influence of surface-area (SA) and volume (V) related processes dictates the relationship between the metabolic scaling slopes (b) and metabolic level (L), when environmental temperature or activity level of organisms increase. The decline in slopes b with temperature-increased L seen only in water-breathing species (i.e., fish) supported the MLBH prediction that the influence of SA-related processes on resting or routine metabolism may become predominant with warming (Glazier, 2005, 2010, 2020). Conversely, the predicted increase in slope b with activity-increased L by the MLBH was only consistent in air-breathing species (i.e., herptiles), indicating that volume-related influences from high muscular demands might not be sufficient to explain the variation observed in fish at different activity levels. The contrasting relationship between slopes b and metabolic level in air- and water-breathing ectothermic vertebrates may be explained by the stark differences in costs of moving dense and viscous water over respiratory exchange surfaces to meet increased oxygen demand in water-breathers, compared with the lower costs of increasing ventilation in air-breathers (Atkinson et al., 2022). Instead of a direct effect of hypoxia on individuals (Pauly & Cheung, 2018; Rubalcaba et al., 2020), the mass-scaling of metabolic rates in fish may have evolved adaptive, plastic responses arising from selection on their ancestors to cope with warming periods and events of increased activity demands (Verberk et al., 2021). Such plastic responses might act as a mechanism to avoid oxygen shortage in large individuals (Atkinson et al., 2006, 2022), so that an aerobic margin can be preserved for other activities (e.g., digestion, fighting diseases, mating; see Jutfelt et al., 2018). To test this hypothesis, further comparative studies and experiments should investigate how different energy allocation strategies may arise to maximise fitness when organisms live under particular thermal conditions and activity requirements (e.g., changes in growth trajectory, reproductive investment or adult body size). In this regard, long-term selection experiments and transgenerational designs (e.g., Wootton et

al., 2022), measuring both biomass production (i.e., growth and reproduction) and metabolic expenditure will help to understand the extent to which benign, realistic changes of temperature or activity affect mass-scaling of metabolic rates. This knowledge will help to predict how energy use during ontogeny may change in wild populations under a scenario of global warming (e.g., Lindmark et al., 2018; Moffett et al., 2018).

Furthermore, to disentangle whether changes in metabolic scaling have evolved as mechanisms to avoid oxygen shortage, future research would benefit from phylogenetically controlled investigations of a broader range of taxa (e.g., Leiva et al., 2019, for thermal tolerance). Specifically, analyses should focus on clades comprising both water- and air-breathing species that share common features (e.g., circulatory system, respiratory organs, body shape), which ultimately enable the comparison among taxa in which different respiration modes have evolved independently. The investigation of respiratory systems and evolved responses will be more meaningful when comparisons are made between more closely related species (Perry et al., 2019). Taxonomic groups comprising terrestrial, semi-aquatic and fully aquatic lineages are therefore of special interest here, such as Vertebrata (e.g., teleosts, lungfishes, amphibians), Conchifera (e.g., cephalopods, bivalves, gastropods), Isopoda (e.g., species of woodlouse and within Suborder Asellota), or Oligochaeta (e.g., tubificids, pot worms, earthworms). Indeed, as I found here for ectothermic vertebrates, contrasting thermal responses of metabolic scaling were observed between two species of oligochaetes with different respiration mode (Lee, 2021). However, a general mechanism to explain such variation in metabolic scaling may still be elusive due to the stark variation in (*i*) life-history strategies, such as semelparity or iteroparity (Glazier, 2015; Tan et al., 2019); (*ii*) breathing mechanisms, such as branchial or cutaneous respiration (Hsia et al., 2013; Perry et al., 2019); (*iii*) thermal adaptations, such as cold-induced diapause or estivation (e.g., Marshall & McQuaid, 2011; Young et al., 2011; Li et al., 2022); (*iv*) cell-size effects on oxygen-supply capacity (Verberk et al., 2022); (*v*) and behavioural activity related to lifestyle, e.g., benthic organisms being able to rest whereas pelagic organisms need to maintain buoyancy in the water column (Glazier, 2006, 2020). Incorporating these organismal traits in models to explain intraspecific metabolic scaling will improve our understanding of how different mechanisms to overcome oxygen shortage may have evolved in animals; additionally, such models will determine which taxa could be more vulnerable or resilient to environmental changes.

2. The interspecific variation in metabolic scaling and growth rates among teleost fish

In Chapter 3, I explored the variation in ontogenetic mass-scaling of metabolic rates and growth rates across a diverse array of teleost fish species. The negative relationship I observed between metabolic scaling slopes (b) and maximum growth rates (i.e., a standard measure to compare growth between species; Pauly, 2010) suggests that, since mass-specific growth rates typically decline over fish ontogeny, a greater contribution of growth demands to resting or routine metabolism leads to lower slopes b. These results support the argument that energetic demands of whole-body processes such as growth or maintenance may underpin differences in b between species (Glazier, 2005, 2015), an idea recently termed the 'growth-scaling hypothesis' (GSH; Tan et al., 2019). Indeed, maximum growth rate showed to be a better predictor of slopes b in these species than environmental temperature, metabolic level, or mass-scaling of gill surface-area. These results indicate that the GSH can provide an alternative explanation of the variation in ontogenetic metabolic scaling to the surface area-related constraints or influences on resource supply posited by the MLBH (Glazier, 2005, 2010, 2014). Following the GSH, the same mechanism, i.e. growth demands dictating mass-scaling of metabolic rates in rapidly-growing species, may be applicable to other taxa. In terrestrial ectotherms, for instance, active foragers and predators such as theridiid spiders and some boid snakes generally exhibit faster growth rates and shallower metabolic scaling slopes b than more sluggish and slow-growing counterparts (Glazier, 2009b). Further research will determine whether growth is also an important determinant of metabolic scaling among spiders or snakes.

Furthermore, I was able to partition metabolic costs of teleost species during growth into overhead costs of growth and maintenance demands, estimated using the Ontogenetic Growth Model (OGM) framework (Moses et al., 2008; Barneche & Allen, 2018). After accounting for body mass at maximum growth rate, I found that overhead costs of growth and maintenance demands increase similarly among species adapted to different temperatures, suggesting that the relative contribution of growth to metabolism remains similar across species occurring from polar to tropical climates. Maintenance metabolism, on the other hand, was relatively higher for pelagic fishes than for demersal and benthopelagic species, which may reflect the increased energetic requirements to support greater locomotory capacities in athletic fish, even at rest (Killen et al., 2010, 2016). Remarkably, the net growth efficiency (i.e., energy gain per assimilated energy) exhibited a relatively small variation among these species and barely decreased with temperature. Growth efficiencies were also largely independent of body

size, lifestyle, and phylogeny, revealing that growth efficiency is relatively conserved across species over evolution (Burger et al., 2021; Brandl et al., 2023). Overall, these results highlight that systematic differences in slopes *b* seen in teleost fish are not random deviations from a 'universal' scaling law, but can arise from different growth rates and maintenance requirements among species (Glazier, 2005, 2015; Killen et al., 2010; Tan et al., 2019). Therefore, overlooking this variation in quantitative models of fish energetics may yield unrealistic predictions of resource demand across species.

Since the relationship between metabolic rates and body mass of growing animals reflects how energy use changes during ontogeny, hypotheses on how energy trade-offs vary among teleost species (Sibly et al., 2015) and more broadly among animals (Harrison, 2017; Harrison et al., 2022), would benefit from investigating how fitness-related traits (e.g., body size, biomass production, self-maintenance, mortality) relate to different patterns of metabolic scaling. Recently, White et al. (2022) presented a model positing that mass-scaling of metabolic rates results from evolutionary optimization of fitness-related traits, namely growth, reproduction, and longevity. According to the predictions of this model, they showed that metabolic scaling slopes (*b*) tend to decrease with growth performance but increase with reproductive output for a diverse set of animals including 12 phyla. Such promising models will contribute to understanding of the ultimate (i.e., evolutionary) causes of variation in metabolic scaling.

3. Metabolic scaling and biomass production during ontogeny and between sexes in a model crustacean

In contrast to the multi-species comparisons of metabolic scaling and growth in Chapters 2 and 3, in Chapter 4 I used a single model crustacean species, *Artemia franciscana*, to investigate how the rate of biomass production and its associated costs align with the variation in metabolic scaling during ontogeny and between sexes. I discussed these relationships through the perspective of the cellular mode of growth seen in this species, dominated by cell multiplication early in ontogeny (i.e., embryo and first larval stages) and subsequently by cell expansion (Freeman, 1986, 1995, 2005). Such change in average cell size during organismal growth may influence either resource-supply capacity per cell or the costs of achieving a given rate of supply to cells, and ultimately the costs of production. My findings

showed parallel shifts in metabolic scaling and growth trajectory during ontogeny indicating that growth and metabolism are strongly linked in this species by the overhead costs of growth. In contrast with the general view of increased growth demands related to rapid mass-specific growth rates early in ontogeny (Riisgård, 1998; Glazier, 2022b), the cost per unit growth during larval development was lower than in post-larval individuals, which may reflect the shift in cellular mode of growth in these organisms. These results agree with the relatively low cost of growth during larval phases in other animal groups such as fish (reviewed in Wieser, 1994; and Rombough, 2011) or insects (e.g., Sears et al., 2012; Ferral et al., 2020).

More comprehensive, meta-analytic approaches using available data from various taxa may help to understand the generality of these changes in costs of growth during ontogeny of diverse life forms (reviewed in Wieser, 1994; and Rombough, 2011). However, laboratory experiments are needed to determine the mechanisms by which growth costs are reduced during the fastest growing phases of early life, and specifically, whether this may be explained by enhanced resource-supply into cells with high ratios of surface-area to volume (Kozłowski et al., 2003; Czarnołeski et al., 2008; Glazier, 2022b) and through other exchange surfaces (e.g., gills or integument; Glazier et al., 2015), or from shorter transport distances within organisms (Glazier, 2022b). Although methodologically challenging, further experimental designs will shed light on how biosynthesis costs are related to metabolic scaling patterns by analysing simultaneously how growth, metabolism, and cellular growth change with organismal size (Cadart & Heald, 2022). For instance, a quantitative experiment recently showed the linkages between cell size, body mass, growth, and metabolism in the planarian *Schmidtea mediterranea* (Thommen et al., 2019), demonstrating that the increase in average cell size by larger intracellular reserves accounted for the ¾ power mass-scaling of metabolic rates in this eutelic species.

Moreover, this chapter showed a difference in metabolic scaling slope (*b*) between males and females, though such difference was only found in single (i.e., isolated, and non-reproductive) individuals but not in reproductive animals after mating. This contrasting results between single and reproductive individuals may arise from the increasing demands of egg formation prior to mating and longer post-maturational growth in *Artemia* females, which could together combine to steepen *b* (Glazier, 2015; Moffett et al., 2022). Conversely, the costs of reproduction and their mass-scaling of males and females may converge in reproductive

individuals due to the increased activity of both sexes required during mating, but also because females are able to switch between reproductive modes and so change offspring production costs. In effect, I found that the cost of producing offspring in *A. franciscana* was determined by the amount of larvae produced, relative to the amount of cysts, which cost less to produce. This finding supports the prediction from the Dynamic Energy Budget theory that developing eggs (here, cysts, which are mainly reserves) cost less energy to produce than embryos (i.e., rapidly growing structure) (Maino et al., 2017), which are supplied by gravid females. Overall, these results show that metabolic scaling not only varies between sexes, but also depends on reproductive state, although the possible causes of this variation remain under debate (Somjee et al., 2022).

Comprehensive models aiming to discern general patterns of metabolic scaling between sexes may still be hindered by the very few studies on this topic (reviewed in Somjee et al., 2022). For this purpose, future research on intraspecific metabolic scaling should, when possible, explore differences between sexes and report mass-scaling slopes (*b*) separately for females and males. Moreover, the emphasis should be placed on organismal costs that can contribute to change the mass-scaling of energetic demands between sexes (reviewed in Moffett et al., 2022; and in Somjee et al., 2022), such as variation in (*i*) post-maturational growth (Glazier, 2015) and thus body size between sexes (i.e., sexual size dimorphism); (*ii*) reproductive mode, since increasing offspring production with female size entails greater costs in viviparous but not in oviparous species (e.g., Angilletta & Sears, 2000; Timmerman & Chapman, 2003; Moffett et al., 2022); and (*iii*) mating, especially when this process involves developing and maintaining exaggerated, sexually selected structures (e.g., weapons; Somjee et al., 2018) or require different activity between sexes (e.g., courtship or mate guarding; Somjee et al., 2022).

4. Conclusions

Overall, this thesis supports growing evidence against a general mass-scaling of metabolic rates among all lifeforms, and demonstrates systematic variation in metabolic scaling following changes in environmental temperature, activity level and biomass production. My findings contrast with the classical view of universal scaling 'laws', either across or within species (West et al., 1997, 1999; Brown et al., 2004; Moses et al., 2008), indicating that

deviations from the proposed central scaling values can be biologically meaningful and not just statistical artifacts (Killen et al., 2010; Glazier, 2022a). I showed that responses of metabolic scaling to factors affecting metabolic demand (temperature, activity) differ between closely-related taxa with different respiration modes, which may reveal adaptive mechanisms to protect aerobic scope in water-breathers (Atkinson et al., 2006, 2022), meriting further research in a broader range of taxa. Moreover, I showed that interspecific differences in ontogenetic metabolic scaling are negatively related to maximum growth rates among teleost fishes, suggesting that variation in energy allocation among fitness-related processes, such as growth and self-maintenance, may influence scaling slopes of species, instead of the proposed surface-area influences on oxygen supply. Using a model crustacean, I also demonstrated that shifts in metabolic scaling during ontogeny and differences between sexes align with biomass production and its energetic costs (Wieser, 1984; Riisgård, 1998; Glazier, 2005, 2022b), pointing to the role of cell-size influences on the costs of resource supply. Hence, this thesis combined various perspectives within the theoretical framework of metabolic scaling in animals, emphasizing evolutionary adaptations, plastic responses, and energetic costs of different activities (growth, maintenance, ventilation, and reproduction, including embryo and cyst production). The findings in this thesis will hopefully help improve quantitative models that predict changes in energy use with body size, accounting for adaptive responses to extrinsic as well as intrinsic factors. Such a multi-mechanistic perspective, as highlighted by Glazier (2014, 2022a), is crucial for a comprehensive understanding of the mechanism(s) underpinning metabolic scaling, but also to make accurate predictions in an uncertain scenario of global change.

References

Abdi, H., & Williams, L. J. (2010). Tukey's honestly significant difference (HSD) test. *Encyclopedia of Research Design*, *3*(1), 1-5.

Agutter, P. S., & Wheatley, D. N. (2004). Metabolic scaling: consensus or controversy?. *Theoretical Biology and Medical Modelling*, *1*, 1-11.

Aho, K., Derryberry, D., & Peterson, T. (2014). Model selection for ecologists: the worldviews of AIC and BIC. *Ecology*, *95*(3), 631-636.

Alami-Durante, H., Fauconneau, B., Rouel, M., Escaffre, A. M., & Bergot, P. (1997). Growth and multiplication of white skeletal muscle fibres in carp larvae in relation to somatic growth rate. *Journal of Fish Biology*, *50*(6), 1285-1302.

Andersen, K. H., Berge, T., Gonçalves, R. J., Hartvig, M., Heuschele, J., Hylander, S., Jacobsen, N. S., Lindemann, C., Martens, E. A., Neuheimer, A. B., Olsson, K., Palacz, A., Prowe, A. E. F., Sainmont, J., Traving, S. J., Visser, A. W., Wadhwa, N., & Kiørboe, T. (2016). Characteristic sizes of life in the oceans, from bacteria to whales. *Annual Review of Marine Science*, *8*, 217-241.

Anderson, J. F. (1994). Comparative energetics of comb-footed spiders (Araneae: Theridiidae). *Comparative Biochemistry and Physiology Part A: Physiology*, *109*(1), 181-189.

Angilletta Jr, M. J., Niewiarowski, P. H., & Navas, C. A. (2002). The evolution of thermal physiology in ectotherms. *Journal of thermal Biology*, *27*(4), 249-268.

Angilletta, Jr, M. J., & Dunham, A. E. (2003). The temperature-size rule in ectotherms: simple evolutionary explanations may not be general. *The American Naturalist*, *162*(3), 332-342.

Angilletta, M. J., & Sears, M. W. (2000). The metabolic cost of reproduction in an oviparous lizard. *Functional Ecology*, *14*(1), 39-45.

Arendt, J. D. (2000). Allocation of cells to proliferation vs. differentiation and its consequences for growth and development. *Journal of Experimental Zoology*, *288*(3), 219-234.

Arendt, J. (2007). Ecological correlates of body size in relation to cell size and cell number: patterns in flies, fish, fruits and foliage. *Biological Reviews*, *82*(2), 241-256.

Árnason, T., Björnsson, B., Steinarsson, A., & Oddgeirsson, M. (2009). Effects of temperature and body weight on growth rate and feed conversion ratio in turbot (*Scophthalmus maximus*). *Aquaculture*, *295*(3-4), 218-225.

Atkinson, D., & Sibly, R. M. (1997). Why are organisms usually bigger in colder environments? Making sense of a life history puzzle. *Trends in Ecology & Evolution*, *12*(6), 235-239.

Atkinson, D., Leighton, G., & Berenbrink, M. (2022). Controversial roles of oxygen in organismal responses to climate warming. *The Biological Bulletin*, *243*(2), 207-219.

Atkinson, D., Morley, S. A., & Hughes, R. N. (2006). From cells to colonies: at what levels of body organization does the 'temperature-size rule'apply?. *Evolution & Development*, *8*(2), 202-214.

Banavar, J. R., Damuth, J., Maritan, A., & Rinaldo, A. (2002). Supply–demand balance and metabolic scaling. *Proceedings of the National Academy of Sciences*, *99*(16), 10506-10509.

Banavar, J. R., Moses, M. E., Brown, J. H., Damuth, J., Rinaldo, A., Sibly, R. M., & Maritan, A. (2010). A general basis for quarter-power scaling in animals. *Proceedings of the National Academy of Sciences*, *107*(36), 15816-15820.

Banse, K. (1979). On weight dependence of net growth efficiency and specific respiration rates among field populations of invertebrates. *Oecologia*, *38*(2), 111-126.

Barlow, D. I., & Sleigh, M. A. (1980). The propulsion and use of water currents for swimming and feeding in larval and adult *Artemia*. In G. Persoone, P. Sorgeloos, O. Roles & E. Jaspers (Eds.), *The Brine Shrimp Artemia* (pp. 61-73). Universa Press.

Barneche, D. R., & Allen, A. P. (2018). The energetics of fish growth and how it constrains food-web trophic structure. *Ecology letters*, *21*(6), 836-844.

Barneche, D. R., Jahn, M., & Seebacher, F. (2019). Warming increases the cost of growth in a model vertebrate. *Functional Ecology*, *33*(7), 1256-1266.

Barneche, D. R., Kulbicki, M., Floeter, S. R., Friedlander, A. M., Maina, J., & Allen, A. P. (2014). Scaling metabolism from individuals to reef-fish communities at broad spatial scales. *Ecology Letters*, *17*(9), 1067-1076.

Barneche, D. R., Robertson, D. R., White, C. R., & Marshall, D. J. (2018). Fish reproductive-energy output increases disproportionately with body size. *Science*, 360(6389), 642-645.

Barton, K. (2018). Package 'MuMIn'. Model selection and model averaging based on information criteria. R package version 3.0.2.

Bayne, B. L. (1976). The biology of mussel larvae. In B. L. Bayne (Ed.), *Marine Mussels: Their Ecology and Physiology* (pp. 81-120). Cambridge University press.

Bayne, B. L. (2000). Relations between variable rates of growth, metabolic costs and growth efficiencies in individual Sydney rock oysters (*Saccostrea commercialis*). *Journal of Experimental Marine Biology and Ecology*, 251(2), 185-203.

Bergmann C. (1847). *Über die Verhältnisse der Wärmeökonomie der Thiere zu ihrer Grösse. Göttinger Studien*, Germany.

Beuchat, C. A., & Vleck, D. (1990). Metabolic consequences of viviparity in a lizard, *Sceloporus jarrovi*. *Physiological Zoology*, 63(3), 555-570.

Bigman, J. S., Pardo, S. A., Prinzing, T. S., Dando, M., Wegner, N. C., & Dulvy, N. K. (2018). Ecological lifestyles and the scaling of shark gill surface area. *Journal of Morphology*, 279(12), 1716-1724.

Björnsson, B., & Steinarsson, A. (2002). The food-unlimited growth rate of Atlantic cod (*Gadus morhua*). *Canadian Journal of Fisheries and Aquatic Sciences*, 59(3), 494-502.

Block, B. A. (1991). Endothermy in fish: thermogenesis, ecology and evolution. In P.W. Hochachka & T.P. Mommsen (Eds.), *Biochemistry and Molecular Biology of Fishes* (pp. 269-311). Elsevier.

Block, B. A., & Finnerty, J. R. (1994). Endothermy in fishes: a phylogenetic analysis of constraints, predispositions, and selection pressures. *Environmental Biology of Fishes*, 40, 283-302.

Bodensteiner, B. L., Agudelo-Cantero, G. A., Arietta, A. A., Gunderson, A. R., Muñoz, M. M., Refsnider, J. M., & Gangloff, E. J. (2021). Thermal adaptation revisited: how conserved are thermal traits of reptiles and amphibians?. *Journal of Experimental Zoology Part A: Ecological and Integrative Physiology*, 335(1), 173-194.

Bokma, F. (2004). Evidence against universal metabolic allometry. *Functional Ecology*, 184-187.

Bradley, D. J., & Forward Jr, R. B. (1984). Phototaxis of adult brine shrimp, *Artemia salina*. *Canadian Journal of Zoology*, *62*(12), 2357-2359.

Brand, M. D. (1990). The contribution of the leak of protons across the mitochondrial inner membrane to standard metabolic rate. *Journal of Theoretical Biology*, *145*(2), 267-286.

Brandl, S. J., Lefcheck, J. S., Bates, A. E., Rasher, D. B., & Norin, T. (2023). Can metabolic traits explain animal community assembly and functioning?. *Biological Reviews*, *98*, 1-18.

Brent, R. P. (1973). *Algorithms for Minimization without Derivatives*. Prentice-Hall.

Brett, J. R. (1965). The relation of size to rate of oxygen consumption and sustained swimming speed of sockeye salmon (*Oncorhynchus nerka*). *Journal of the Fisheries Board of Canada*, *22*(6), 1491-1501.

Brett, J. R., & Glass, N. R. (1973). Metabolic rates and critical swimming speeds of sockeye salmon (*Oncorhynchus nerka*) in relation to size and temperature. *Journal of the Fisheries Board of Canada*, 30(3), 379-387.

Brett, J. R., & Groves, T. D. D. (1979). Physiological energetics. *Fish Physiology*, *8*(6), 280-352.

Brill, R. W. (1996). Selective advantages conferred by the high performance physiology of tunas, billfishes, and dolphin fish. *Comparative Biochemistry and Physiology Part A: Physiology*, *113*(1), 3-15.

Britton, R. H., de Groot, E. R., & Johnson, A. R. (1986). The daily cycle of feeding activity of the Greater Flamingo in relation to the dispersion of the prey *Artemia*. *Wildfowl*, *37*, 151-155.

Brody S. & Procter R.C. (1932). Relationship between basal metabolism and mature body-weight in different species of mammals and birds. *University of Missouri Agricultural Experiment Station Research Bulletin*, *116*, 89–101.

Brown, J. H., & Sibly, R. M. (2012). The Metabolic Theory of Ecology and Its Central Equation. In R. M. Sibly, J. H. Brown & A. Kodric-Brown (Eds.), *Metabolic Ecology: A Scaling Approach* (pp. 21-33). John Wiley & Sons, Ltd.

Brown, J. H., Burger, J. R., Hou, C., & Hall, C. A. (2022). The pace of life: metabolic energy, biological time, and life history. *Integrative and Comparative Biology*, *62*(5), 1479-1491.

Brown, J. H., Gillooly, J. F., Allen, A. P., Savage, V. M., & West, G. B. (2004). Toward a metabolic theory of ecology. *Ecology*, *85*(7), 1771-1789.

Brown, J. H., Hall, C. A., & Sibly, R. M. (2018). Equal fitness paradigm explained by a trade-off between generation time and energy production rate. *Nature Ecology & Evolution*, *2*(2), 262-268.

Brown, J. H., Marquet, P. A., & Taper, M. L. (1993). Evolution of body size: consequences of an energetic definition of fitness. *The American Naturalist*, *142*(4), 573-584.

Browne, R. A., & Wanigasekera, G. (2000). Combined effects of salinity and temperature on survival and reproduction of five species of *Artemia*. *Journal of Experimental Marine Biology and Ecology*, *244*(1), 29-44.

Browne, R. A., Sallee, S. E., Grosch, D. S., Segreti, W. O., & Purser, S. M. (1984). Partitioning genetic and environmental components of reproduction and lifespan in *Artemia*. *Ecology*, *65*(3), 949-960.

Buckel, J. A., Steinberg, N. D., & Conover, D. O. (1995). Effects of temperature, salinity, and fish size on growth and consumption of juvenile bluefish. *Journal of Fish Biology*, *47*(4), 696-706.

Burger, J. R., Hou, C., AS Hall, C., & Brown, J. H. (2021). Universal rules of life: metabolic rates, biological times and the equal fitness paradigm *Ecology Letters*, *24*(6), 1262-1281.

Bürkner, P. C. (2017). brms: An R package for Bayesian multilevel models using Stan. *Journal of Statistical Software*, *80*, 1-28.

Bürkner, P. C. (2018). Advanced Bayesian multilevel modeling with the R package brms. *The R Journal*, *10*(1), 395-411.

Burpee, J. L., Bardsley, E. L., Dillaman, R. M., Watanabe, W. O., & Kinsey, S. T. (2010). Scaling with body mass of mitochondrial respiration from the white muscle of three phylogenetically, morphologically and behaviorally disparate teleost fishes. *Journal of Comparative Physiology B*, *180*, 967-977.

Cadart, C., & Heald, R. (2022). Scaling of biosynthesis and metabolism with cell size. *Molecular Biology of the Cell*, *33*(9), 1-6.

Calder, W. A. (1996). *Size, Function, and Life History*. Harvard University Press.

Carey, F. G., Teal, J. M., Kanwisher, J. W., Lawson, K. D., & Beckett, J. S. (1971). Warm-bodied fish. *American Zoologist*, *11*(1), 137-143.

Carey, N., & Sigwart, J. D. (2014). Size matters: plasticity in metabolic scaling shows body-size may modulate responses to climate change. *Biology letters*, *10*(8), 20140408.

Caudell, J. N., & Conover, M. R. (2006). Energy content and digestibility of brine shrimp (*Artemia franciscana*) and other prey items of eared grebes (*Podiceps nigricollis*) on the Great Salt Lake, Utah. *Biological Conservation*, *130*(2), 251-254.

Chang, J., Rabosky, D. L., Smith, S. A., & Alfaro, M. E. (2019). An R package and online resource for macroevolutionary studies using the ray-finned fish tree of life. *Methods in Ecology and Evolution*, *10*(7), 1118-1124.

Clarke, A. (2004). Is there a universal temperature dependence of metabolism?. *Functional Ecology*, *18*(2), 252-256.

Clarke, A. (2017). Temperature, growth and size. In A. Clarke (Ed.), *Principles of Thermal ecology: Temperature, Energy and Life* (pp. 285-307). Oxford University Press.

Clarke, A. (2019). Energy flow in growth and production. *Trends in Ecology & Evolution*, *34*(6), 502-509.

Clarke, A., & Johnston, I. A. (1996). Evolution and adaptive radiation of Antarctic fishes. *Trends in Ecology & Evolution*, *11*(5), 212-218.

Clarke, A., & Johnston, N. M. (1999). Scaling of metabolic rate with body mass and temperature in teleost fish. *Journal of Animal Ecology*, *68*(5), 893-905.

Claunch, N. M., Nix, E., Royal, A. E., Burgos, L. P., Corn, M., DuBois, P. M., Ivey, K. N., King, E. C., Rucker, K. A., Shea, T. K., Stepanek, J., Vansdadia, S. & Taylor, E. N.

(2021). Body size impacts critical thermal maximum measurements in lizards. *Journal of Experimental Zoology Part A: Ecological and Integrative Physiology*, *335*(1), 96-107.

Conceição, L. E. C., Dersjant-Li, Y., & Verreth, J. A. J. (1998). Cost of growth in larval and juvenile African catfish (*Clarias gariepinus*) in relation to growth rate, food intake and oxygen consumption. *Aquaculture*, *161*(1-4), 95-106.

Cornwallis, C. K., & Uller, T. (2010). Towards an evolutionary ecology of sexual traits. *Trends in Ecology & Evolution*, *25*(3), 145-152.

Cribari-Neto, F., & Zeileis, A. (2010). Beta regression in R. *Journal of Statistical Software*, *34*, 1-24.

Criel, G. R., & Macrae, T. H. (2002). Artemia morphology and structure. In T. J. Abatzopoulos, J.A. Beardmore, J.S. Clegg & P. Sorgeloos (Eds.), *Artemia: Basic and Applied Biology* (pp. 1-37). Springer Dordrecht.

Cumminns, K. W., & Wuycheck, J. C. (1971). Caloric Equivalents for Investigations in Ecological Energetics. *Internationale Vereinigung für Theoretische und Angewandte Limnologie: Mitteilungen*, *18*(1), 1-158.

Czarnołęski, M., Kozłowski, J., Dumiot, G., Bonnet, J. C., Mallard, J., & Dupont-Nivet, M. (2008). Scaling of metabolism in *Helix aspersa* snails: changes through ontogeny and response to selection for increased size. *Journal of Experimental Biology*, *211*(3), 391-400.

da Silva, J. K. L., Garcia, G. J., & Barbosa, L. A. (2006). Allometric scaling laws of metabolism. *Physics of Life Reviews*, *3*(4), 229-261.

Davies, K. J. (1995). Oxidative stress: the paradox of aerobic life. *Biochemical Society Symposia*, *61*, 1-31.

Davison, J. (1955). Body weight, cell surface, and metabolic rate in anuran Amphibia. *The Biological Bulletin*, *109*(3), 407-419.

Dawson, G., Suthers, I. M., Brodie, S., & Smith, J. A. (2020). The bioenergetics of a coastal forage fish: Importance of empirical values for ecosystem models. *Deep Sea Research Part II: Topical Studies in Oceanography*, 175, 104700.

Dejours, P. (1981). *Principles of Comparative Respiratory Physiology*. Elsevier.

DeLong, J. P., Okie, J. G., Moses, M. E., Sibly, R. M., & Brown, J. H. (2010). Shifts in metabolic scaling, production, and efficiency across major evolutionary transitions of life. *Proceedings of the National Academy of Sciences*, *107*(29), 12941-12945.

Deutsch, C., Penn, J. L., Verberk, W. C., Inomura, K., Endress, M. G., & Payne, J. L. (2022). Impact of warming on aquatic body sizes explained by metabolic scaling from microbes to macrofauna. *Proceedings of the National Academy of Sciences*, *119*(28), e2201345119.

Dmi'el, R. (1972). Effect of activity and temperature on metabolism and water loss in snakes. *American Journal of Physiology*, *223*(3), 510-516.

Dmitriew, C. M. (2011). The evolution of growth trajectories: what limits growth rate?. *Biological Reviews*, *86*(1), 97-116.

Du Preez, H. H., Mclachlan, A., & Marais, J. F. K. (1988). Oxygen consumption of two nearshore marine elasmobranchs, *Rhinobatos annulatus* (Muller & Henle, 1841) and *Myliobatus aquila* (Linnaeus, 1758). *Comparative Biochemistry and Physiology Part A*: *Physiology*, *89*(2), 283-294.

Ducret, V., Videlier, M., Moureaux, C., Bonneaud, C., & Herrel, A. (2020). Do female frogs have higher resting metabolic rates than males? A case study with *Xenopus allofraseri*. *Journal of Zoology*, *312*(4), 221-226.

Ehnes, R. B., Rall, B. C., & Brose, U. (2011). Phylogenetic grouping, curvature and metabolic scaling in terrestrial invertebrates. *Ecology Letters*, *14*(10), 993-1000.

Einum, S., Bech, C., & Kielland, Ø. N. (2021). Quantitative mismatch between empirical temperature-size rule slopes and predictions based on oxygen limitation. *Scientific Reports*, *11*(1), 23594.

Elliott, J. M., & Davison, W. (1975). Energy equivalents of oxygen consumption in animal energetics. *Oecologia*, *19*, 195-201.

Evjemo, J. O., & Olsen, Y. (1999). Effect of food concentration on the growth and production rate of *Artemia franciscana* feeding on algae (T. iso). *Journal of Experimental Marine Biology and Ecology*, *242*(2), 273-296.

Evjemo, J. O., Vadstein, O., & Olsen, Y. (2000). Feeding and assimilation kinetics of *Artemia franciscana* fed *Isochrysis galbana* (clone T. Iso). *Marine Biology*, *136*, 1099-1109.

Fernández-i-Marín, X. (2016). ggmcmc: Analysis of MCMC samples and Bayesian inference. *Journal of Statistical Software, 70*, 1-20.

Ferral, N., Gomez, N., Holloway, K., Neeter, H., Fairfield, M., Pollman, K., Huang, Y.-W. & Hou, C. (2020). The extremely low energy cost of biosynthesis in holometabolous insect larvae. *Journal of Insect Physiology*, *120*, 103988.

Finkler, M. S., Hayes, C. J., & Rifai, L. (2014). Sexual dimorphisms in metabolism, organ mass, and reproductive energetics in pre-breeding American toads (*Anaxyrus americanus*). *Copeia*, *2014*(3), 447-453.

Fonds, M., Cronie, R., Vethaak, A. D., & Van der Puyl, P. (1992). Metabolism, food consumption and growth of plaice (*Pleuronectes platessa*) and flounder (*Platichthys flesus*) in relation to fish size and temperature. *Netherlands Journal of Sea Research*, *29*(1-3), 127-143.

Forster, J., & Hirst, A. G. (2012). The temperature-size rule emerges from ontogenetic differences between growth and development rates. *Functional Ecology*, *26*(2), 483-492.

Forster, J., Hirst, A. G., & Atkinson, D. (2012). Warming-induced reductions in body size are greater in aquatic than terrestrial species. *Proceedings of the National Academy of Sciences*, *109*(47), 19310-19314.

Fossen, E. I., Pélabon, C., & Einum, S. (2019). Genetic and environmental effects on the scaling of metabolic rate with body size. *Journal of Experimental Biology*, *222*(7), jeb193243.

Freeman, J. A. (1986). Epidermal cell proliferation during thoracic development in larvae of *Artemia*. *Journal of Crustacean Biology*, *6*(1), 37-48.

Freeman, J. A. (1995). Epidermal cell cycle and region-specific growth during segment development in *Artemia*. *Journal of Experimental Zoology*, *271*(4), 285-295.

Freeman, J. A. (2005). Cell differentiation is a primary growth process in developing limbs of *Artemia*. *The Biological Bulletin*, *208*(3), 189-199.

Froese, R., & Pauly, D. (2010). FishBase. www.fishbase.org

Funk, D. H., Sweeney, B. W., & Jackson, J. K. (2021). Oxygen limitation fails to explain upper chronic thermal limits and the temperature size rule in mayflies. *Journal of Experimental Biology*, *224*(1), jeb233338.

Fusco, G., & Minelli, A. (2021). The development of arthropod segmentation across the embryonic/post-embryonic divide–an evolutionary perspective. *Frontiers in Ecology and Evolution*, *9*, 622482.

Gabry, J., Simpson, D., Vehtari, A., Betancourt, M., & Gelman, A. (2019). Visualization in Bayesian workflow. *Journal of the Royal Statistical Society Series A-Statistics in Society*, *182*(2), 382-402.

Gaitán-Espitia, J. D., Bruning, A., Mondaca, F., & Nespolo, R. F. (2013). Intraspecific variation in the metabolic scaling exponent in ectotherms: testing the effect of latitudinal cline, ontogeny and transgenerational change in the land snail *Cornu aspersum. Comparative Biochemistry and Physiology Part A: Molecular & Integrative Physiology*, *165*(2), 169-177.

Gajardo, G. M., & Beardmore, J. A. (1989). Ability to switch reproductive mode in *Artemia* is related to maternal heterozygosity. *Marine Ecology Progress Series*, *55*(2), 191-195.

Gajardo, G. M., & Beardmore, J. A. (2012). The brine shrimp Artemia: adapted to critical life conditions. *Frontiers in Physiology*, *3*, 1-8.

Garland Jr, T. (1984). Physiological correlates of locomotory performance in a lizard: an allometric approach. *American Journal of Physiology*, *247*(5), R806-R815.

Garland, Jr, T., & Ives, A. R. (2000). Using the past to predict the present: confidence intervals for regression equations in phylogenetic comparative methods. *The American Naturalist*, *155*(3), 346-364.

Geffen, A. J., Van der Veer, H. W., & Nash, R. D. M. (2007). The cost of metamorphosis in flatfishes. *Journal of Sea Research*, *58*(1), 35-45.

Gelman, A. (2003). A Bayesian formulation of exploratory data analysis and goodness-of-fit testing. *International Statistical Review*, *71*(2), 369-382.

Gelman, A., & Hill, J. (2006). *Data Analysis Using Regression and Multilevel/Hierarchical Models*. Cambridge University Press.

Gifford, M. E., Clay, T. A., & Peterman, W. E. (2013). The effects of temperature and activity on intraspecific scaling of metabolic rates in a lungless salamander. *Journal of Experimental Zoology Part A: Ecological Genetics and Physiology*, *319*(4), 230-236.

Giguère, L. A., Côté, B., & St-Pierre, J. F. (1988). Metabolic rates scale isometrically in larval fishes. *Marine Ecology Progress Series*, *50*, 13-19.

Gillooly, J. F., & Allen, A. P. (2007). Changes in body temperature influence the scaling of and aerobic scope in mammals. *Biology Letters*, *3*(1), 100-103.

Gillooly, J. F., Brown, J. H., West, G. B., Savage, V. M., & Charnov, E. L. (2001). Effects of size and temperature on metabolic rate. *Science*, *293*(5538), 2248-2251.

Gillooly, J. F., Charnov, E. L., West, G. B., Savage, V. M., & Brown, J. H. (2002). Effects of size and temperature on developmental time. *Nature*, *417*(6884), 70-73.

Gillooly, J. F., Gomez, J. P., Mavrodiev, E. V., Rong, Y., & McLamore, E. S. (2016). Body mass scaling of passive oxygen diffusion in endotherms and ectotherms. *Proceedings of the National Academy of Sciences*, *113*(19), 5340-5345.

Gillooly, J. F., Gomez, J. P., Mavrodiev, E. V., Rong, Y., & McLamore, E. S. (2016). Body mass scaling of passive oxygen diffusion in endotherms and ectotherms. *Proceedings of the National Academy of Sciences*, *113*(19), 5340-5345.

Gittleman, J. L., & Thompson, S. D. (1988). Energy allocation in mammalian reproduction. *American Zoologist*, *28*(3), 863-875.

Given, M. F. (1988). Growth rate and the cost of calling activity in male carpenter frogs, *Rana virgatipes*. *Behavioral Ecology and Sociobiology*, *22*(3), 153-160.

Gkioulekas, I., & Papageorgiou, L. G. (2019). Piecewise regression analysis through information criteria using mathematical programming. *Expert Systems with Applications*, *121*, 362-372.

Glazier, D. S. (2005). Beyond the '3/4-power law': variation in the intra-and interspecific scaling of metabolic rate in animals. *Biological Reviews*, *80*(4), 611-662.

Glazier, D. S. (2006). The 3/4-power law is not universal: evolution of isometric, ontogenetic metabolic scaling in pelagic animals. *BioScience*, *56*(4), 325-332.

Glazier, D. S. (2008). Effects of metabolic level on the body size scaling of metabolic rate in birds and mammals. *Proceedings of the Royal Society B: Biological Sciences*, *275*(1641), 1405-1410.

Glazier, D. S. (2009a). Metabolic level and size scaling of rates of respiration and growth in unicellular organisms. *Functional Ecology*, *23*(5), 963-968.

Glazier, D. S. (2009b). Ontogenetic body-mass scaling of resting metabolic rate covaries with species-specific metabolic level and body size in spiders and snakes. *Comparative Biochemistry and Physiology Part A: Molecular & Integrative Physiology*, *153*(4), 403-407.

Glazier, D. S. (2009c). Activity affects intraspecific body-size scaling of metabolic rate in ectothermic animals. *Journal of Comparative Physiology B*, *179*, 821-828.

Glazier, D. S. (2010). A unifying explanation for diverse metabolic scaling in animals and plants. *Biological Reviews*, *85*(1), 111-138.

Glazier, D. S. (2014). Scaling of metabolic scaling within physical limits. *Systems*, *2*(4), 425-450.

Glazier, D. S. (2015). Is metabolic rate a universal 'pacemaker' for biological processes?. *Biological Reviews*, *90*(2), 377-407.

Glazier, D. S. (2018a). Effects of contingency versus constraints on the body-mass scaling of metabolic rate. *Challenges*, *9*(1), 4.

Glazier, D. S. (2018b). Resource Supply and Demand Both Affect Metabolic Scaling: A Response to Harrison. *Trends in Ecology & Evolution*, 33(4), 237-238.

Glazier, D. S. (2020). Activity alters how temperature influences intraspecific metabolic scaling: testing the metabolic-level boundaries hypothesis. *Journal of Comparative Physiology B*, *190*(4), 445-454.

Glazier, D. S. (2021). Biological scaling analyses are more than statistical line fitting. *Journal of Experimental Biology*, *224*(11), jeb241059.

Glazier, D. S. (2022a). Variable metabolic scaling breaks the law: from 'Newtonian' to 'Darwinian' approaches. *Proceedings of the Royal Society B: Biological Sciences*, *289*(1985), 20221605.

Glazier, D. S. (2022b). How metabolic rate relates to cell size. *Biology*, *11*(8), 1106.

Glazier, D. S., & Calow, P. (1992). Energy allocation rules in *Daphnia magna*: clonal and age differences in the effects of food limitation. *Oecologia*, *90*(4), 540-549.

Glazier, D. S., & Paul, D. A. (2017). Ecology of ontogenetic body-mass scaling of gill surface area in a freshwater crustacean. *Journal of Experimental Biology*, *220*(11), 2120-2127.

Glazier, D. S., Borrelli, J. J., & Hoffman, C. L. (2020). Effects of fish predators on the mass-related energetics of a keystone freshwater crustacean. *Biology*, *9*(3), 40.

Glazier, D. S., Hirst, A. G., & Atkinson, D. (2015). Shape shifting predicts ontogenetic changes in metabolic scaling in diverse aquatic invertebrates. *Proceedings of the Royal Society B: Biological Sciences*, *282*(1802), 20142302.

Goss, R. J. (1966). Hypertrophy versus Hyperplasia: How much organs can grow depends on whether their functional units increase in size or in number. *Science*, *153*(3744), 1615-1620.

Gould, S. J. (1966). Allometry and size in ontogeny and phylogeny. *Biological Reviews*, *41*(4), 587-638.

Grafen, A. (1989). The phylogenetic regression. *Philosophical Transactions of the Royal Society of London. B, Biological Sciences, 326*(1233), 119-157.

Graham, J. B., & Wegner, N. C. (2010). Breathing air in water and in air: the air-breathing fishes. In G. Nilsson (Ed.), *Respiratory physiology of vertebrates: Life With and Without Oxygen* (pp. 174-221). Cambridge University Press.

Gulbrandsen, J. (2001). *Artemia* swarming—mechanisms and suggested reasons. *Journal of Plankton Research*, *23*(7), 659-669.

Harrison, J. F. (2017). Do performance–safety tradeoffs cause hypometric metabolic scaling in animals?. *Trends in Ecology & Evolution*, *32*(9), 653-664.

Harrison, J. F., Biewener, A., Bernhardt, J. R., Burger, J. R., Brown, J. H., Coto, Z. N., Duell, M. E. D., Lynch, M., Moffett, E. R., Norin, T. N., Pettersen, A. K., Smith, F. A., Somjee,

U., Traniello, J. F. A. & Williams, T. M. (2022). White paper: an integrated perspective on the causes of hypometric metabolic scaling in animals. *Integrative and Comparative Biology*, *62*(5), 1395-1418.

Harrison, X. A., Donaldson, L., Correa-Cano, M. E., Evans, J., Fisher, D. N., Goodwin, C. E., Robinson, B. S., Hodgson, D. J., & Inger, R. (2018). A brief introduction to mixed effects modelling and multi-model inference in ecology. *PeerJ*, *6*, e4794.

Hatton, I. A., Dobson, A. P., Storch, D., Galbraith, E. D., & Loreau, M. (2019). Linking scaling laws across eukaryotes. *Proceedings of the National Academy of Sciences*, *116*(43), 21616-21622.

Hayward, A., & Gillooly, J. F. (2011). The cost of sex: quantifying energetic investment in gamete production by males and females. *PLoS One*, *6*(1), e16557.

Hemmingsen, A. M. (1960). Energy metabolism as related to body size and respiratory surface, and its evolution. *Reports of the Steno Memorial Hospital and the Nordisk Insulin Laboratorium (Copenhagen)*, *9*, 1-110.

Higgins, P. J., & Thorpe, J. E. (1990). Hyperplasia and hypertrophy in the growth of skeletal muscle in juvenile Atlantic salmon, *Salmo salar* L. *Journal of Fish Biology*, *37*(4), 505-519.

Hirst, A. G., & Forster, J. (2013). When growth models are not universal: evidence from marine invertebrates. *Proceedings of the Royal Society B: Biological Sciences*, *280*(1768), 20131546.

Hirst, A. G., Glazier, D. S., & Atkinson, D. (2014). Body shape shifting during growth permits tests that distinguish between competing geometric theories of metabolic scaling. *Ecology Letters*, *17*(10), 1274-1281.

Hoffman, M. D., & Gelman, A. (2014). The No-U-Turn sampler: adaptively setting path lengths in Hamiltonian Monte Carlo. *Journal of Machine Learning Research*, *15*(1), 1593-1623.

Hoppeler, H., Kayar, S. R., Claasen, H., Uhlmann, E., & Karas, R. H. (1987). Adaptive variation in the mammalian respiratory system in relation to energetic demand: III. Skeletal muscles: setting the demand for oxygen. *Respiration Physiology*, *69*(1), 27-46.

Horn, S., & de la Vega, C. (2016). Relationships between fresh weight, dry weight, ash free dry weight, carbon and nitrogen content for selected vertebrates. *Journal of Experimental Marine Biology and Ecology*, *481*, 41-48.

Hou, C., Zuo, W., Moses, M. E., Woodruff, W. H., Brown, J. H., & West, G. B. (2008). Energy uptake and allocation during ontogeny. *Science*, *322*(5902), 736-739.

Hsia, C. C., Schmitz, A., Lambertz, M., Perry, S. F., & Maina, J. N. (2013). Evolution of air breathing: oxygen homeostasis and the transitions from water to land and sky. *Comprehensive Physiology*, *3*(2), 849-915.

Hu, T. M. (2022). A general biphasic bodyweight model for scaling basal metabolic rate, glomerular filtration rate, and drug clearance from birth to adulthood. *The AAPS Journal*, *24*(3), 1-19.

Hughes, A. L. (1985). Male size, mating success, and mating strategy in the mosquitofish *Gambusia affinis* (Poeciliidae). *Behavioral Ecology and Sociobiology*, 17, 271-278.

Humphries, M. M., & McCann, K. S. (2014). Metabolic ecology. *Journal of Animal Ecology*, *83*(1), 7-19.

Hutchison, V. H., & Dupré, R. K. (1992). Thermoregulation. In M. R. Feder & W. W. Burggren (Eds.), *Environmental physiology of the amphibians* (pp. 206-249). University of Chicago Press.

Imsland, A. K., & Jonassen, T. M. (2001). Regulation of growth in turbot (*Scophthalmus maximus* Rafinesque) and Atlantic halibut (*Hippoglossus hippoglossus* L.): aspects of environment× genotype interactions. *Reviews in Fish Biology and Fisheries*, *11*, 71-90.

Isaac, N. J., & Carbone, C. (2010). Why are metabolic scaling exponents so controversial? Quantifying variance and testing hypotheses. *Ecology Letters*, *13*(6), 728-735.

Johnston, I. A., Calvo, J., Guderley, H., Fernandez, D., & Palmer, L. I. S. A. (1998). Latitudinal variation in the abundance and oxidative capacities of muscle mitochondria in perciform fishes. *The Journal of Experimental Biology*, *201*(1), 1-12.

Jorgensen, C. B. (1988). Metabolic costs of growth and maintenance in the toad, *Bufo bufo*. *Journal of Experimental Biology*, *138*(1), 319-331.

Jutfelt, F. (2020). Metabolic adaptation to warm water in fish. *Functional Ecology*, *34*(6), 1138-1141.

Jutfelt, F., Norin, T., Åsheim, E. R., Rowsey, L. E., Andreassen, A. H., Morgan, R., Clark, T. D., & Speers-Roesch, B. (2021). 'Aerobic scope protection' reduces ectotherm growth under warming. *Functional Ecology*, *35*(7), 1397-1407.

Kamler, E. (1992). *Early Life History of Fish: An Energetics Approach*. Chapman & Hall.

Karkach, A. S. (2006). Trajectories and models of individual growth. *Demographic Research*, 15, 347-400.

Kay, M. (2022). tidybayes: Tidy data and geoms for Bayesian models. R package version 3.0.2.

Kearney, M. R., & White, C. R. (2012). Testing metabolic theories. *The American Naturalist*, *180*(5), 546-565.

Killen, S. S., Atkinson, D., & Glazier, D. S. (2010). The intraspecific scaling of metabolic rate with body mass in fishes depends on lifestyle and temperature. *Ecology Letters*, *13*(2), 184-193.

Killen, S. S., Costa, I., Brown, J. A., & Gamperl, A. K. (2007). Little left in the tank: metabolic scaling in marine teleosts and its implications for aerobic scope. *Proceedings of the Royal Society B: Biological Sciences*, *274*(1608), 431-438.

Killen, S. S., Glazier, D. S., Rezende, E. L., Clark, T. D., Atkinson, D., Willener, A. S., & Halsey, L. G. (2016). Ecological influences and morphological correlates of resting and maximal metabolic rates across teleost fish species. *The American Naturalist*, *187*(5), 592-606.

Kiørboe, T., & Hirst, A. G. (2014). Shifts in mass scaling of respiration, feeding, and growth rates across life-form transitions in marine pelagic organisms. *The American Naturalist*, *183*(4), E118-E130.

Kiørboe, T., Møhlenberg, F., & Hamburger, K. (1985). Bioenergetics of the planktonic copepod *Acartia tonsa*: relation between feeding, egg production and respiration, and composition of specific dynamic action. *Marine Ecology Progress Series*, *26*(1-2), 85-97.

Kiørboe, T., Munk, P., & Richardson, K. (1987). Respiration and growth of larval herring *Clupea harengus*: relation between specific dynamic action and growth efficiency. *Marine Ecology Progress Series*, 40(1-2), 1-10.

Kleiber, M. (1932). Body size and metabolism. *Hilgardia*, *6*(11), 315-353.

Koch, R. E., Buchanan, K. L., Casagrande, S., Crino, O., Dowling, D. K., Hill, G. E., Hood, W. R., McKenzie, M., Mariette, M. M., Noble, D. W. A., Pavlova, A., Seebacher, F., Sunnucks, P., Udino, E., White, C. R., Salin, K., & Stier, A. (2021). Integrating mitochondrial aerobic metabolism into ecology and evolution. *Trends in Ecology & Evolution*, *36*(4), 321-332.

Kooijman, S. A. L. M. (1986). Energy budgets can explain body size relations. *Journal of Theoretical Biology*, *121*(3), 269-282.

Kooijman, S. A. L. M. (2000). Dynamic energy and mass budgets in biological systems. Cambridge university press.

Kooijman, S. A. L. M. (2010). Dynamic Energy Budget Theory for Metabolic Organisation. Cambridge University Press.

Kozłowski, J., Konarzewski, M., & Czarnoleski, M. (2020). Coevolution of body size and metabolic rate in vertebrates: a life-history perspective. *Biological Reviews*, *95*(5), 1393-1417.

Kozłowski, J., Konarzewski, M., & Gawelczyk, A. T. (2003). Cell size as a link between noncoding DNA and metabolic rate scaling. *Proceedings of the National Academy of Sciences*, *100*(24), 14080-14085.

Kutschera, U., & Niklas, K. J. (2012). Organ-specific rates of cellular respiration in developing sunflower seedlings and their bearing on metabolic scaling theory. *Protoplasma*, *249*, 1049-1057.

Lee, L., Atkinson, D., Hirst, A. G., & Cornell, S. J. (2020). A new framework for growth curve fitting based on the von Bertalanffy Growth Function. *Scientific Reports*, *10*(1), 1-12.

Lee, L. (2021). *Towards improved predictions of growth and metabolism in the animal kingdom*. PhD Dissertation, University of Liverpool.

Lefébure, R., Larsson, S., & Byström, P. (2011). A temperature-dependent growth model for the three-spined stickleback *Gasterosteus aculeatus*. *Journal of Fish Biology*, *79*(7), 1815-1827.

Léger, P., Bengtson, D. A., Sorgeloos, P., Simpson, K. L., & Beck, A. D. (1987). The nutritional value of *Artemia*: a review. *Artemia Research and its Applications*, *3*, 357-372.

Leiva, F. P., Calosi, P., & Verberk, W. C. (2019). Scaling of thermal tolerance with body mass and genome size in ectotherms: a comparison between water- and air-breathers. *Philosophical Transactions of the Royal Society B*, *374*(1778), 20190035.

Lent, C. M. (1977). The mechanism for co-ordinating metachronal limb movements between joined male and female *Artemia salina* during precopulatory behaviour. *Journal of Experimental Biology*, *66*(1), 127-140.

Lewandowski, D., Kurowicka, D., & Joe, H. (2009). Generating random correlation matrices based on vines and extended onion method. *Journal of Multivariate Analysis*, *100*(9), 1989-2001.

Li, Y., Ding, Y., & Pan, L. (2022). Effects of increasing temperature and aestivation on biogenic amines, signal transduction pathways and metabolic enzyme activities in the sea cucumber (*Apostichopus japonicus*). *Marine Biology*, 169, 1-16.

Lindeman, R. L. (1942). The trophic-dynamic aspect of ecology. *Ecology*, *23*(4), 399-417.

Lindmark, M., Huss, M., Ohlberger, J., & Gårdmark, A. (2018). Temperature-dependent body size effects determine population responses to climate warming. *Ecology Letters*, *21*(2), 181-189.

Lindmark, M., Ohlberger, J., & Gårdmark, A. (2022). Optimum growth temperature declines with body size within fish species. *Global Change Biology*, *28*(7), 2259-2271.

Lüdecke et al., (2021). performance: An R Package for Assessment, Comparison and Testing of Statistical Models. *Journal of Open Source Software*, *6*(60), 3139.

Lyman, C. P. (1968). Body temperature of exhausted salmon. *Copeia*, 1968(3), 631-633.

Maino, J. L., Kearney, M. R., Nisbet, R. M., & Kooijman, S. A. (2014). Reconciling theories for metabolic scaling. *Journal of Animal Ecology*, *83*(1), 20-29.

Maino, J. L., Pirtle, E. I., & Kearney, M. R. (2017). The effect of egg size on hatch time and metabolic rate: theoretical and empirical insights on developing insect embryos. *Functional Ecology*, *31*(1), 227-234.

Makarieva, A. M., Gorshkov, V. G., & Li, B. L. (2004). Ontogenetic growth: models and theory. *Ecological Modelling*, *176*(1-2), 15-26.

Makarieva, A. M., Gorshkov, V. G., Li, B. L., Chown, S. L., Reich, P. B., & Gavrilov, V. M. (2008). Mean mass-specific metabolic rates are strikingly similar across life's major domains: evidence for life's metabolic optimum. *Proceedings of the National Academy of Sciences*, *105*(44), 16994-16999.

Manzanares, M., Marco, R., & Garesse, R. (1993). Genomic organization and developmental pattern of expression of the engrailed gene from the brine shrimp *Artemia*. *Development*, *118*(4), 1209-1219.

Marchant, R. (1978). The energy balance of the Australian brine shrimp, *Parartemia zietziana* (Crustacea: Anostraca). *Freshwater Biology*, *8*(5), 481-489.

Marshall, D. J., & McQuaid, C. D. (2011). Warming reduces metabolic rate in marine snails: adaptation to fluctuating high temperatures challenges the metabolic theory of ecology. *Proceedings of the Royal Society B: Biological Sciences*, *278*(1703), 281-288.

Marshall, D. J., & White, C. R. (2019a). Have we outgrown the existing models of growth?. *Trends in Ecology & Evolution*, *34*(2), 102-111.

Marshall, D. J., & White, C. R. (2019b). Aquatic life history trajectories are shaped by selection, not oxygen limitation. *Trends in Ecology & Evolution*, *34*(3), 182-184.

Michonneau, F., Brown, J. W., & Winter, D. J. (2016). rotl: an R package to interact with the Open Tree of Life data. *Methods in Ecology and Evolution*, *7*(12), 1476-1481.

Mitz, S. V., & Newman, M. C. (1989). Allometric relationship between oxygen consumption and body weight of mosquitofish, *Gambusia affinis*. *Environmental Biology of Fishes*, *24*, 267-273.

Moffett, E. R., Fryxell, D. C., Benavente, J. N., Kinnison, M. T., Palkovacs, E. P., Symons, C. C., & Simon, K. S. (2022). The effect of pregnancy on metabolic scaling and population energy demand in the viviparous fish *Gambusia affinis*. *Integrative and Comparative Biology*, *62*(5), 1419-1428.

Moffett, E. R., Fryxell, D. C., Palkovacs, E. P., Kinnison, M. T., & Simon, K. S. (2018). Local adaptation reduces the metabolic cost of environmental warming. *Ecology*, *99*(10), 2318-2326.

Moran, D., & Wells, R. M. (2007). Ontogenetic scaling of fish metabolism in the mouse-to-elephant mass magnitude range. *Comparative Biochemistry and Physiology Part A: Molecular & Integrative Physiology*, *148*(3), 611-620.

Moses, M. E., Hou, C., Woodruff, W. H., West, G. B., Nekola, J. C., Zuo, W., & Brown, J. H. (2008). Revisiting a model of ontogenetic growth: estimating model parameters from theory and data. *The American Naturalist*, *171*(5), 632-645.

Muggeo, V. M. (2008). Segmented: an R package to fit regression models with broken-line relationships. *R News*, *8*(1), 20-25.

Muir, B. S., & Hughes, G. M. (1969). Gill dimensions for three species of tunny. *Journal of Experimental Biology*, *51*(2), 271-285.

Navarro, J. M., Paschke, K., Ortiz, A., Vargas-Chacoff, L., Pardo, L. M., & Valdivia, N. (2019). The Antarctic fish *Harpagifer antarcticus* under current temperatures and salinities and future scenarios of climate change. *Progress in Oceanography*, *174*, 37-43.

Nielsen, A. M., Eriksen, N. T., Iversen, J. L., & Riisgård, H. U. (1995). Feeding, growth and respiration in the polychaetes *Nereis diversicolor* (facultative filter-feeder) and *N. virens* (omnivorous)-a comparative study. *Marine Ecology Progress Series*, *125*, 149-158.

Nilsson, G. E., Dymowska, A., & Stecyk, J. A. (2012). New insights into the plasticity of gill structure. *Respiratory Physiology & Neurobiology*, *184*(3), 214-222.

Ohlberger, J., Mehner, T., Staaks, G., & Hölker, F. (2012). Intraspecific temperature dependence of the scaling of metabolic rate with body mass in fishes and its ecological implications. *Oikos*, *121*(2), 245-251.

Oikawa, S., Itazawa, Y., & Gotoh, M. (1991). Ontogenetic change in the relationship between metabolic rate and body mass in a sea bream *Pagrus major* (Temminck & Schlegel). *Journal of Fish Biology*, *38*(4), 483-496.

Orme, D., Freckleton, R., Thomas, G., Petzoldt, T., Fritz, S., Isaac, N., & Pearse, W. (2018). The caper package: comparative analysis of phylogenetics and evolution in R. R package version 1.0.1.

Pace, D. A., & Manahan, D. T. (2007). Efficiencies and costs of larval growth in different food environments (Asteroidea: *Asterina miniata*). *Journal of Experimental Marine Biology and Ecology*, *353*(1), 89-106.

Paloheimo, J. E. D., & Dickie, L. M. (1965). Food and Growth of Fishes.: I. A Growth Curve Derived from Experimental Data. *Journal of the Fisheries Board of Canada*, *22*(2), 521-542.

Paradis, E., & Schliep, K. (2019). ape 5.0: an environment for modern phylogenetics and evolutionary analyses in R. *Bioinformatics*, *35*(3), 526-528.

Parry, G. D. (1983). The influence of the cost of growth on ectotherm metabolism. *Journal of Theoretical Biology*, *101*(3), 453-477.

Pauly, D. (2010). *Gasping Fish and Panting Squids: Oxygen, Temperature and the Growth of Water Breathing Animals*. International Ecology Institute, Oldendorf/Luhe.

Pauly, D. (2021). The gill-oxygen limitation theory (GOLT) and its critics. *Science Advances*, *7*(2), eabc6050.

Pauly, D., & Cheung, W. W. (2018). Sound physiological knowledge and principles in modeling shrinking of fishes under climate change. *Global Change Biology*, *24*(1), e15-e26.

Peck, L. (2020). The ecophysiology of responding to change in polar marine benthos. In G. Di Prisco, H. Edwards, J. Elster, & A. Huiskes (Eds.), *Life in Extreme Environments: Insights in Biological Capability* (pp. 184-217). Cambridge University Press.

Peck, L. S. (2018). Antarctic marine biodiversity: adaptations, environments and responses to change. In S. J. Hawkins, A. J. Evans, A. C. Dale, L. B. Firth & I. P. Smith (Eds.), *Oceanography and Marine Biology: An Annual Review* (pp. 105-235). CRC Press.

Perry, S. F., Lambertz, M., & Schmitz, A. (2019). *Respiratory Biology of Animals: evolutionary and functional morphology*. Oxford University Press.

Peters, R. H. (1986). *The Ecological Implications of Body Size*. Cambridge university press.

Post, J. R., & Lee, J. A. (1996). Metabolic ontogeny of teleost fishes. *Canadian Journal of Fisheries and Aquatic Sciences*, *53*(4), 910-923.

Price, C. A., Weitz, J. S., Savage, V. M., Stegen, J., Clarke, A., Coomes, D. A., Dodds, P. S., Etienne, R. S., Kerkhoff, A. J., McCulloh, K., Niklas, K. J., Olff, H., & Swenson, N. G. (2012). Testing the metabolic theory of ecology. *Ecology Letters*, *15*(12), 1465-1474.

Provasoli, L., & Shiraishi, K. (1959). Axenic cultivation of the brine shrimp *Artemia salina*. *The Biological Bulletin*, *117*(2), 347-355.

Pütter, A. (1920). Studien über physiologische Ähnlichkeit. VI. Wachstumsähnlichkeiten. *Pflüger's Archiv für die Gesamte Physiologie des Menschen und der Tiere*, *180*(1), 298-340.

R Core Team (2022). R: A language and environment for statistical computing. R Foundation for Statistical Computing, Vienna, Austria. https://www.R-project.org/

Rao, G. M. M. (1968). Oxygen consumption of rainbow trout (*Salmo gairdneri*) in relation to activity and salinity. *Canadian Journal of Zoology*, *46*(4), 781-786.

Reeve, M. R. (1963). The filter-feeding of *Artemia*: I. In pure cultures of plant cells. *Journal of Experimental Biology, 40*(1), 195-205.

Revell, L. J. (2012). phytools: an R package for phylogenetic comparative biology (and other things). *Methods in Ecology and Evolution*, *3*(2), 217-223.

Rhen, T., & Lang, J. W. (1995). Phenotypic plasticity for growth in the common snapping turtle: effects of incubation temperature, clutch, and their interaction. *The American Naturalist*, *146*(5), 726-747.

Ricklefs, R. E. (2003). Is rate of ontogenetic growth constrained by resource supply or tissue growth potential? A comment on West et al.'s model. *Functional Ecology*, *17*(3), 384-393.

Ricklefs, R. E., & Wikelski, M. (2002). The physiology/life-history nexus. *Trends in Ecology & Evolution*, *17*(10), 462-468.

Riisgård, H. U. (1998). No foundation of a '3/4 power scaling law' for respiration in biology. *Ecology Letters*, *1*(2), 71-73.

Rode, N. O., Charmantier, A., & Lenormand, T. (2011). Male–female coevolution in the wild: Evidence from a time series in *Artemia franciscana*. *Evolution*, *65*(10), 2881-2892.

Rohatgi, A. (2020). Webplotdigitizer: Version 4.4. https://automeris. io/WebPlotDigitizer

Rolfe, D. F., & Brown, G. C. (1997). Cellular energy utilization and molecular origin of standard metabolic rate in mammals. *Physiological Reviews*, *77*(3), 731-758.

Rombough, P. (2006). Developmental costs and the partitioning of metabolic energy. In S. J. Warburton, W. W. Burggren, B. Pelster, C. L Reiber & J. Spicer (Eds.), *Comparative Developmental Physiology: Contributions, Tools and Trends* (pp. 99-123). Oxford University Press.

Rombough, P. (2011). The energetics of embryonic growth. *Respiratory Physiology & Neurobiology*, *178*(1), 22-29.

Rombough, P. J. (1994). Energy partitioning during fish development: additive or compensatory allocation of energy to support growth?. *Functional Ecology*, *8*(2), 178-186.

Roosenburg, W. M., & Kelley, K. C. (1996). The effect of egg size and incubation temperature on growth in the turtle, *Malaclemys terrapin*. *Journal of Herpetology*, 198-204.

Rosenfeld, J., Van Leeuwen, T., Richards, J., & Allen, D. (2015). Relationship between growth and standard metabolic rate: measurement artefacts and implications for habitat use and life-history adaptation in salmonids. *Journal of Animal Ecology*, *84*(1), 4-20.

Rubalcaba, J. G., Verberk, W. C., Hendriks, A. J., Saris, B., & Woods, H. A. (2020). Oxygen limitation may affect the temperature and size dependence of metabolism in aquatic ectotherms. *Proceedings of the National Academy of Sciences*, *117*(50), 31963-31968.

Rubner, Max (1883): Ueber den Einfluss der Körpergrösse auf Stoff- und Kraftwechsel. *Zeitschrift für Biologie*, *19*, 535–562.

Sarrus, F., & Rameaux, J. F. (1839). Application des sciences accessoires et principalement des mathématiques à la physiologie générale (Rapport sur une mémoire adressé à l'Académic royale de Médecine, séance du 23 juillet 1839). *Bulletin de L'Académie Nationale de Médecine.(Paris)*, *3*, 1094-1100.

Savage, V. M., Gillooly, J. F., Woodruff, W. H., West, G. B., Allen, A. P., Enquist, B. J., & Brown, J. H. (2004). The predominance of quarter-power scaling in biology. *Functional Ecology*, *18*(2), 257-282.

Schrehardt, A. (1987). A scanning electron-microscope study of the post-embryonic development of *Artemia*. *Artemia* research and its applications, *1*, 5-32.

Sears, K. E., Kerkhoff, A. J., Messerman, A., & Itagaki, H. (2012). Ontogenetic scaling of metabolism, growth, and assimilation: testing metabolic scaling theory with *Manduca sexta* larvae. *Physiological and Biochemical Zoology*, *85*(2), 159-173.

Seebacher, F., White, C. R., & Franklin, C. E. (2015). Physiological plasticity increases resilience of ectothermic animals to climate change. *Nature Climate Change*, *5*(1), 61-66.

Sender, R., & Milo, R. (2021). The distribution of cellular turnover in the human body. *Nature Medicine*, *27*(1), 45-48.

Shelton, G., Jones, D.R. & Milsom, W.K. (1986). Control of breathing in ectothermic vertebrates. In A. F. Fishman, F.J. Chernlack, J.G. Widdlcombe & S.R. Geiger (Eds.), *Handbook of Physiology* (pp. 857-909). John Wiley & Sons Inc.

Sibly, R. M., Baker, J., Grady, J. M., Luna, S. M., Kodric-Brown, A., Venditti, C., & Brown, J. H. (2015). Fundamental insights into ontogenetic growth from theory and fish. *Proceedings of the National Academy of Sciences*, *112*(45), 13934-13939.

Siems, W. G., Schmidt, H., Gruner, S., & Jakstadt, M. (1992). Balancing of energy-consuming processes of K 562 cells. *Cell Biochemistry and Function*, *10*(1), 61-66.

Smith, R. W., & Ottema, C. (2006). Growth, oxygen consumption, and protein and RNA synthesis rates in the yolk sac larvae of the African catfish (*Clarias gariepinus*). *Comparative Biochemistry and Physiology Part A: Molecular & Integrative Physiology*, *143*(3), 315-325.

Snyder, G. K. (1975). Respiratory metabolism and evaporative water loss in a small tropical lizard. *Journal of Comparative Physiology*, *104*(1), 13-18.

Somjee, U. (2021). Positive allometry of sexually selected traits: Do metabolic maintenance costs play an important role?. *BioEssays*, *43*(6), 2000183.

Somjee, U., Shankar, A., & Falk, J. J. (2022). Can Sex-Specific Metabolic Rates Provide Insight into Patterns of Metabolic Scaling?. *Integrative and Comparative Biology*, *62*(5), 1460-1470.

Somjee, U., Woods, H. A., Duell, M., & Miller, C. W. (2018). The hidden cost of sexually selected traits: the metabolic expense of maintaining a sexually selected weapon. *Proceedings of the Royal Society B: Biological Sciences*, *285*(1891), 20181685.

Spicer, J. I. (1994). Ontogeny of cardiac function in the brine shrimp *Artemia franciscana* Kellogg 1906 (Branchiopoda: Anostraca). *Journal of Experimental Zoology*, *270*(6), 508-516.

Stearns, S. C. (1989). Trade-offs in life-history evolution. *Functional Ecology*, *3*(3), 259-268.

Steyermark, A. C., & Spotila, J. R. (2001). Effects of maternal identity and incubation temperature on snapping turtle (*Chelydra serpentina*) growth. *Functional Ecology*, *15*(5), 624-632.

Strauss, K., & Reinhold, K. (2010). Scaling of metabolic rate in the lesser wax moth *Achroia grisella* does not fit the 3/4-power law and shows significant sex differences. *Physiological Entomology*, *35*(1), 59-63.

Takatsuka, H., & Umeda, M. (2014). Hormonal control of cell division and elongation along differentiation trajectories in roots. *Journal of Experimental Botany*, *65*(10), 2633-2643.

Tan, H., Hirst, A. G., Glazier, D. S., & Atkinson, D. (2019). Ecological pressures and the contrasting scaling of metabolism and body shape in coexisting taxa: cephalopods versus teleost fish. *Philosophical Transactions of the Royal Society B*, *374*(1778), 20180543.

Tapia, C., Parra, L., Pacheco, B., Palma, R., Gajardo, G., & Quiroz, A. (2015). Courtship behavior and potential indications for chemical communication in *Artemia franciscana* (Kellog 1906). *Gayana*, *79*(2), 152.

Thommen, A., Werner, S., Frank, O., Philipp, J., Knittelfelder, O., Quek, Y., Fahmy, K., Shevchenko, A., Friedrich, B. M., Jülicher , F., & Rink, J. C. (2019). Body size-dependent energy storage causes Kleiber's law scaling of the metabolic rate in planarians. *Elife*, 8, e38187.

Timmerman, C. M., & Chapman, L. J. (2003). The effect of gestational state on oxygen consumption and response to hypoxia in the sailfin molly, *Poecilia latipinna*. *Environmental Biology of Fishes*, *68*, 293-299.

Ursin, E. (1967). A mathematical model of some aspects of fish growth, respiration, and mortality. *Journal of the Fisheries Board of Canada*, *24*(11), 2355-2453.

Vahl, O. (1984). The relationship between specific dynamic action (SDA) and growth in the common starfish, *Asterias rubens* L. *Oecologia*, *61*, 122-125.

van der Meer, J. (2006). An introduction to Dynamic Energy Budget (DEB) models with special emphasis on parameter estimation. *Journal of Sea Research*, *56*(2), 85-102.

Vanhaecke, P., & Sorgeloos, P. (1982). International study on *Artemia*. XVIII. The hatching rate of *Artemia* cysts—a comparative study. *Aquacultural Engineering*, *1*(4), 263-273.

Verberk, W. C., & Atkinson, D. (2013). Why polar gigantism and Palaeozoic gigantism are not equivalent: effects of oxygen and temperature on the body size of ectotherms. *Functional Ecology*, *27*(6), 1275-1285.

Verberk, W. C., Atkinson, D., Hoefnagel, K. N., Hirst, A. G., Horne, C. R., & Siepel, H. (2021). Shrinking body sizes in response to warming: explanations for the temperature–size rule with special emphasis on the role of oxygen. *Biological Reviews*, *96*(1), 247-268.

Verberk, W. C., Sandker, J. F., van de Pol, I. L., Urbina, M. A., Wilson, R. W., McKenzie, D. J., & Leiva, F. P. (2022). Body mass and cell size shape the tolerance of fishes to low oxygen in a temperature-dependent manner. *Global Change Biology*, *28*(19), 5695-5707.

Versichele, D., & Sorgeloos, P. (1980). Controlled production of *Artemia* cysts in batch cultures. In G. Persoone, P. Sorgeloos, O. Roles & E. Jaspers (Eds.), *The Brine Shrimp Artemia* (pp. 231-246). Universa Press.

Von Bertalanffy, L. (1938). A quantitative theory of organic growth (inquiries on growth laws. II). *Human Biology*, *10*(2), 181-213.

von Bertalanffy, L. (1951). Metabolic types and growth types. *The American Naturalist*, *85*(821), 111-117.

Von Bertalanffy, L. (1957). Quantitative laws in metabolism and growth. *The Quarterly Review of Biology*, *32*(3), 217-231.

von Bertalanffy, L. (1964). Basic concepts in quantitative biology of metabolism. *Helgoland Marine Research*, *9*(1), 5-37.

Walton, M. (1988). Relationships among metabolic, locomotory, and field measures of organismal performance in the Fowler's toad (*Bufo woodhousei fowleri*). *Physiological Zoology*, *61*(2), 107-118.

Warton, David I., Duursma, Remko A., Falster, Daniel S. & Taskinen, S. (2012). smatr 3 - an R package for estimation and inference about allometric lines. *Methods in Ecology and Evolution*, *3*(2), 257-259.

Weibel, E. R., & Hoppeler, H. (2005). Exercise-induced maximal metabolic rate scales with muscle aerobic capacity. *Journal of Experimental Biology*, *208*(9), 1635-1644.

Weisz, P. B. (1946). The space-time pattern of segment formation in *Artemia salina*. *The Biological Bulletin*, *91*(2), 119-140.

Welch, H. E. (1968). Relationships between assimilation efficiencies and growth efficiencies for aquatic consumers. *Ecology*, *49*(4), 755-759.

Wesley, C. C., Mishra, S., & Levy, D. L. (2020). Organelle size scaling over embryonic development. *Wiley Interdisciplinary Reviews: Developmental Biology*, *9*(5), e376.

West, G. B., Brown, J. H., & Enquist, B. J. (1997). A general model for the origin of allometric scaling laws in biology. *Science*, *276*(5309), 122-126.

West, G. B., Brown, J. H., & Enquist, B. J. (1999). The fourth dimension of life: fractal geometry and allometric scaling of organisms. *Science*, *284*(5420), 1677-1679.

West, G. B., Brown, J. H., & Enquist, B. J. (2001). A general model for ontogenetic growth. *Nature*, *413*(6856), 628-631.

White, C. R. (2010). There is no single p. *Nature*, *464*(7289), 691-693.

White, C. R., Alton, L. A., Bywater, C. L., Lombardi, E. J., & Marshall, D. J. (2022). Metabolic scaling is the product of life-history optimization. *Science*, *377*(6608), 834-839.

White, C. R., Cassey, P., & Blackburn, T. M. (2007). Allometric exponents do not support a universal metabolic allometry. *Ecology*, *88*(2), 315-323.

Wickham, H. (2016). ggplot2: *Elegant Graphics for Data Analysis*. Springer.

Wieser, W. (1984). A distribution must be made between the ontogeny the phylogeny of metabolism in order to understand the mass exponent of energy metabolism. *Respiration Physiology*, *55*(1), 1-9.

Wieser, W. (1994). Cost of growth in cells and organisms: general rules and comparative aspects. *Biological Reviews*, *69*(1), 1-33.

Winemiller, K. O., & Rose, K. A. (1992). Patterns of life-history diversification in North American fishes: implications for population regulation. *Canadian Journal of Fisheries and Aquatic Sciences*, *49*(10), 2196-2218.

Wolfe, A. F. (1973) Observations on the clasping behaviour of *Artemia salina*. *American Zoologist*, *13*, 1340.

Wood, S. C., Johansen, K., Glass, M. L., & Maloiy, G. M. O. (1978). Aerobic metabolism of the lizard *Varanus exanthematicus*: effects of activity, temperature, and size. *Journal of Comparative Physiology*, *127*(4), 331-336.

Woods, H. A., Moran, A. L., Atkinson, D., Audzijonyte, A., Berenbrink, M., Borges, F. O., Burnett, K. G., Burnett, L. E., Coates, C. J., Collin, R., Costa-Paiva, E. M., Duncan, M. I., Ern, R., Laetz, E. M. J., Levin, L. A., Lindmark, M., Lucey, N. M., McCormick, L. R., Pierson, J. J., ... Verberk, W. C. (2022). Integrative approaches to understanding organismal responses to aquatic deoxygenation. *The Biological Bulletin*, *243*(2), 85-103.

Wootton, H. F., Morrongiello, J. R., Schmitt, T., & Audzijonyte, A. (2022). Smaller adult fish size in warmer water is not explained by elevated metabolism. *Ecology Letters*, *25*(5), 1177-1188.

Wright, J. C. (1986). Effects of body temperature, mass, and activity on aerobic and anaerobic metabolism in juvenile *Crocodylus porosus*. *Physiological Zoology*, *59*(5), 505-513.

Yeannes, M. I., & Almandos, M. E. (2003). Estimation of fish proximate composition starting from water content. *Journal of Food Composition and Analysis*, *16*(1), 81-92.

Young, K. M., Cramp, R. L., White, C. R., & Franklin, C. E. (2011). Influence of elevated temperature on metabolism during aestivation: implications for muscle disuse atrophy. *Journal of Experimental Biology*, *214*(22), 3782-3789.

Yu, G., Smith, D. K., Zhu, H., Guan, Y., & Lam, T. T. Y. (2017). ggtree: an R package for visualization and annotation of phylogenetic trees with their covariates and other associated data. *Methods in Ecology and Evolution*, *8*(1), 28-36.

Zuur, A. F., & Ieno, E. N. (2016). A protocol for conducting and presenting results of regression-type analyses. *Methods in Ecology and Evolution*, *7*(6), 636-645.

Supplementary data

The data supporting the analyses within this thesis are available via Google Drive using the following link:

https://drive.google.com/drive/folders/1yaK9S2PDD9z8bqOBTHSNNavuVtQX09zS?usp=share_link

Table S2.1. Metabolic rate-body mass scaling relationships performed at various temperatures from experiments in ectothermic vertebrates at low activity.

Table S2.2. Metabolic rate-body mass scaling relationships performed at various temperatures from experiments in ectothermic vertebrates at different activity levels.

Table S3.1. Data on metabolic scaling, growth, lifestyle, climate zone, and mass-scaling of gill surface-area of the teleost species studied in Chapter 3.

Table S4.1. Data collected in Chapter 4 for individuals of *Artemia franciscana* at different points of the ontogeny, including body mass, developmental stage, metabolic rate, specific growth rate, growth rate (i.e., absolute increase in body mass per unit time), and sex (in post-larval individuals).

Table S4.2. Data collected in Chapter 4 for reproductive individuals of *A. franciscana* after reproduction experiments, including body mass, metabolic rate, offspring production rate (i.e., total, cysts or larvae mass produced per unit time), as well as the proportion of offspring that were larvae.

Appendix

A2. Appendix for Chapter 2

Combining theoretical approaches to understanding the intraspecific variation in metabolic scaling: Responses to temperature and activity differ between water- and air-breathing ectothermic vertebrates

This file includes:

A2.1. Data comparability between datasets of water- and air-breathers

A2.2. Checking the potential influence of acclimation period on metabolic scaling

A2.3. Controlling for the effect of body mass on metabolic level in the models

A2.4. Description of Bayesian models

A2.5. Phylogenetic trees used in the models

A2.6. Temperature correction of metabolic level in Figures 2.3-2.4

A2.1. Data comparability between datasets of water- and air-breathers

I checked for differences between datasets for air- and water-breathing species in (1) the ranges of body mass covered by scaling regressions and (2) the increases in metabolic levels (L) with either temperature (Table S2.1) or locomotory activity (Table S2.2). These two factors could influence the relationship between the slope b and L (Glazier, 2020). I observed that regressions compiled for water- and air-breathing species measured similar ranges of body mass in my datasets (Fig. A2.1A, B), covering generally from 0.5 to 2.5 orders of magnitude (mean 1.4 – 1.5). Most of regressions in the datasets of water- and air-breathers (range 62.8 – 76.9%) covered mass ranges of ≥1 order of magnitude. Moreover, the increases in metabolic level (L) by only changing temperature (Fig. A2.1C) or activity level (Fig. A2.1D) were similar between water- and air-breathing species, mostly below 1 mg O_2 g^{-1} h^{-1}, though slightly higher for activity-increased L in air-breathers. This difference is partially due to almost all experiments in air-breathers covering from minimal to maximal L, but also because of the higher aerobic scopes of these species (0.34 vs 1.35 mg O_2 g^{-1} h^{-1}).
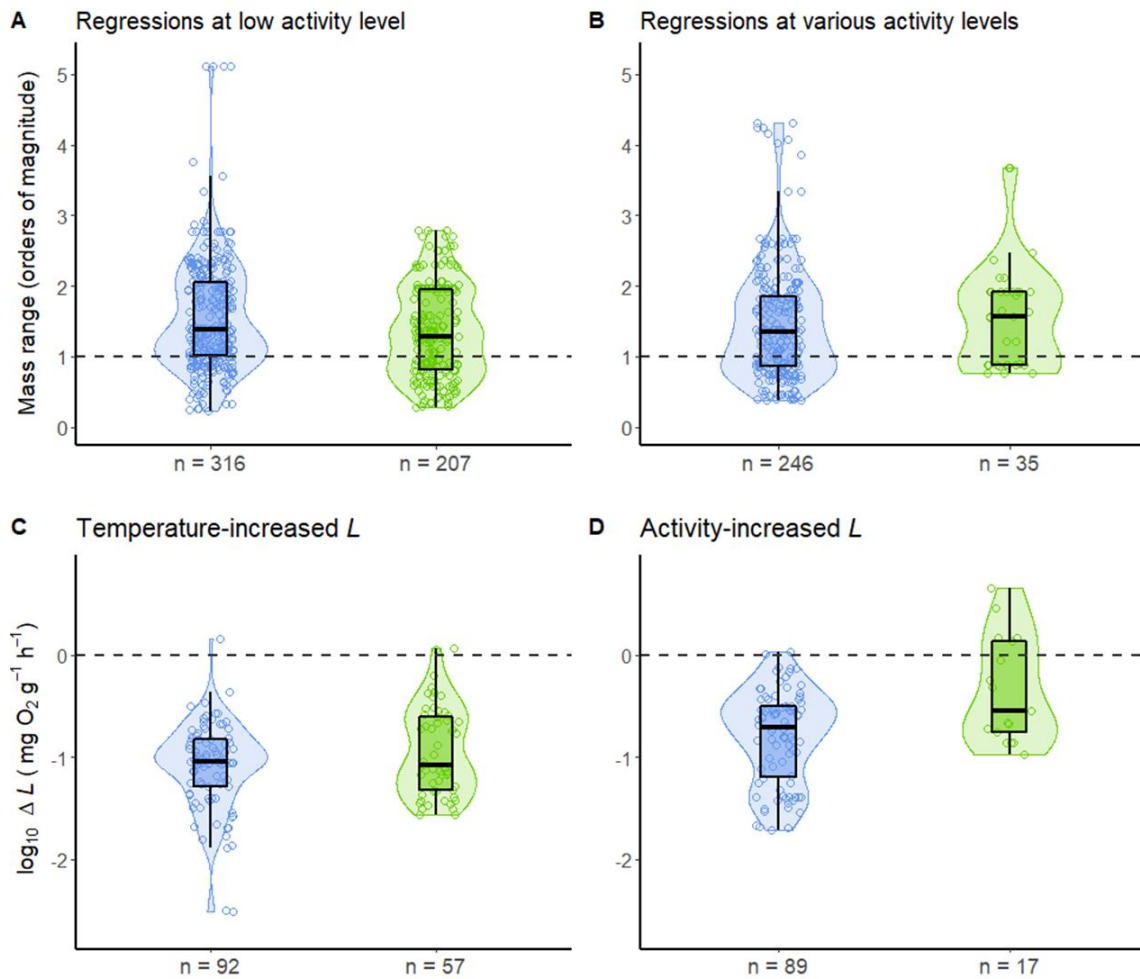
Figure A2.1. The ranges of body mass covered by scaling regressions and the increases in metabolic level (Δ L, as $\log_{10}$) measured by experiments of water- (blue) and air-breathing (green) species. Upper panels show regressions measured (**A**) in low-activity animals acclimatised at various temperatures, and (**B**) in animals at various activity levels. The lower panels show experiments where L was exclusively increased by (**C**) temperature or (**D**) activity. The solid line within each box marks the median, box boundaries indicate 25th and 75th percentiles, and whiskers indicate the largest and smallest value within 1.5 times the interquartile range beyond either box boundary. Shading around boxes show kernel densities. The number of regressions (A, B) or experiments (C, D) is indicated below each box. Dashed lines denote a reference value of one order of magnitude in A and B, and the increase of 1 mg O_2 g^{-1} h^{-1} in metabolic level in C and D.

A2.2. Checking the potential influence of acclimation period on metabolic scaling

Acclimation periods in experiments that measured metabolic scaling of inactive animals at various temperatures (Table S2.1) were, overall, longer in water-breathers than in air-breathers (Fig. A2.2A). From the studies that reported acclimation times (86.0% in water- and 78.9% in air-breathers), the average acclimation duration in experiments of water- and air-breathers was respectively ca. 362.6 and 89.5 hours, with 92.3% and 53.3% of the experiments lasting $\geq$ 24 hours. This difference between water- and air-breathers may be due to the lower effect of acclimation duration on metabolic rates in terrestrial ectotherms (Seebacher et al., 2015), and thus experiments in air-breathing ectotherms in my data, almost all terrestrial, would not require acclimation periods as long as in water-breathers. If the duration of the acclimation period influenced the strength of the temperature response, I would expect that longer acclimation periods would let animals stabilise their metabolism better at experimental temperatures, thus leading to smaller variation in b among temperature conditions within experiments. However, the acclimation duration showed no trend with the amount of variation (i.e., standard deviation) of slopes b within experiments (Fig. A2.2B). This suggests that the duration of the acclimation period had no obvious influence on the differences in metabolic scaling observed in this paper.

While the ideal dataset for this study would consist of metabolic scaling experiments on animals growing from eggs in laboratory conditions at constant temperatures, this type of experiments is unfortunately very scarce in the literature. Indeed, I might expect differences in metabolic rates due to organismal growth after a period at a given temperature, but this thermal effect would be less likely to be detected in short-term experiments. Yet, physiological changes during acclimation are associated with rapid changes in growth metabolism, i.e., an increased temperature can cause immediate increases in growth rate, though these effects are usually difficult to detect in short-term experiments (Parry, 1983). Acclimation within individuals occurs through rapid signalling systems such as thyroid or growth hormone (Little et al., 2013), whose levels increase with warming, and this is, in turn, generally associated with increased growth rates within the benign thermal range of species (Deane & Woo, 2009). Acclimation temperature can first act as a seasonal cue, making individuals adjust their growth metabolism accordingly, activating hormonal production and accelerating metabolic rates as temperatures get closer to those experienced during the growing season (see Table 4 in Parry, 1983; Deane & Woo, 2009). For most experiments included in my analyses, I therefore expect that

temperature-dependent growth overheads contributed importantly to the metabolic rate of individuals.
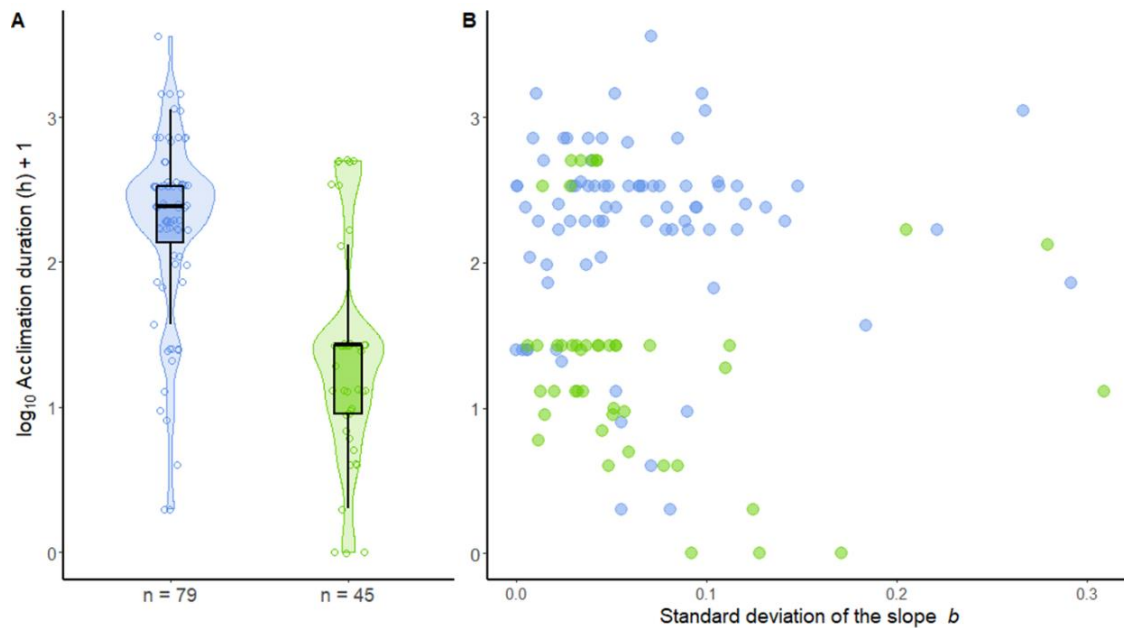
Figure A2.2. The mean duration of the acclimation period (as $\log_{10}$ (acclimation time + 1), to include no acclimation) from experiments that measured metabolic scaling in inactive animals acclimatised at various temperatures (**A**), and the comparison between the acclimation duration and the standard deviation of the slopes b within these experiments (**B**). The acclimation period was not specified in some studies, and thus those experiments are not shown here. Symbols as in Fig. A2.1.

A2.3. Controlling for the effect of body mass on metabolic level in the models

Metabolic level (*L*) generally decreases with increasing body mass (see discussion in Glazier, 2008), which may hinder tests of the relationship between slopes *b* and *L* due to increasing temperature or activity level. In my models, the inverse relationship between *L* and mass was controlled by incorporating as a random effect the experiment from which a set of scaling regressions was produced, as regressions within an experiment generally measure similar body mass ranges. Moreover, to cope with the variation in *L* between regressions from the same experiment due to slight differences in body mass range, I further excluded regressions whose geometric mass-midpoints were too dissimilar to the rest of the set from an experiment, i.e., differing > 0.5 orders of magnitude. By doing this, I was able to minimise the effect of body mass on metabolism, ensuring that most of the variation in *L* within experiments was due to changes in either temperature or activity level (Fig. A2.3).
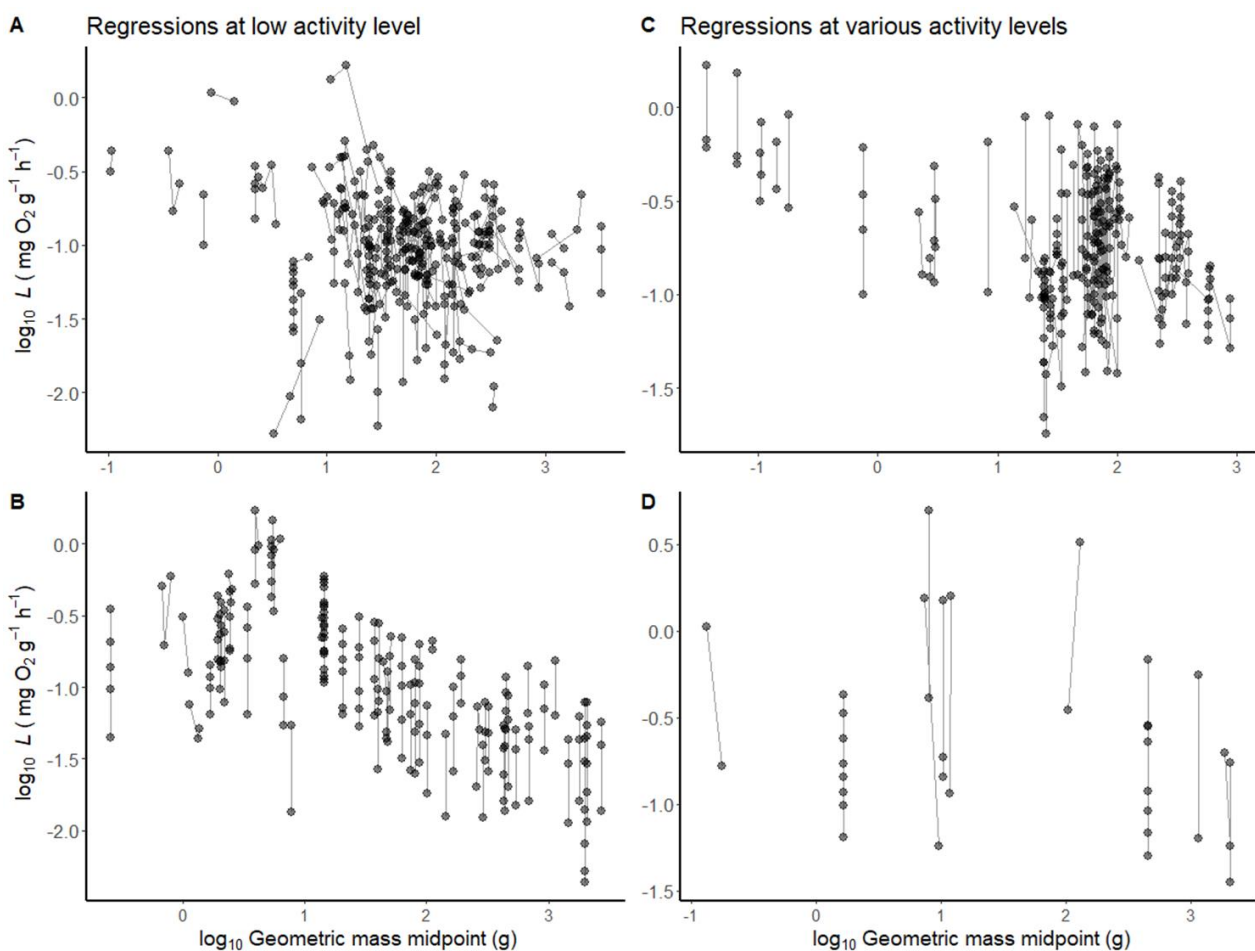
Figure A2.3. The relationship between the $\log_{10}$ metabolic level (*L*) and the $\log_{10}$ geometric midpoint of the body mass ranges covered by scaling regressions. Left panels show measurements in inactive animals of water- (**A**) and air-breathing (**B**) species, where lines join

measurements made at different temperatures of single experiments in the same species. Right panels show values for animals under different activity levels and temperatures of water- (**C**) and air-breathing (**D**) species, where lines join experiments made at a single temperature and species. Since L values were estimated at a similar point in ontogeny (i.e., geometric mass midpoints) between regressions from the same experiment, the differences in L within experiments (vertical variation of joined points) was mainly due to changes in temperature or activity level, and not to differences in body mass.

A2.4. Description of Bayesian models

A2.4.1. Model fitting:

I fitted models in a Bayesian phylogenetic multilevel framework using the package 'brms' (Burkner, 2017, 2019) in R version 4.0.2 (R Core Team, 2022). I used Student's t distribution to describe the slopes b because this is robust against outliers (Gelman & Hill, 2006; see example in ecology in Roycroft et al., 2020). To analyse the effect of temperature-increased metabolic level (L) on the scaling slope b, and whether this effect differs between water and air-breathing species, I fitted a model using data from Table S2.1, defined as:

$$b_{ijk} \sim \text{Student's } t(\nu, \mu_{ijk}, \sigma),$$

$$\mu_{ijk} = \beta_0 + \beta_L \log_{10} L_{ijk} + \beta_g g_k + \beta_{Lg} \log_{10} L_{ijk} g_k + \phi_{0j} + \phi_{Lj} \log_{10} L_{ijk} + \psi_k,$$

$$\begin{pmatrix} \phi_{0j} \\ \phi_{Lj} \end{pmatrix} \sim N(\mathbf{0}, \mathbf{V}),$$

$$\psi \sim N\left(\mathbf{0}, \sigma_{\text{species}}^2 \mathbf{K}\right),$$

where b_{ijk} is the ith slope b estimate from the jth experiment on the kth species, $\text{Student's } t(\nu, \mu, \sigma)$ is a non-standardized Student's t distribution with degrees of freedom ν, location μ and scale σ (Jackman, 2006), β_0 is the global intercept parameter, β_L is the global effect of $\log_{10} L$, β_g is the effect of the animal group (air- or water-breather), β_{Lg} is the effect of the interaction between $\log_{10} L$ and group, L_{ijk} is the metabolic level for the ith slope estimate from the jth experiment on the kth species, g_k is an indicator variable representing the group for the kth species:

$$g_k = \begin{cases} 1, \text{if organism is water-breather,} \\ 0, \text{if organism is air-breather.} \end{cases}$$

The random factor of experiments was defined by the group-level intercept ϕ_{0j} and coefficient ϕ_{Lj} for the jth experiment, assumed to come from a bivariate normal distribution $N(\mathbf{0}, \mathbf{V})$ with mean vector $\mathbf{0}$ and covariance matrix $\mathbf{V}$, which is parameterized as a correlation matrix Ω and a vector of standard deviations $\boldsymbol{\sigma}_{\text{experiment}}$ through:

$$\mathbf{V} = D(\boldsymbol{\sigma}_{\text{experiment}}) \Omega D(\boldsymbol{\sigma}_{\text{experiment}}),$$

where $D(\boldsymbol{\sigma}_{\text{experiment}})$ denotes the diagonal matrix with elements $\begin{pmatrix} \sigma_{\phi_{0j}} & 0 \\ 0 & \sigma_{\phi_{Lj}} \end{pmatrix}$ The random factor of phylogeny was defined as the effect ψ_k of the kth species, with the vector of these effects $\boldsymbol{\psi}$

drawn from a multivariate normal distribution with mean vector **0** and covariance $\sigma^2_{\text{species}}\mathbf{K}$, where **K** is a known correlation matrix representing phylogenetic effects.

To analyse the effect of activity-increased L on the slope b, I fitted a similar model to the above, but including experimental temperature (in °C) as an additional covariate. The effect of temperature was included because temperature and activity level are expected to show opposite effects on b by the MLBH (see Fig. 2.1). The linear predictor was defined as:

$$\mu_{\text{ijk}} = \beta_0 + \beta_L \log_{10} L_{\text{ijk}} + \beta_g g_k + \beta_{Lg} \log_{10} L_{\text{ijk}}\, g_k + \beta_T T_{\text{ijk}} + \phi_{0j} + \phi_{Lj} \log_{10} L_{\text{ijk}} + \psi_k,$$

where β_T is the effect of experimental temperature, and T_{ijk} is the experimental temperature for the ith slope estimate from the jth experiment on the kth species.

A2.4.2. Selection of priors

I used a mix of weakly informative and informative priors. For models analysing the effect of temperature-increased metabolic level (L) on the slope b, I used an empirical estimate observed between species for the coefficient of metabolic level (see Killen et al., 2010). The prior of β_L was thus defined as:

$$\beta_L \sim N(-0.1, 0.5)$$

For the overall intercept (β_0), which correspond to a high L (when $\log_{10} L = 0$, $L = 1$ mg O_2 g^{-1} h^{-1}), I used the MLBH prediction, that the slope b approaches 2/3 at high L with warming (Glazier, 2010), defined as:

$$\beta_0 \sim N(0.67, 0.5)$$

For models analysing the effect of activity-increased L, I used the opposite effect of that estimated by temperature-increased L following the MLBH predictions (Fig. 2.1), and hence:

$$\beta_L \sim N(0.1, 0.5)$$

For the overall intercept, I followed the MLBH prediction that the slope b approaches 1 at high activity levels and so high L (at $L = 1$ mg O_2 g^{-1} h^{-1}), and thus:

$$\beta_0 \sim N(1, 0.5)$$

For the remaining model parameters, I set weakly informative priors as follows:

$$\beta_g \sim N(0, 1),$$

$$\beta_{Lg} \sim N(0, 1),$$

$$\beta_T \sim N(0, 1),$$

$$\sigma \sim \text{half Student's } t(3, 0, 2.5),$$
$$\sigma_{\phi_{0j}} \sim \text{half Student's } t(3, 0, 2.5),$$

$$\sigma_{\phi_{Lj}} \sim \text{half Student's } t(3, 0, 2.5),$$

$$\Omega \sim \text{LKJ}(\zeta),$$

$$\sigma_{\text{species}} \sim \text{half Student's } t(3, 0, 2.5),$$
$$\nu \sim \text{left truncated Gamma}(2, 0.1, 1),$$

where half Student's $t(\cdot)$ is the positive half of the Student's t distribution, LKJ is the LKJ correlation prior with shape parameter $\zeta = 1$ (Lewandowski et al., 2009; Burkner, 2017), left truncated Gamma$(\alpha, \beta, 1)$ is a gamma distribution with shape parameter α and inverse scale parameter β, left-truncated at 1. Note that left-truncation of the prior for the degrees of freedom at 1 ensures that the mean but not necessarily the variance of each b_{ijk} exists.

A2.4.3. Model performance

To assess the performance of the latter models, I checked whether I could recover known parameter values with simulated data. I first generated 10 simulated data sets with the same structure as the real data (Table S2.1) with posterior mean parameter values from the temperature-effect model. Then, I fitted the latter model to the simulated data sets. For all parameters in this model, posterior values were clearly centred on the true parameter values (Fig. A2.4).
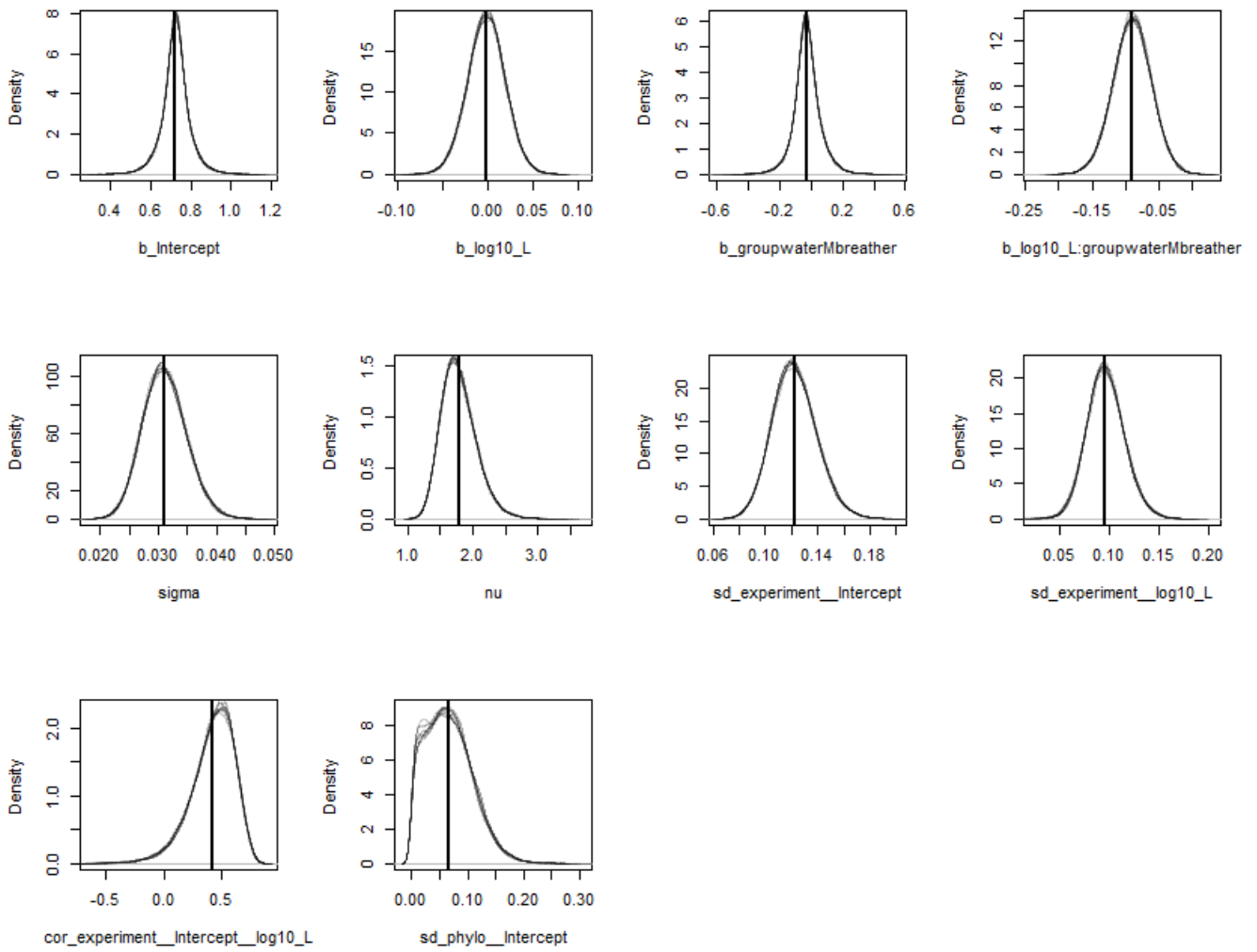
Figure A2.4. The posterior estimates of parameters in the temperature-effect model, fitted to 10 simulated data sets with the same structure as the real data, generated using posterior mean parameter values. Abbreviations of model parameters are b_intercept for β_0, b_log10_L for β_L, b_groupwaterMbreather for β_g, b_log10_L:groupwaterMbreather for β_{Lg}, sigma for σ, nu for ν, sd_experiment_Intercept for ϕ_{0j}, sd_experiment_log10_L for ϕ_{Lj}, cor_experiment_Intercept_log10_L for Ω, and sd_phylo_Intercept for ψ_k.

142

A2.5. Phylogenetic trees used in the models

I used package 'rotl' (Michonneau et al., 2016) to search and match the species names in the Open Tree of Life (OTL, https://tree.opentreeoflife.org), which were used to build the phylogenetic trees (Fig. A2.5). I then calculated the variance-covariance matrices of species incorporated as a random effect in the models using package 'ape' (Paradis & Schliep, 2019). Following Grafen's method (Grafen, 1989), branch lengths of phylogenetic trees were set equal to the number of descendant branch tips minus one.

Figure A2.5. Phylogenetic trees built using 'rotl' package for the species included in Table S2.1 (**A**) and S2.2 (**B**). Water-breathing species (i.e., elasmobranchs and teleost fish) are coloured in blue, whereas air-breathing species (i.e., reptiles and amphibians) are indicated in green. Species names showed here were first checked with Open Tree of Life (OTL, https://tree.opentreeoflife.org) using the same R package. One polytomy, present in both trees, was resolved using function *multi2di* in the package 'ape' (Paradis & Schliep, 2019).

A2.6. Temperature correction of metabolic level in Figures 2.3-2.4

To compare visually between activity-increased metabolic levels (L) at various temperatures in Figure 2.3 and 2.4 in the main text, I adjusted L values to a common temperature of 20 °C, which was approximately the mean experimental temperature across all the compiled metabolic regressions in Table S2.2. Following Killen et al. (2010), the Q_{10} value (0 – 30 °C) for L was estimated from the relationship between $\log_{10} L$ and temperature in °C using the equation:

$$(R_{30}/R_0)^{(10/(30-0))},$$

where R_{30} and R_0 are metabolic rates at 30 and 0 °C estimated from the fit of separate linear mixed-effects models for water- and air-breathing species using package lmerTest (Kuznetsova et al., 2017) in R. The latter models used L measurements of inactive animals acclimatised at various temperatures (Table S2.1) and these temperatures (in °C) as the only predictor. To account for different experimental conditions, I incorporated the experiments from which each set of measurements was produced as a random effect in these models. I obtained a similar temperature effect on $\log_{10} L$ for water- and air-breathers through these models (estimate = 0.036 and 0.035, respectively; both $p < 0.001$), from which I estimated a Q_{10} of 2.30 and 2.25, respectively.

A3. Appendix for Chapter 3

Understanding the adaptive significance of metabolic scaling: interspecific variation in mass-scaling slopes may reflect different growth demands among teleost fish

The following appendix contains supplementary information on:

A3.1. Derivation of the von Bertalanffy growth model (VBG)

A3.2. Checking temperatures recorded in growth and metabolic data

A3.3. Estimation of ontogenetic body mass covered by metabolic scaling relationships

A3.4. Results of Ordinary Least Squares (OLS) models and model selection to explain the interspecific variation in metabolic scaling slopes

A3.5. Phylogenetic tree of the sampled species and results of the Phylogenetic Generalised Least Squares (PGLS) models

A3.1. Derivation of the von Bertalanffy growth model (VBG)

The classical VBG equation describes fish growth in the form:

$$l(t) = L_\infty\left(1 - e^{-K(t-t_0)}\right) = L_\infty\left(1 - \left(1 - \frac{l_0}{L_\infty}\right)e^{-Kt}\right), \qquad \text{[S1]}$$

where $l(t)$ is the predicted mean length of fish at age t, t_0 is the theoretical age at length zero, l_0 is length at time 0, L_∞ is their mean final or asymptotic length (i.e. the length at an infinitely old age), and K is a factor of dimensions time $^{-1}$ (e.g., d^{-1}) by which $l(t)$ approaches L_∞. The length-based VBG expression (eq. [S1], in cm) can be then transformed in mass (g) through length-weight relationships of the form (von Bertalanffy, 1938):

$$m = a_L l^{b_L}, \qquad \text{[S2]}$$

where a_L (g cm$^{-b_L}$) and b_L (dimensionless) are the scaling coefficient and exponent that describe the change in body shape over ontogeny. Following the derivations in Barneche & Allen (2018), by using the parameters in the length-weight relationship (eq. [S2]) the mass-based VBG can be described as:

$$m(t) = a_L\left(L_\infty\left(1 - \left(1 - \frac{l_0}{L_\infty}\right)e^{-Kt}\right)\right)^{b_L} = M_\infty\left(1 - \left(1 - \left(\frac{m_0}{M_\infty}\right)^{1/b_L}\right)e^{-Kt}\right)^{b_L} \quad \text{[S3]}$$

Growth in body mass, dm/dt, can be obtained by the first derivative of the latter equation:

$$\frac{dm}{dt} = b_L K M\left(1 - \left(\frac{m_0}{M_\infty}\right)^{1/b_L}\right)e^{-Kt}\left(1 - \left(1 - \left(\frac{m_0}{M_\infty}\right)^{1/b_L}\right)e^{-Kt}\right)^{b_L-1} \qquad \text{[S4]}$$

Finally, the mass-based version of the VBG results from combining eq. [S4] and [S5]:

$$\frac{dm}{dt} = b_L K M_\infty^{1/b_L} m^{\frac{b_L-1}{b_L}} - b_L K m \qquad \text{[S5]}$$

which describes the ontogenetic growth trajectory of a species. This equation (eq. [S5]) can be used to calculate the maximum growth rate (g_{max}, g d^{-1}) of a species from the body mass at which maximum growth rate is achieved (m_{gmax}, g) (see eq. [9] in the main tex). For the case where $\alpha = b_L K M_\infty^{1/b_L}$, $\beta = b_L K$, $h = \frac{b_L-1}{b_L} = 1 - \frac{1}{b_L}$, and $c = 1$, then yields eq. [6] in the main text:

$$\frac{dm}{dt} = \alpha m^h - \beta m^c \qquad \text{[S6]}$$

Furthermore, eq. [S6] provides a bridge between the VBG and the Ontogenetic Growth Model (Moses et al., 2008; Barneche & Allen, 2018). However, whereas h is typically 2/3 in the VBG for organisms with isomorphic growth (i.e., whose $b_L = 3$), h in the OGM represents the mass-scaling exponent of metabolic rates, which is assumed to be $b = 3/4$ (West et al., 1997, 2001). This study, in contrast, uses actual b values from species-specific metabolic scaling relationships (see 2.2 in Material & Methods). In any case, as explained in the main text (section 2.3), the calculations of m_{gmax} and g_{max} are expected to be almost identical if length-based data from FishBase are used following the VBG (i.e., $h = 2/3$) or the present approach ($h = b$), which allows the use of these data to compare growth and metabolic rates among the species compiled here.

A3.2. Checking temperatures recorded in growth and metabolic data

For the species compiled in this study, the mean temperatures recorded in FishBase for growth data and measurement temperatures from metabolic studies were highly correlated [Pearson correlation, $r = 0.83$, 95% CI (0.74, 0.89), df $= 74$, $p < 0.001$]. One temperature record of T $= 20$ °C corresponding to the polar species *Electrona antarctica* was not included here because this likely corresponds to an error, as this temperature value is remarkably higher than the thermal range for this species (-0.2 – 1.2°C; www.fishbase.org). Hence, no temperature correction was made to link the estimated growth and metabolic rates of these species. The measurement temperatures of metabolic studies were used in the analyses of this chapter because these values were available for all compiled species (temperature data were not available in FishBase for 37 species), but also precisely measured in controlled conditions.
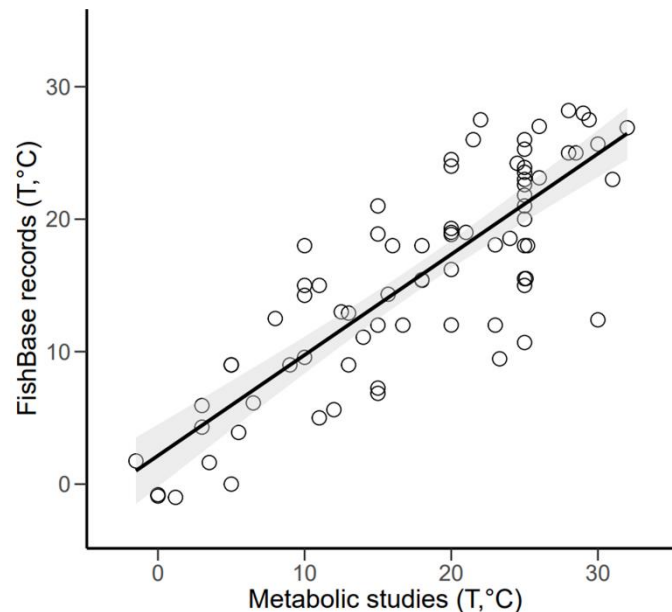
Figure A3.1. The mean temperature recorded for the growth data in FishBase against the measurement temperature from the metabolic studies. Black line and grey bands denote the regression line and 95% confidence intervals of the Pearson correlation.

A3.3. Estimation of ontogenetic body mass covered by metabolic scaling relationships

The variation in metabolic scaling slopes was investigated in this chapter after a further screening step that excluded species for which metabolic scaling relationships covered body mass ranges < 5% of the total ontogenetic mass range (following Killen et al., 2010). The percentage of ontogenetic body mass range spanned by metabolic scaling relationships was calculated as:

$$\frac{(m_{max} - m_{min})}{M_{\infty}} \times 100 \qquad [S7]$$

where m_{max} and m_{min} are respectively the maximum and minimal body mass included in metabolic scaling relationships, and M_{∞} is the mean final body mass of species reported in FishBase (all in grams). Here, M_{∞} was used as the upper end of the ontogenetic mass range, whereas the initial ontogenetic mass was assumed to be negligible relative to M_{∞}.

A3.4. Results of Ordinary Least Squares (OLS) models and model selection to explain the interspecific variation in metabolic scaling slopes

Table A3.1. Comparison of ordinary least squares models (OLS) testing metabolic scaling slopes as explained by $\log_{10}$ maximum growth rate (g_{max}, g d^{-1}), $\log_{10}$ metabolic level (L, mg O$_2$ g^{-1} d^{-1}), and temperature (T, °C) across all sampled species here (n = 118). Abbreviations: df, degrees of freedom; AICc, Akaike's Information Criterion corrected for small samples; weight, Akaike model's weight. The best model (i.e., lowest AICc value) is highlighted in bold.

variable	predictor	df	logLik	AICc	delta	weight
Metabolic scaling slope (b)	**$\log_{10} g_{max}$ + T**	**4**	**74.20**	**-140.05**	**0.00**	**0.36**
	$\log_{10} g_{max}$ + $\log_{10} L$	4	73.83	-139.31	0.75	0.24
	$\log_{10} g_{max}$	3	72.35	-138.48	1.57	0.16
	$\log_{10} g_{max}$ + $\log_{10} L$ + T	5	74.47	-138.40	1.65	0.16
	T	3	70.88	-135.56	4.50	0.04
	$\log_{10} L$	3	70.26	-134.30	5.75	0.02
	$\log_{10} L$ + T	4	71.30	-134.25	5.80	0.02
	null	2	67.75	-131.40	8.66	0.00

Table A3.2. Results of the OLS model describing the variation in metabolic scaling slope (b) as explained by $\log_{10}$ maximum growth rate (g d^{-1}), $\log_{10}$ metabolic level (mg O$_2$ g^{-1} d^{-1}), and temperature (°C) across all sampled teleost species (n = 118). Significant effects ($p < 0.05$) are shown in bold.

variable	predictor	estimate	std. error	t-value	p	R^2
Metabolic scaling slope (b)	intercept	0.801	0.029	27.819	**<0.001**	
	Maximum growth rate	-0.031	0.012	-2.507	**0.014**	0.08
	Metabolic level	-0.029	0.040	-0.719	0.474	
	Temperature	-0.002	0.002	-1.115	0.267	

Table A3.3. Comparison of OLS models testing metabolic scaling slopes as explained by $\log_{10}$ maximum growth rate (g_{max}, g d^{-1}), $\log_{10}$ metabolic level (L, mg O$_2$ g^{-1} d^{-1}), temperature (T, °C), and gill SA scaling slope (b_G) for the set of species with available data on b_G (n = 21). The best model (i.e., lowest AICc value) is highlighted in bold. Abbreviations as in Table A3.1.

variable	predictor	df	logLik	AICc	delta	weight
	$\log_{10} g_{max}$	**3**	**20.63**	**-33.84**	**0.00**	**0.51**
	$\log_{10} g_{max}$ + T	4	21.07	-31.64	2.20	0.17
	$\log_{10} g_{max}$ + b_G	4	20.63	-30.75	3.09	0.11
	$\log_{10} g_{max}$ + $\log_{10} L$	4	20.63	-30.75	3.09	0.11
	$\log_{10} g_{max}$ + $\log_{10} L$ + T	5	21.19	-28.39	5.45	0.03
	$\log_{10} g_{max}$ + b_G + T	5	21.13	-28.26	5.59	0.03
	$\log_{10} g_{max}$ + b_G + $\log_{10} L$	5	20.63	-27.25	6.59	0.02
Metabolic	$\log_{10} g_{max}$ + b_G + $\log_{10} L$ + T	6	21.21	-24.52	9.32	0.00
scaling	$\log_{10} L$	3	15.14	-22.87	10.97	0.00
slope (b)	T	3	14.51	-21.61	12.23	0.00
	b_G + T	4	15.90	-21.29	12.55	0.00
	b_G + $\log_{10} L$	4	15.66	-20.82	13.02	0.00
	null	3	12.64	-20.62	13.22	0.00
	$\log_{10} L$ + T	4	15.55	-20.60	13.24	0.00
	b_G	3	13.43	-19.44	14.40	0.00
	b_G + $\log_{10} L$ + T	5	16.46	-18.92	14.92	0.00

Table A3.4. Results of the OLS model describing the variation in metabolic scaling slope (b) as explained by $\log_{10}$ maximum growth rate (g d^{-1}), $\log_{10}$ metabolic level (mg O$_2$ g^{-1} d^{-1}), and temperature (°C) for the set of species with available data on b_G (n = 21). Significant effects ($p < 0.05$) are shown in bold.

variable	predictor	estimate	std. error	t-value	p	R^2
	intercept	0.828	0.151	5.502	**<0.001**	
Metabolic	Maximum growth rate	-0.087	0.029	-3.045	**0.008**	
scaling	Metabolic level	0.042	0.094	0.453	0.657	0.45
slope (b)	Temperature	-0.003	0.003	-0.998	0.333	
	Gill SA scaling slope (b_G)	-0.048	0.151	-0.319	0.754	

A3.5. Phylogenetic tree of the sampled species and results of the Phylogenetic Generalised Least Squares (PGLS) models
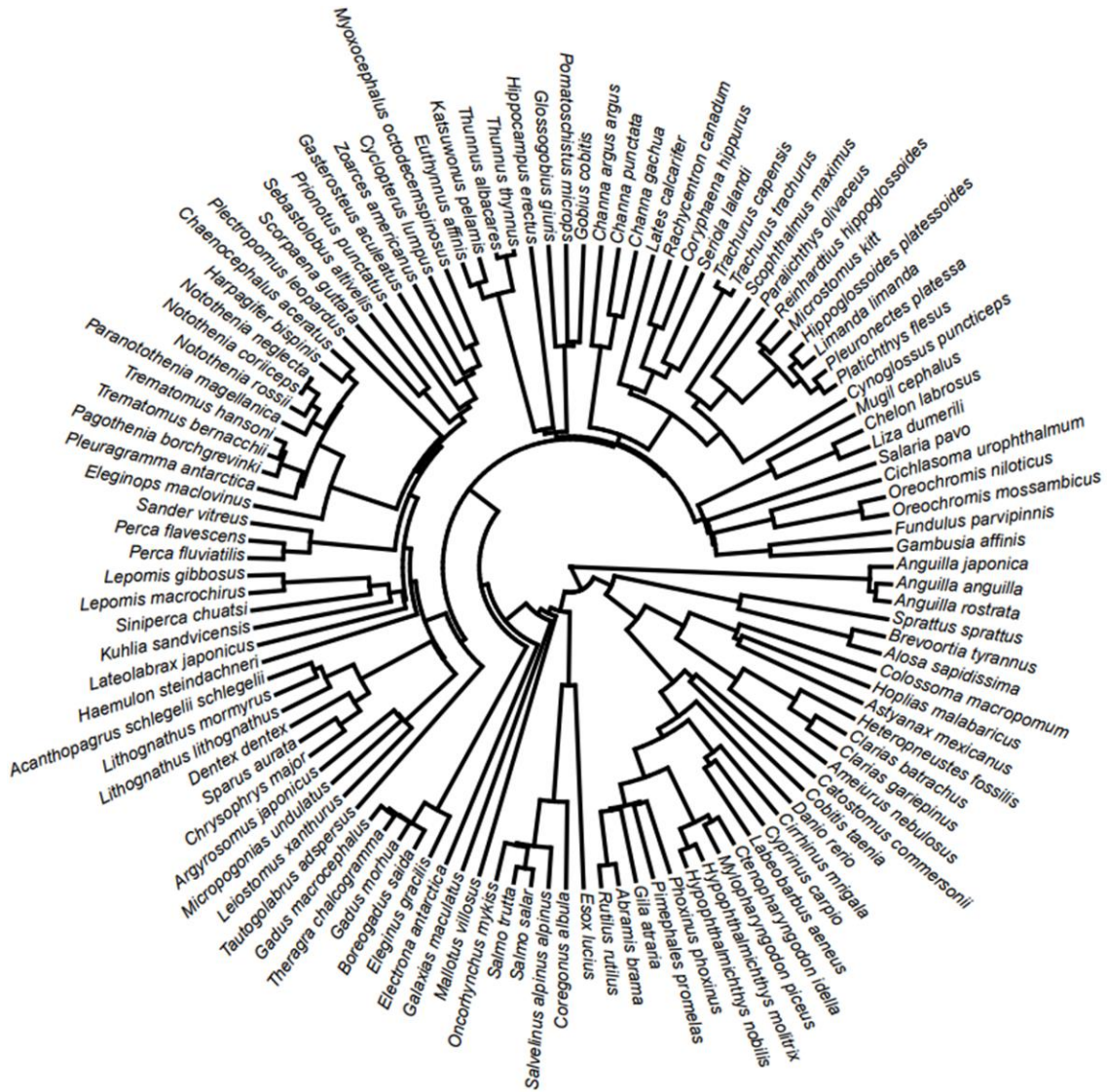

Figure A3.2. Phylogenetic tree of the teleost species used in this study. Three of the 118 sampled species are missing in this tree because their phylogenetic data was not available in The Fish Tree Of Life (Chang et al., 2019).

Table A3.5. Results of the phylogenetic generalised least squares (PGLS) model describing the variation in metabolic scaling slope (b) as explained by $\log_{10}$ maximum growth rate (g d^{-1}), $\log_{10}$ metabolic level (mg O$_2$ g^{-1} d^{-1}), and temperature (°C) for all sampled species with phylogenetic data available (n = 115). Pagel's lambda was not significantly different from 0 (λ = 0.00, 95% CI: NA, 0.58). Significant effects ($p < 0.05$) are shown in bold.

variable	predictor	estimate	std. error	t-value	p	R^2
Metabolic scaling slope (b)	intercept	0.800	0.029	27.384	**<0.001**	
	Maximum growth rate	-0.030	0.013	-2.397	**0.018**	0.08
	Metabolic level	-0.031	0.040	-0.776	0.439	
	Temperature	-0.002	0.002	-0.992	0.323	

Table A3.6. Results of the PGLS model describing the variation in metabolic scaling slope (b) as explained by $\log_{10}$ maximum growth rate (g d^{-1}), $\log_{10}$ metabolic level (mg O$_2$ g^{-1} d^{-1}), and temperature (°C) for all sampled species with phylogenetic data available (n = 21). Pagel's lambda was not significantly different from 0 (λ = 0.20, 95% CI: NA, NA). Significant effects ($p < 0.05$) are shown in bold.

variable	predictor	estimate	std. error	t-value	p	R^2
Metabolic scaling slope (b)	intercept	0.842	0.150	5.608	**<0.001**	
	Maximum growth rate	-0.081	0.028	-2.879	**0.011**	
	Metabolic level	0.049	0.090	0.549	0.590	0.43
	Temperature	-0.004	0.003	-1.219	0.241	
	Gill SA scaling slope b_G	-0.046	0.148	-0.312	0.759	

Table A3.7. Results of the PGLS model describing the variation in the overhead costs of growth (C_g) and maintenance metabolism (R_m) as explained by body mas (g), temperature (°C), and lifestyle across the 114 species with phylogenetic data available (one bathy-demersal was not included here due to be the only representative of this lifestyle category). All metabolic costs as well as body mass were $\log_{10}$-transformed. The OLS and PGLS models yielded very similar estimates for the temperature effect on both $\log_{10} C_g$ ($\beta_T = 0.015$ *vs.* 0.017, respectively) and $\log_{10} R_m$ ($\beta_T = 0.018$ *vs.* 0.020). Pagel's lambda ($\lambda \pm 95\%$ CI) and R^2 are indicated for each model, whereas significant effects ($p < 0.05$) are shown in bold.

variable	predictor	df	*F*-value	*p*	Pagel's λ	R^2
Overhead cost of growth (C_g, mg O_2 g^{-1})	Body mass	1	10.333	**0.002**	0.21 (NA, 0.79)	0.16
	Temperature	1	13.086	**<0.001**		
	Lifestyle	3	0.582	0.628		
Maintenance metabolism (R_m, mg O_2 g^{-1} d^{-1})	Body mass	1	29.247	**<0.001**	0.54 (0.16, 0.82)	0.36
	Temperature	1	29.330	**<0.001**		
	Lifestyle	3	2.612	**0.055**		

Table A3.8. PGLS regression describing the variation in net growth efficiency as explained by $\log_{10}$ body mas (g), temperature (°C), and lifestyle across the 114 species with phylogenetic data available. Net growth efficiencies were logit transformed here for comparison with the Beta regression model (BRM) in the main text. The BRM and PGLS model yielded very similar estimates for the temperature effect ($\beta_T = -0.019$ *vs.* -0.022, respectively). Pagel's lambda ($\lambda \pm 95\%$ CI) and R^2 are indicated for each model, whereas significant effects ($p < 0.05$) are shown in bold.

predictor	df	*F*-value	*p*	Pagel's λ	R^2
Body mass	1	0.944	0.334	0.00 (NA, 0.49)	0.04
Temperature	1	7.344	**0.008**		
Lifestyle	3	0.480	0.697		

A4. Appendix for Chapter 4

The cost of biomass production changes during ontogeny and between reproductive modes in a model crustacean

The following appendix contains supplementary information on:

A4.1. Monitoring individual rates of development and growth in cultures

A4.2. Conversion of body length into body mass

A4.3. Assumption of negligible body growth in reproductive individuals

A4.4. Non-linear squares models describing the variation in specific growth rates with body mass

A4.5. Sexual differences in metabolic scaling and growth trajectory in single individuals

A4.6. Differences in the metabolic costs between production of cysts and larvae

A4.1. Monitoring individual rates of development and growth in cultures

Individual rates of growth and development were tracked by using cylindrical cages made of plankton mesh floating into the batch cultures. These cages consisted of a cylinder of plankton mesh with a supporting plastic ring in the upper end, which incorporated circular floaters to maintain buoyancy, and enabled marking each cage so different individuals could be monitored simultaneously. The pore size of the plankton nets ranged from 40 to 150 μm depending on animal size, allowing water and food move through these cages (cell size of algal blend was 1.5 – 12 μm; RG Complete, Reef Nutrition®), but preventing individuals from escaping. Different cage dimensions and mesh sizes were used to accommodate the whole range of body sizes of animals studied here (Fig. A4.1).

Individuals were introduced and monitored in these cages for short periods ranging from 1 to 5 days, depending on their body size. Body length and developmental stage were recorded before and after this period in these individuals, which were finally placed in the respirometer where their metabolic rates were measured. To ensure that no individual was measured twice, monitored animals did not return to the cultures. Furthermore, the growth performance of individuals monitored through these cages was checked by comparing data on body length (mm) vs. age (days) with previous studies under similar conditions of temperature, salinity, and food ration (Evjemo & Olsen, 1999; Forster & Hirst, 2012) (Fig. A4.2).
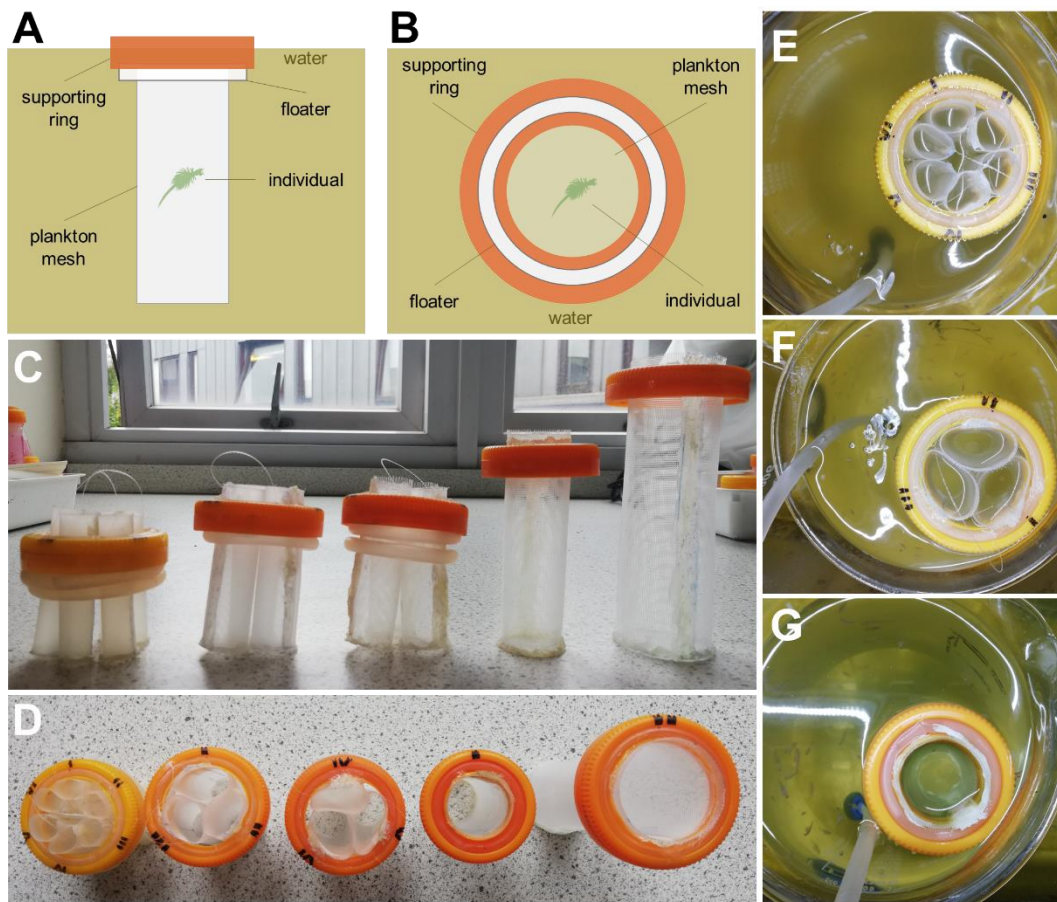
Figure A4.1. Cages used in this study to monitor individual growth and developmental rates in batch cultures. Schematic of a cage immersed in culture water and containing an individual, shown in lateral view (**A**) and from above (**B**). In **C,** an example of the different cages used to accommodate the entire range of body sizes throughout the ontogeny of *A. franciscana*, showing the circular floaters that maintained buoyancy. Cage dimensions (height $\times$ diameter), from left to right, were 6$\times$1, 8$\times$2 (duplicated), 10$\times$3, and 12$\times$4 cm. Pore size of plankton mesh in these cages were 40 µm in the smallest cage (left), and 120 µm in all the others. **D** shows the upper section and cylindrical shape of the cages, as well as the numeration of the individual cages to track animals throughout the experiment. **E**, **F** and **G** show examples of small (6$\times$1 cm), medium (8$\times$2 cm), and large (10$\times$3 cm) cages, as these were used in the cultures.
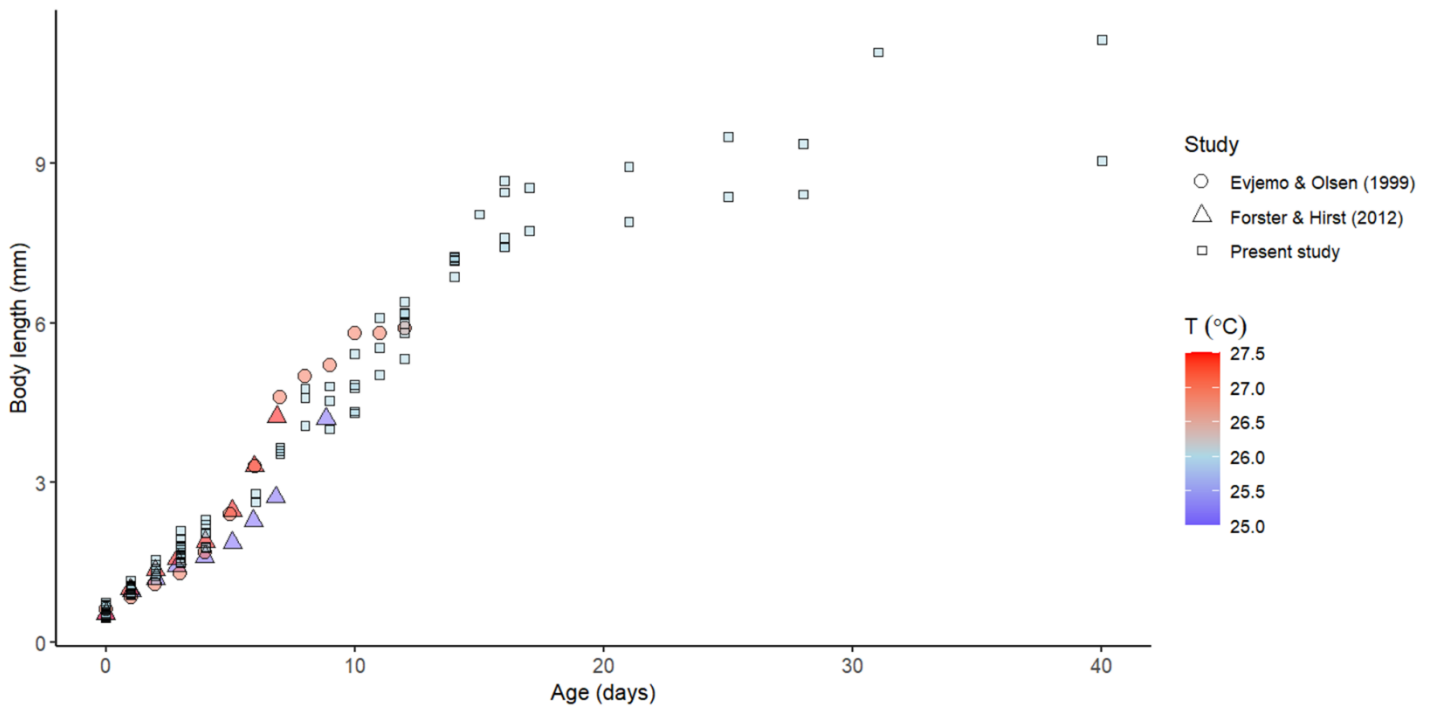
Figure A4.2. The increase in body length with age in individuals of *A. franciscana* observed in the present study (squares). Data from previous studies are shown for comparison, as mean body length at age under various conditions. Data from Evejmo & Olsen (1999) (circles) show cultures maintained at a temperature of 26 – 28 °C and 34 ppt of salinity, fed live *Isochrysis galbana* at a concentration of 10 mg of carbon L^{-1} (optimum ration), whereas the density of individuals in this study was decreased deliberately over time (from 18 to 0.48 ind. mL^{-1}). Data from Forster & Hirst (2012) (triangles) shows cultures where a total of 50 individuals were placed in 900 mL beakers at the start of the experiment (0.06 ind. mL^{-1}), fed Spirulina powder (*Arthrospira plantensis*), and maintained at temperatures of 25 and 27.5 °C. Temperature is colour coded form blue to red.

A4.2. Conversion of body length into body mass

To estimate the dry body mass of individuals from body length, I used the relationship between $\log_{10}$ body length (in mm) and $\log_{10}$ dry body mass (in µg) measured in a previous experiment. In this experiment, cultures of *A. franciscana* were fed live *Dunialella tertiolecta* and kept at 20 °C, 33 ppt of salinity, and at densities of $0.4 – 0.8$ individuals L^{-1}. A total of 504 individuals in these cultures were used, including from cysts to adults of *A. franciscana* (Fig. A4.3). Individuals were first photographed under a stereomicroscope and measured in body length from the anterior tip of the head to the base of the caudal furcae (Reeve, 1963), using the Motic Images Plus 2.0 software. Second, these individuals were dried at 80 °C for 24 h, and finally weighted in a microscale to get dry body mass (Mason, 1963). After comparing these data with other studies, culture conditions showed no obvious influence on the relationship between body length and mass in *A. franciscana* (Fig. A4.3), supporting previous observations by Evjemo & Olsen (1999).
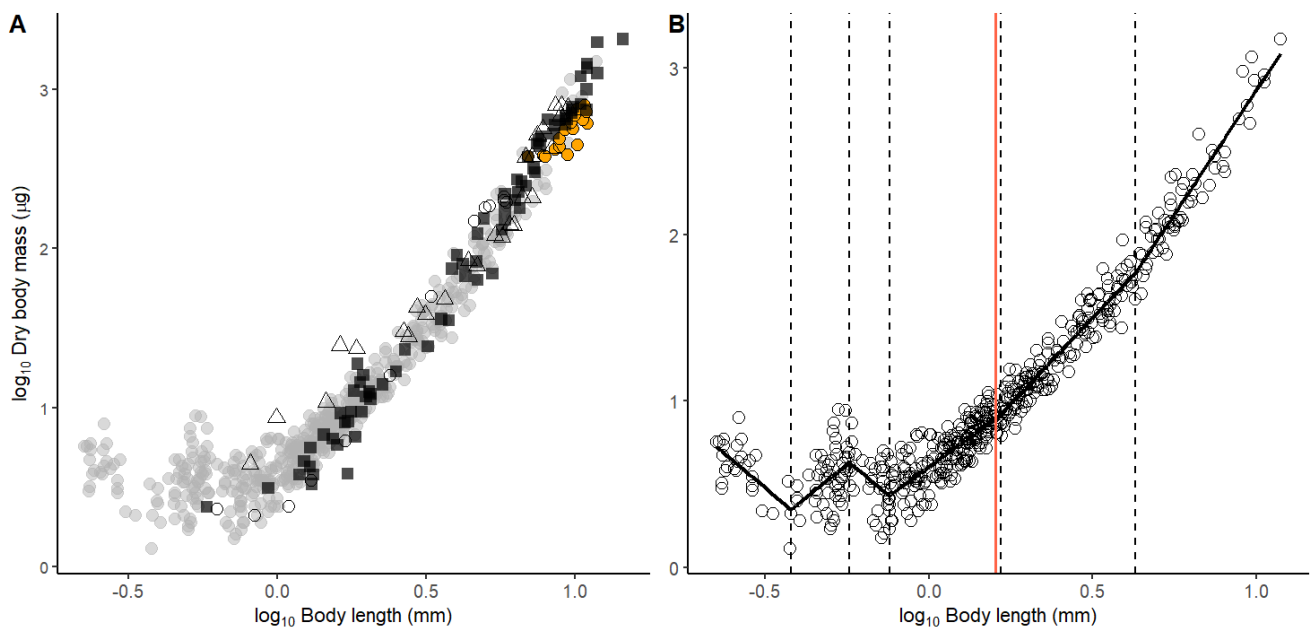

Figure A4.3. The relationship between $\log_{10}$ body length and $\log_{10}$ dry body mass in *Artemia franciscana*, from cysts to adults. **A** shows data on 504 individuals collected from cultures fed *Dunialella tertiolecta*, kept at 20 °C, 33 ppt of salinity, and at densities of $0.4 – 0.8$ individuals L^{-1}. For comparison, data are shown from other studies that used various experimental conditions: Reeve (1963), black squares: Mason (1963), triangles (for individuals grown in laboratory) and orange circles for a wild population from Mono Lake, California; Evjemo & Olsen (1999), empty circles. **B** shows the results of the piece-wise regression, which showed five breakpoints (dashed lines) over ontogeny, with six different slopes (see Table A1). The

parameters of the segmented regression were used in this study to estimate dry body mass from body length measurements of experimental individuals. The red line denotes the breakpoint at which Forster & Hirst (2012) estimated the change in slope from the thoracic to abdominal phase in *Artemia*, using data from Reeve (1963).

The relationship between individual body length and dry mass was analysed through a piece-wise regression (Muggeo, 2008), after $\log_{10}$ conversion of the variables. This method is described in detail in the main text (see section 4.2.7). This piece-wise regression yielded five breakpoints and six segments, each of those segments with respective intercepts and slopes (Table A4.1). These parameters were finally used to estimate the dry body mass from body length measurements of the individuals investigated in the present study.

Table A4.1. Results of the piece-wise regression for the relationship between $\log_{10}$ body length (mm) and $\log_{10}$ body dry mass (µg), indicating breakpoints (i.e., body length at which regression changes) as well as parameters (intercepts and slopes) of the regression segments used in this study to estimate dry mass from length measurements.

Breakpoints	Regression parameters	
Body length (*L*, mm)	intercept	slope
$L \leq 0.379$	-0.356	-1.675
$0.379 < L \leq 0.572$	1.009	1.565
$0.572 < L \leq 0.758$	0.275	-1.617
$0.758 < L \leq 1.664$	0.605	1.436
$1.664 < L \leq 4.260$	0.465	2.070
$L > 4.260$	-0.096	2.961

A4.3. Assumption of negligible body growth in reproductive individuals

To avoid perturbation of the individuals forming sexual pairs, body length was not measured in reproductive males and females prior to the reproduction experiments (see section 2.4 in the main text). Instead, growth in body mass in these animals was expected to be negligible, and hence biomass production was assumed to be solely due to offspring in females. While this assumption may have overlooked some variation in body mass during the reproduction experiments, the specific growth rates of these individuals, according to their body mass, were expected to be very close to zero (Fig. A4.4). Moreover, to ensure reproductive success during mating periods, most resources are presumably directed towards reproductive activities in both individuals of the pair (e.g., swimming, gamete production, fertilisation), as well as biosynthesis of offspring mass in females, and therefore little energy was expected to be left for somatic growth.
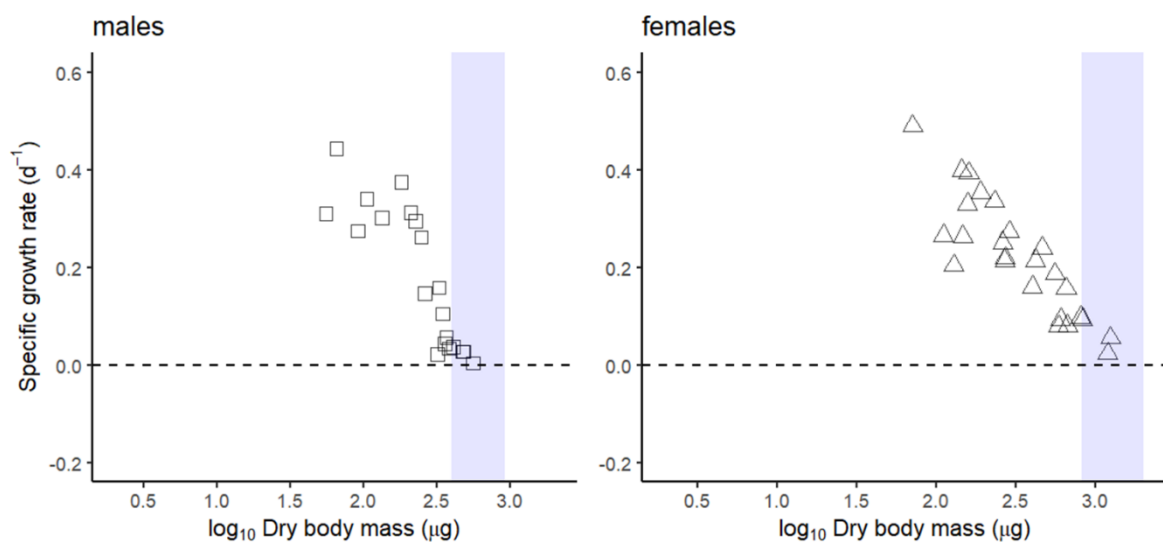

Figure A4.4. The decrease in specific growth rates with $\log_{10}$ body mass in single males (left) and females (right) observed in this study. Vertical blue bands denote the range of body sizes of reproductive individuals from sexual pairs in the reproduction experiments.

A4.4. Non-linear squares (NLS) models describing the variation in specific growth rates with body mass

Table A4.2. Results of the non-linear squares (NLS) models to describe the variation in specific growth rates (SGR, d^{-1}) of individuals as explained by $\log_{10}$ dry body mass (M, μg) over the ontogeny of *A. franciscana*. Second-, third-, and fourth-degree polynomial equations were implemented to data and compared through BIC values. The best model (i.e., lowest BIC value) is indicated by in bold.

Equation	Parameter	Estimate	t	p	BIC
$SGR = a + b \log_{10}m + c \log_{10}m^2$	a	-0.118	-2.01	0.047	
	b	0.666	7.78	< 0.001	-144.77
	c	-0.214	-8.55	< 0.001	
$\boldsymbol{SGR = a + b \log_{10}m + c \log_{10}m^2 + d \log_{10}m^3}$	a	-0.517	-4.45	< 0.001	
	b	1.587	6.36	< 0.001	-154.84
	c	-0.814	-5.23	< 0.001	
	d	0.116	3.90	< 0.001	
$SGR = a + b \log_{10}m + c \log_{10}m^2 + d \log_{10}m^3 + e \log_{10}m^4$	a	-0.943	-3.61	< 0.001	
	b	2.958	3.72	< 0.001	
	c	-2.267	-2.78	0.006	-153.61
	d	0.723	2.16	0.034	
	e	-0.087	-1.82	0.072	

A4.5. Sexual differences in metabolic scaling and growth trajectory in single individuals

The relationship between metabolic rates (R) and body mass (M) differed between single males and females (see Table 4.2). The OLS regression equations were $\log_{10} R = -0.85 + 0.61 \log_{10} M$ (df: 23, $t = 14.73$, $R^2 = 0.90$, $p < 0.001$) for females, and $\log_{10} R = -0.48 + 0.46 \log_{10} M$ (df: 18, $t = 8.55$, $R^2 = 0.79$, $p < 0.001$) for males. Similar OLS models were fitted to describe the relationship between specific growth rates (SGR) and $\log_{10}$ body mass (M) in these individuals, assuming that SGR decline linearly during post-larval ontogeny (Fig. A4.5). These equations are $\log_{10} SGR = 1.00 - 0.31 \log_{10} M$ (df: 23, $t = -8.93$, $R^2 = 0.77$, $p < 0.001$) for females, and $\log_{10} SGR = 1.18 - 0.42 \log_{10} M$ (df: 18, $t = -7.12$, $R^2 = 0.72$, $p < 0.001$) for males. Although SGR decreased more steeply over ontogeny in males than in females, a further OLS model incorporating data on both females and males showed that such decline in SGR with body mass was not significantly different between sexes, as denoted by the interaction term between sex and $\log_{10} M$ in this model (OLS, df: 41, $t = -1.69$, $p = 0.099$).
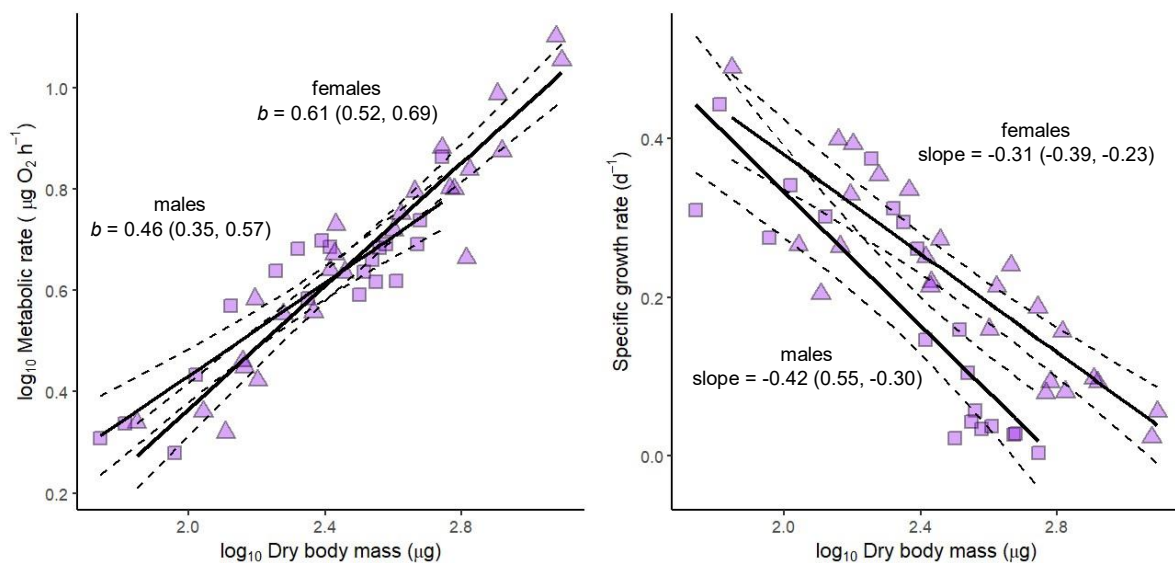

Figure A4.5. Left panel shows the relationship between $\log_{10}$ metabolic rates (R) and $\log_{10}$ body mass (M) of single females (triangles) and males (squares) in this study. Right panel shows the decrease in specific growth rates (SGR) with $\log_{10}$ body mass (M) of single females and males. Thick and dashed lines denote regression lines and 95% confidence intervals from OLS models, whereas regression slopes and 95% CI are indicated in the plots.

A4.6. Differences in the metabolic costs between production of cysts and larvae

The metabolic costs of offspring production showed to be influenced by the reproductive mode of females (see Table 4.3). The OLS regression equations for the relationship between mass-specific metabolic rate and each reproductive mode alone (all in J g^{-1} h^{-1}; Fig. A4.6) were $Y = 141.61 - 0.46\ X$ (df = 15, $t = -0.78$, $R^2 = -0.02$, $p = 0.447$) for cyst production; and $Y = 98.17 - 1.82\ X$ (df = 15, $t = 4.05$, $R^2 = 0.49$, $p = 0.001$), for larvae production.
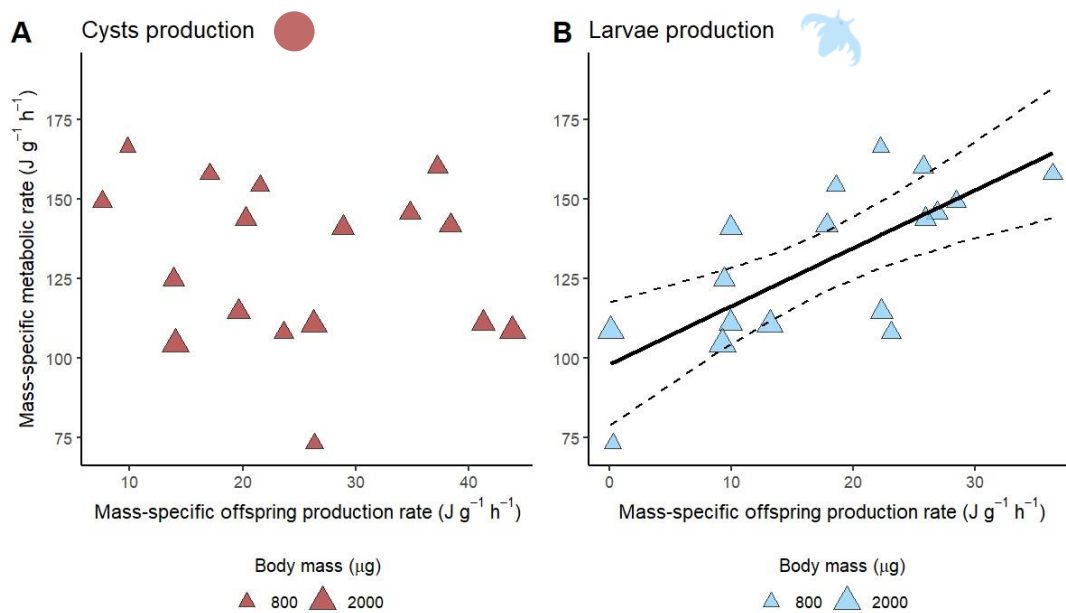

Figure A4.6. The relationship between mass-specific rates of metabolism and production of cysts mass (A) and larvae mass (B) by reproducing females. Thick and dashed lines denote regression lines and 95% confidence intervals from statistically significant models ($p < 0.05$).

References

Barneche, D. R., & Allen, A. P. (2018). The energetics of fish growth and how it constrains food-web trophic structure. *Ecology letters*, *21*(6), 836-844.

Bürkner, P. C. (2017). brms: An R package for Bayesian multilevel models using Stan. *Journal of Statistical Software*, *80*, 1-28

Chang, J., Rabosky, D. L., Smith, S. A., & Alfaro, M. E. (2019). An R package and online resource for macroevolutionary studies using the ray-finned fish tree of life. *Methods in Ecology and Evolution*, *10*(7), 1118-1124.

Deane, E. E., & Woo, N. Y. (2009). Modulation of fish growth hormone levels by salinity, temperature, pollutants and aquaculture related stress: a review. *Reviews in Fish Biology and Fisheries*, *19*, 97-120.

Evjemo, J. O., & Olsen, Y. (1999). Effect of food concentration on the growth and production rate of *Artemia franciscana* feeding on algae (T. iso). *Journal of Experimental Marine Biology and Ecology*, *242*(2), 273-296

Forster, J., & Hirst, A. G. (2012). The temperature-size rule emerges from ontogenetic differences between growth and development rates. *Functional Ecology*, *26*(2), 483-492.

Gelman, A. & Hill, J. (2006). *Data Analysis Using Regression and Multilevel/Hierarchical Models* (pp. 124-125). Cambridge University Press.

Glazier, D. S. (2009c). Ontogenetic body-mass scaling of resting metabolic rate covaries with species-specific metabolic level and body size in spiders and snakes. *Comparative Biochemistry and Physiology Part A: Molecular & Integrative Physiology*, *153*(4), 403-407.

Glazier, D. S. (2010). A unifying explanation for diverse metabolic scaling in animals and plants. *Biological Reviews*, *85*(1), 111-138.

Glazier, D. S. (2020). Activity alters how temperature influences intraspecific metabolic scaling: testing the metabolic-level boundaries hypothesis. *Journal of Comparative Physiology B*, *190*(4), 445-454.

Grafen, A. (1989). The phylogenetic regression. *Philosophical Transactions of the Royal Society of London. B*, *Biological Sciences, 326*(1233), 119-157.

Jackman, S. (2009). *Bayesian analysis for the social sciences* (p. 507). Wiley.

Killen, S. S., Atkinson, D., & Glazier, D. S. (2010). The intraspecific scaling of metabolic rate with body mass in fishes depends on lifestyle and temperature. *Ecology Letters*, *13*(2), 184-193.

Kuznetsova, A., Brockhoff, P. B., & Christensen, R. H. (2017). lmerTest package: tests in linear mixed effects models. *Journal of Statistical Software*, *82*(13), 1-26.

Lewandowski, D., Kurowicka, D., & Joe, H. (2009). Generating random correlation matrices based on vines and extended onion method. *Journal of Multivariate Analysis*, *100*(9), 1989-2001.

Little, A.G., Kunisue, T., Kannan, K., & Seebacher, F. (2013). Thyroid hormone actions are temperature-specific and regulate thermal acclimation in zebrafish (*Danio rerio*). *BMC Biology*, 11, 1-15.

Mason, D. T. (1963). The growth response of *Artemia salina* (L.) to various feeding regimes. *Crustaceana*, 5(2), 138-150.

Michonneau, F., Brown, J. W., & Winter, D. J. (2016). rotl: an R package to interact with the Open Tree of Life data. *Methods in Ecology and Evolution*, *7*(12), 1476-1481.

Moses, M. E., Hou, C., Woodruff, W. H., West, G. B., Nekola, J. C., Zuo, W., & Brown, J. H. (2008). Revisiting a model of ontogenetic growth: estimating model parameters from theory and data. *The American Naturalist*, *171*(5), 632-645.

Muggeo, V. M. (2008). Segmented: an R package to fit regression models with broken-line relationships. *R News*, *8*(1), 20-25.

Paradis, E., & Schliep, K. (2019). ape 5.0: an environment for modern phylogenetics and evolutionary analyses in R. *Bioinformatics*, *35*(3), 526-528.

Parry, G. D. (1983). The influence of the cost of growth on ectotherm metabolism. *Journal of Theoretical Biology*, *101*(3), 453-477.

Reeve, M. R. (1963). The filter-feeding of *Artemia*: I. In pure cultures of plant cells. *Journal of Experimental Biology*, *40*(1), 195-205.

Roycroft, E. J., Nations, J. A., & Rowe, K. C. (2020). Environment predicts repeated body size shifts in a recent radiation of Australian mammals. *Evolution*, *74*(3), 671-680.

Seebacher, F., White, C. R., & Franklin, C. E. (2015). Physiological plasticity increases resilience of ectothermic animals to climate change. *Nature Climate Change*, *5*(1), 61-66.

Von Bertalanffy, L. (1938). A quantitative theory of organic growth (inquiries on growth laws. II). *Human Biology*, *10*(2), 181-213.

West, G. B., Brown, J. H., & Enquist, B. J. (1997). A general model for the origin of allometric scaling laws in biology. *Science*, *276*(5309), 122-126.

West, G. B., Brown, J. H., & Enquist, B. J. (2001). A general model for ontogenetic growth. *Nature*, *413*(6856), 628-631.